CHALMERS

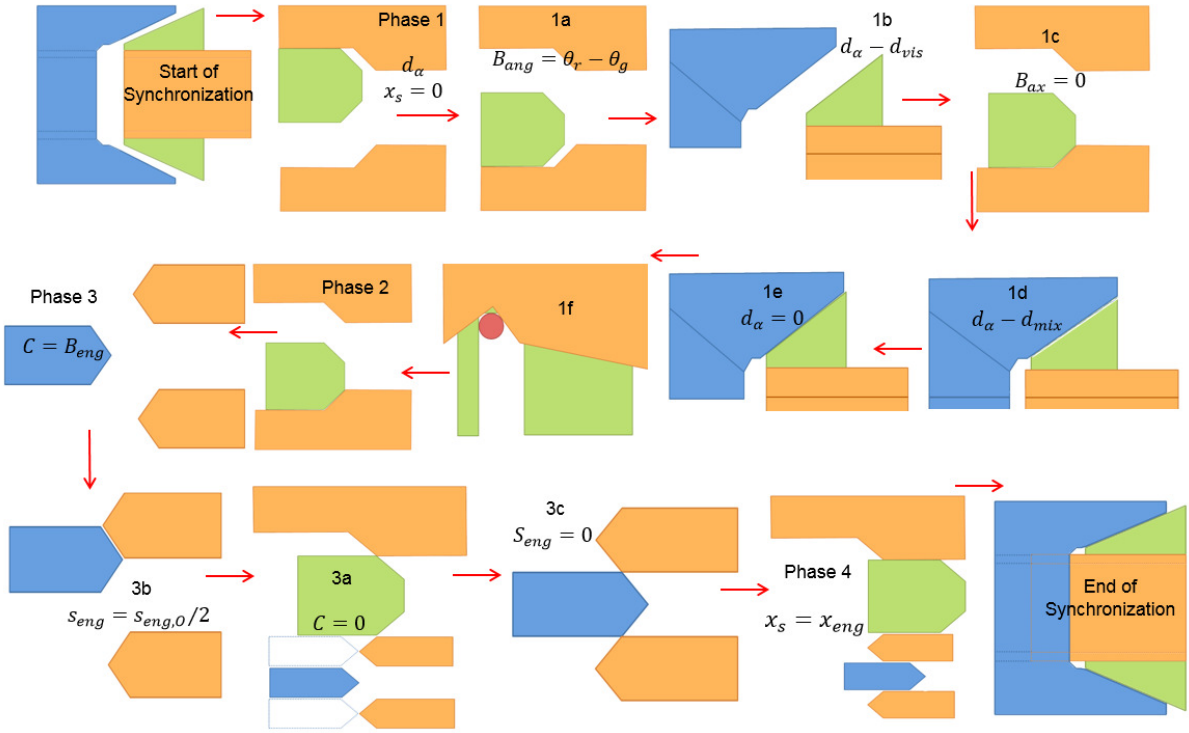

Research report 2015:05

Constrained Lagrangian Formulation for Modelling and Analysis of Transmission Synchronizers

MUHAMMAD IRFAN, VIKTOR BERBYUK AND HÅKAN JOHANSSON

Department of Applied Mechanics
CHALMERS UNIVERSITY OF TECHNOLOGY
Göteborg, Sweden 2015

Research report 2015:05

Constrained Lagrangian Formulation for Modelling and Analysis of Transmission Synchronizers

by

MUHAMMAD IRFAN, VIKTOR BERBYUK AND HÅKAN JOHANSSON

Department of Applied Mechanics
CHALMERS UNIVERSITY OF TECHNOLOGY
Göteborg, Sweden, 2015

Constrained Lagrangian Formulation for Modelling and Analysis of Transmission Synchronizers

MUHAMMAD IRFAN, VIKTOR BERBYUK AND
HÅKAN JOHANSSON

© MUHAMMAD IRFAN, VIKTOR BERBYUK AND
HÅKAN JOHANSSON, 2015

Research report 2015:05
ISSN 1652-8549

Department of Applied Mechanics
Chalmers University of Technology
SE-412 96 Göteborg
Sweden
Telephone +46 (0)31 772 1000

Abstract

An engineering model of a generic synchronizer is considered. The generic synchronizer is modeled consisting of the selector sleeve with engaging teeth and frictional cone, the synchronizing ring with blocker and the gearwheel with engaging teeth. It is assumed that for the sleeve and synchronizing ring translational and rotational motions are feasible, for the gearwheel only rotational motion is feasible. The motion of the generic synchronizer is performed under the external and internal loads. The external loads comprise the vehicle resistance torque and the control force applied to the sleeve and the drag torque due to the clutch. The internal loads comprise the forces and torques arises due to interaction between the sleeve, the synchronizing ring, the gearwheel as well as oil splash during the synchronization process. A feasible synchronization process of a generic synchronizer is divided into four main phases: pre-synchronization, main synchronization, blocker transition (indexing for the ring), and engagement. Pre-synchronization and blocker transition are further divided into several sub-phases. The generic synchronizer is fully parametrized and together with description of all phases constitutes kinematics of synchronization process in question.

Due to the nature of synchronization process in transmission system a motion of a synchronizer mechanism is subjected to unilateral or/and bilateral constraints imposed on generalized coordinates or/and generalized velocities of the synchronizer. Constrained Lagrangian Formalism (CLF) has been proposed as an approach for developing mathematical and computational models of a generic synchronizer dynamics. The CLF gives possibility to formulate direct dynamics, semi-inverse dynamics and inverse dynamics problems for a generic synchronizer in unified and efficient way. It is shown that CLF can be promising and useful for advanced dynamic analysis of the existing synchronizer mechanisms and to design novel optimized ones.

In the present report mathematical and computational models of a generic synchronizer with five degrees of freedom have been developed using CLF. Application of CLF on the modelling of the synchronization process gives system of differential-algebraic equations (DAE). Analysis of the generic synchronizer performance diagrams has shown that the CLF based model is able to predict the synchronization process characteristics reasonably well. The developed model has been validated by using measurement data from test rig at CV AB Scania. Performance of the generic synchronizer is also analyzed in case of driveline vibrations. Sensitivity analysis of the synchronizer mechanism performance with respect to cone angle, coefficient of friction, maximum value of shift force and rate of applying shift force has been done.

Next, the developed models will be used to get further insight into synchronizer design and its performance diagrams with aid of global sensitivity analysis and Pareto optimization.

Contents

Abstract 1
1. Introduction 3
1.1 Background 3
1.2 Working Principle of Synchronization 3
1.3 Project Aim and Objective 4
1.3.1 Current objectives 5
2. Multibody System and Equations of Motion 6
2.1 DAE Solution 8
3. A Generic Synchronizer 10
3.1 A general description and equations of motion 10
3.2 Models of Different Phases for the Generic Synchronizer 13
3.2.1 Phase 1-Pre-synchronization 15
3.2.7 Phase 2- Main synchronization 30
3.2.8 Phase 3-Blocker transition 32
3.2.9 Phase 4-Engagement 40
4. Problem Formulation 42
5. Simulation Results 44
5.1 Force Control 44
5.2 Kinematic control 49
5.3 Sensitivity Analysis 51
5.4 Validation: Modified Generic Synchronizer to validate with the Scania Test Rig 57
6. Conclusions and Future Work 61
ACKNOWLEDGMENTS 61
References 62
Appendix 63
A.1 Constraints and equations of motion for generic synchronizer 63
A.2 Alternative case of phase 3: small clearance 77
A.3 Modified synchronizer for test rig comparison 94

1. Introduction

1.1 Background

The transmission system is a key element in motorized vehicles to transfer mechanical power from the engine to the wheels. It has great impact on the vehicle fuel consumption, power efficiency, noise and shift comfort. For manual transmission, synchronizer mechanisms were developed in the 1920s to allow smooth gear changing both for the durability of the transmission and the comfort for the users [1].

The demand of decreasing vehicle emission has led to higher demands on gearboxes and gear synchronizers by lower engine speeds, leading to higher torque and torque variations and by more frequent and faster shifts to keep engine running at optimal speed.

1.2 Working Principle of Synchronization

The synchronization is a part of the gear shifting which is the process of engagement of gearbox input shaft with output shaft. A common layout of synchronizer consists of sleeve, friction cones, ring, spring and gear which are depicted in *Figure 1*. Frictional cones of synchronizer are used to bring speed difference of output shaft and input shaft to zero. One of the inner frictional cones is part of the blocker ring which has teeth with the purpose of blocking engagement before the speed difference is small enough. When the two shafts rotate at same speed the sleeve slide axially and connect output and input shafts for transmission. For the main gear synchronizers, the sleeve is rotating together with output shaft and output shaft is connected with vehicle wheels to ground. The sleeve is therefore assumed to have roughly constant speed during the short time duration of synchronization because of high rotating inertia of the vehicle. Input shaft together with ring has varying speed during the process.

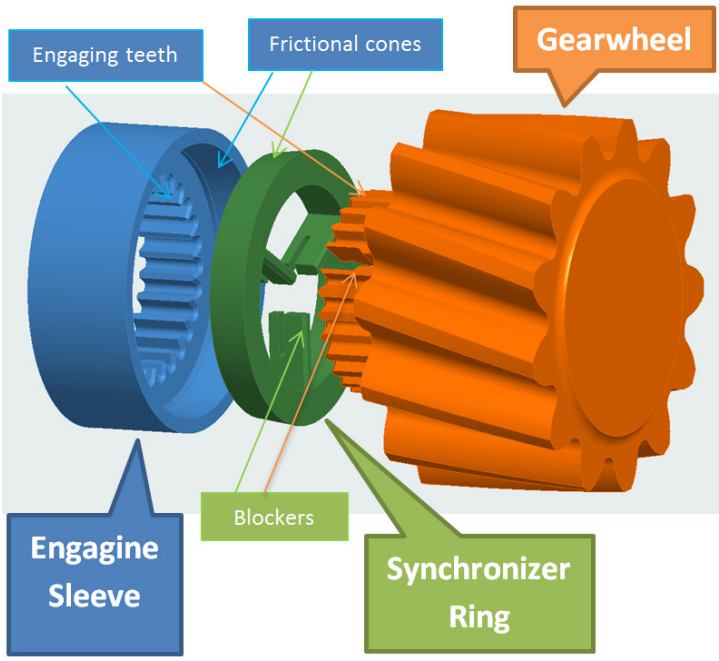

Figure 1: A common layout of a synchronizer.

1.3 Project Aim and Objective

Shift force required and time needed to change gears are typical ways to define shift quality. Basically the shift quality depends upon interaction of different parts of synchronizer, which is defined in terms of a set of design parameters (cone angle, chamfer angle, spring stiffness and many more). It is a time consuming and expensive task to figure out by trial and error which design gives the best performance. Therefore it is desirable to develop an efficient dynamic model especially for manual transmissions of heavy vehicles that can be used for quantitative assessment of shift quality and thereby serve as basis for sensitivity study and optimization. As a way to quantify synchronizer quality, a set of performance measures is to be defined. These include the shift force and time to change gear, and will be detailed in section 4.

The overall objective of the project is develop simulation tools that help engineers design synchronizers with minimal synchronization time while maintaining shift quality for the gearbox over its entire life. A synchronizer must function over a large span of different situations, which are represented by a set of synchronization scenarios. The performance of the synchronizer is predicted from a mechanical model, and is measured in terms of performance measures which include shift time, energy loss (frictional work of conical surfaces), shift comfort (maximum shift force, magnitude of second bump) and other. Robustness is considered by the choice of scenarios and the weighting of these.

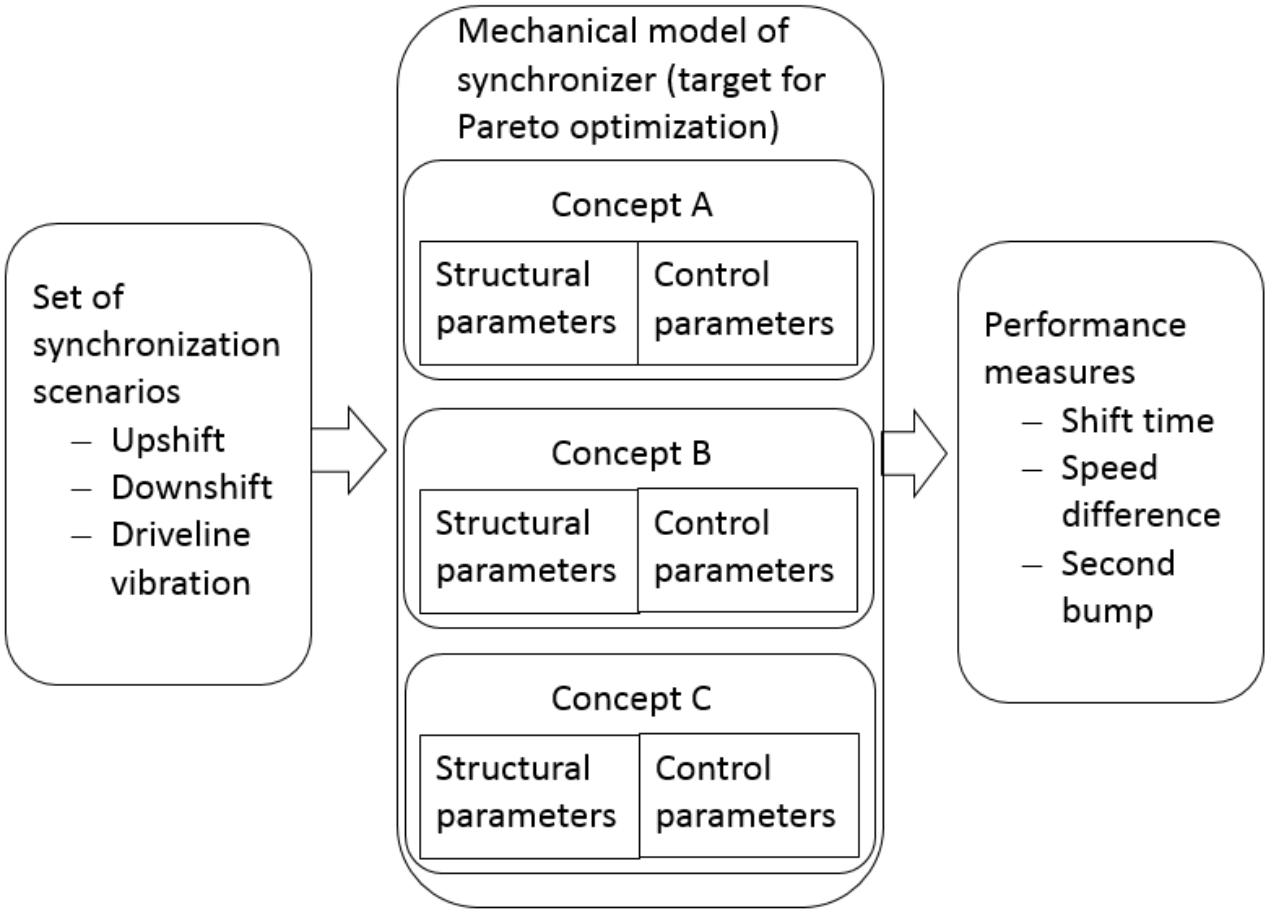

Figure 2. Flow process to develop the optimized and robust synchronizers.

The mechanical model of a given concept of synchronizer is parameterized with a set of structural parameters (cone angle, chamfer angle, radius etc.) and control parameters

(defining the applied sleeve force). The optimization of a synchronizer mechanism can be done on different levels. The first being to find the optimal control parameters for a given concept and given structural parameters. The second level is to find the most suitable structural parameters for a given concept and optimal control parameters. The third is to find the best concept, where each concept (A, B, C…) is assigned its optimal structural and control parameters. Since there is several conflicting performance measures under consideration, Pareto optimization [2] is to be employed to find the trade-off curve between the considered performance measures.

1.3.1 Current objectives

The first objective to reach the overall aim is the development of a mathematical and computational models that can predict synchronizer performance for a given concept. The models should include relevant physical parameters of synchronizer and be able to highlight the parameters that most influence the synchronizer performance. As a starting point to highlight the main features of a generic design of synchronizer will be studied. Since the synchronizer consists of several mechanical parts interaction can be described by different constraints where a constrained Lagrangian formalism is used to formulate such a mathematical model of a generic synchronizer.

In the study of dynamic model development of transmission system a few models have been reported in literature aiming at specific objectives. A simulated technique with an analytical model of movement and contact force of the synchronizer is implemented in ADAMS [3]. A dynamic model of the entire synchronizer, selector mechanism, driveline and transmission has been created in MATLAB Simulink and ADAMS [4]. A MATLAB program of synchronization performance based on existing Scania in-house code in MS Excel was developed and verified by physical testing [5].

This report is organized as follows; firstly the general multibody formalism is outlined. Thereafter, a generic synchronizer is described in terms of constrained multibody formalism, and the numerical method to solve the relevant set of equations is outlined. Finally simulation results are shown before the report ends with conclusion and outlook.

2. Multibody System and Equations of Motion

Before turning to the specific case of synchronizer, a brief introduction to constrained Lagrangian formalism is given. In depth elaborations can be found in [6]. Consider a mechanical system consisting of nb rigid bodies

$$MBS = \{RB_1, RB_2, \dots, RB_{nb}\} \tag{2.1}$$

Let $O(x, y, z)$ be an inertial reference frame, and

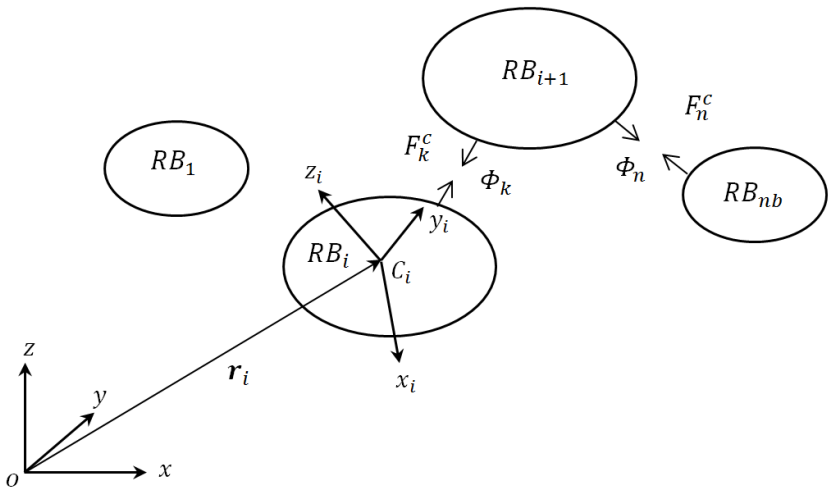

Figure 3: Multibody System of $\boldsymbol{nb}$ bodies.

F_k^c is constraint force associated with some constraint Φ_k between RB_i and RB_{i+1}, $C_i(x_i, y_i, z_i)$ is a body fixed reference frame for RB_i with its origin at the centre of mass of the body, point C_i, for each body , and

$$\boldsymbol{q}_i = [x_i, y_i, z_i, \theta_i, \psi_i, \varphi_i]^T \qquad i = 1, \dots, nb \tag{2.2}$$

is the vector of generalized coordinates of RB_i. Here, $\boldsymbol{r}_i = [x_i, y_i, z_i]^T$ is a position vector from O to C_i and, $[\theta_i, \psi_i, \varphi_i]$ are the Euler angles of body fixed reference frame $C_i(x_i, y_i, z_i)$ w.r.t. inertial reference frame $O(x, y, z)$.

All degrees of freedom of MBS are collected in one vector $\boldsymbol{q}$ as

$$\boldsymbol{q} = [\boldsymbol{q}_1^T, \boldsymbol{q}_2^T, \dots, \boldsymbol{q}_{nb}^T]^T \tag{2.3}$$

To determine the motion of MBS under the action of external forces and torques, Lagrangian formalism is adopted. To this end we assume that a potential energy $U = U(\boldsymbol{q})$ and kinetic energy denoted $T = T(\boldsymbol{q}, \dot{\boldsymbol{q}})$ are used, defining the Lagrangian L of the system as

$$L = T(\boldsymbol{q}, \dot{\boldsymbol{q}}) - U(\boldsymbol{q}) \tag{2.4}$$

If generalized coordinates $\boldsymbol{q}$ are independent then the motion of the system is described by Lagrange's equations

$$\left[\frac{d}{dt}\left(\frac{\partial L}{\partial \dot{\boldsymbol{q}}}\right)\right]^T - \left[\frac{\partial L}{\partial \boldsymbol{q}}\right]^T = \boldsymbol{Q}^A \tag{2.5}$$

where $\boldsymbol{Q}^A$ is a vector of generalized forces due to external non-conservative loads.

In contrast, if the coordinates $\boldsymbol{q}$ are not independent, but is subjected to holonomic kinematic constraints of the form

$$\boldsymbol{\Phi}(\boldsymbol{q}, \boldsymbol{t}) = [\Phi_1(\boldsymbol{q}, t), \ldots \Phi_{nc}(\boldsymbol{q}, t)]^T = \boldsymbol{0} \tag{2.6}$$

the Lagrange multiplier theorem [6] guarantees existence of a Lagrange multiplier vector $\boldsymbol{\lambda}$,

$$\boldsymbol{\lambda} = [\lambda_1, \ldots, \lambda_{nc}]^T \tag{2.7}$$

such that motion of the system is described by the following equations

$$\left[\frac{d}{dt}\left(\frac{\partial L}{\partial \dot{\boldsymbol{q}}}\right)\right]^T - \left[\frac{\partial L}{\partial \boldsymbol{q}}\right]^T + \left[\frac{\partial \boldsymbol{\Phi}}{\partial \boldsymbol{q}}\right]^T \boldsymbol{\lambda} = \boldsymbol{Q}^A \tag{2.8}$$

$$\boldsymbol{\Phi}(\boldsymbol{q}, t) = \boldsymbol{0} \tag{2.9}$$

This is the constrained form of Lagrange equations of motion of MBS with holonomic kinematic constraints.

The vector of generalized non-conservative forces $\boldsymbol{Q}^A$ is further divided into $\boldsymbol{Q}^A = \boldsymbol{Q}^A_{fric} + \boldsymbol{Q}^A_{app}$ where $\boldsymbol{Q}^A_{fric}$ are generalized forces arising due to friction between bodies or other losses and $\boldsymbol{Q}^A_{app}$ are generalized forces due to applied forces arising from external stimuli. Sometimes, $\boldsymbol{Q}^A_{fric}$ is determined from a dissipation function $R(\dot{\boldsymbol{q}})$ as $\boldsymbol{Q}^A_{fric} = \left[-\frac{\partial R}{\partial \dot{\boldsymbol{q}}}\right]^T$, and a classical example of $R(\dot{\boldsymbol{q}})$ is that of Rayleigh dissipation function $R = \frac{1}{2}\dot{\boldsymbol{q}}^T \boldsymbol{C} \dot{\boldsymbol{q}}$.

<u>Remark 1</u>

If time does not appear explicitly in the constraint equations (2.6), these holonomic constraints are called stationary or scleronomic otherwise these are called time dependent or Rheonomic. Constraints that cannot be written in the form (2.6) are called nonholonomic constraints. □

<u>Remark 2</u>

The differential equations (2.8) together with algebraic equations (2.9) constitute $(6nb + nc)$ system of DAE for $(6nb + nc)$ unknown coordinates $q_1, q_2 \ldots, q_{6nb}$ and Lagrangian multiplier $\lambda_1, \ldots, \lambda_{nc}$. □

In (2.8) the constraint Jacobian matrix is evaluated as

$$\frac{\partial \boldsymbol{\Phi}}{\partial \boldsymbol{q}} = \begin{pmatrix} \frac{\partial \Phi_1(\boldsymbol{q},t)}{\partial q_1} & \frac{\partial \Phi_1(\boldsymbol{q},t)}{\partial q_2} \dots\dots & \frac{\partial \Phi_1(\boldsymbol{q},t)}{\partial q_{6nb}} \\ \frac{\partial \Phi_2(\boldsymbol{q},t)}{\partial q_1} & \frac{\partial \Phi_2(\boldsymbol{q},t)}{\partial q_2} \dots\dots & \frac{\partial \Phi_1(\boldsymbol{q},t)}{\partial q_{6nb}} \\ \vdots & \vdots & \vdots \\ \frac{\partial \Phi_{nc}(\boldsymbol{q},t)}{\partial q_1} & \frac{\partial \Phi_{nc}(\boldsymbol{q},t)}{\partial q_2} \dots\dots & \frac{\partial \Phi_{nc}(\boldsymbol{q},t)}{\partial q_{6nb}} \end{pmatrix} \tag{2.10}$$

which together with $\boldsymbol{\lambda}$ can be identified as the force vector needed to upholding the constraints

$$\boldsymbol{F}^c = -\left[\frac{\partial \boldsymbol{\Phi}}{\partial \boldsymbol{q}}\right]^T \boldsymbol{\lambda} \tag{2.11}$$

Note that these are workless forces, which can be computed from the Lagrange multipliers after solving DAE (2.8), (2.9).

In particular, we can identify the constraint force

$$(F_k^c)_j = -\frac{\partial \Phi_k}{\partial q_j}\lambda_k\,, \quad k = 1,2 \dots n_c \tag{2.12}$$

which is the force due to constraint k related to generalized coordinate j.

2.1 DAE Solution

Several methods to solve DAE systems on the form (2.8) and (2.9) exist. A predictor-corrector method described below such that on at each time-step acceleration is computed from which displacements and velocities at next time step are determined. A more in depth description can be found in [6].

To obtain accelerations $\ddot{\boldsymbol{q}}$ and Lagrangian multipliers $\boldsymbol{\lambda}$, it is noted that (2.8) can be written on matrix form as

$$\boldsymbol{M}\ddot{\boldsymbol{q}} + \boldsymbol{\Phi}_{\boldsymbol{q}}^{\boldsymbol{T}}\boldsymbol{\lambda} = \boldsymbol{Q}^A = \boldsymbol{Q}_{fric,ext}^A + \boldsymbol{Q}_{app}^A \tag{2.13}$$

where $\boldsymbol{\Phi}_{\boldsymbol{q}} = \frac{\partial \boldsymbol{\Phi}}{\partial \boldsymbol{q}}$ is the constraint Jacobian.

Next, the constraint equation (2.9) is differentiated twice w.r.t time, $\boldsymbol{q} = \boldsymbol{q}(t)$, which gives

$$\boldsymbol{\Phi}_{\boldsymbol{q}}\ddot{\boldsymbol{q}} = -\left[\frac{\partial}{\partial \boldsymbol{q}}\left(\frac{\partial \boldsymbol{\Phi}}{\partial \boldsymbol{q}}\dot{\boldsymbol{q}}\right)\dot{\boldsymbol{q}}\right] - 2\frac{\partial}{\partial \boldsymbol{q}}\left(\frac{\partial \boldsymbol{\Phi}}{\partial t}\right)\dot{\boldsymbol{q}} - \frac{\partial}{\partial t}\left(\frac{\partial \boldsymbol{\Phi}}{\partial t}\right) \equiv \boldsymbol{\gamma} \tag{2.14}$$

From this, a system to compute accelerations that satisfy the constraints can be formed as

$$\begin{bmatrix} \boldsymbol{M} & \boldsymbol{\Phi}_q^T \\ \boldsymbol{\Phi}_q & \boldsymbol{0} \end{bmatrix} \begin{bmatrix} \ddot{\boldsymbol{q}} \\ \boldsymbol{\lambda} \end{bmatrix} = \begin{bmatrix} \boldsymbol{Q}^A \\ \boldsymbol{\gamma} \end{bmatrix} \tag{2.15}$$

Hence, following [6], the algorithm to solve the DAE (2.8) and (2.9) a predictor-corrector algorithm of Adams-Bashforth type can be summarized as follows:

<u>From time t_i to t_{i+1}</u>

At time t_i for given position $[\boldsymbol{q}]_i$ and velocity $[\dot{\boldsymbol{q}}]_i$ solve for $\left[\ddot{\boldsymbol{q}}^T \;\; \boldsymbol{\lambda}^T\right]_i^T$ from the acceleration equation (2.15)

- ➢ Predictor step

- Compute an approximation for position $[\boldsymbol{q}]_{i+1}$ and velocity $[\dot{\boldsymbol{q}}]_{i+1}$ from the acceleration $[\ddot{\boldsymbol{q}}]_i$
  - $[\dot{\boldsymbol{q}}]_{i+1}^P = [\dot{\boldsymbol{q}}]_{t_i} + h\left[\ddot{\boldsymbol{q}}\right]_i$
  - $[\boldsymbol{q}]_{i+1}^P = [\boldsymbol{q}]_{t_i} + h\left[\dot{\boldsymbol{q}}\right]_i$
- Update $[\boldsymbol{q}]_{i+1}^P$ to satisfy $\boldsymbol{\Phi}(\boldsymbol{q}_{i+1}^P, t_{i+1}) = \boldsymbol{0}$
- Update $[\dot{\boldsymbol{q}}]_{i+1}^P$ to satisfy $\boldsymbol{\Phi}_q \dot{\boldsymbol{q}}_{i+1}^P + \boldsymbol{\Phi}_t = \boldsymbol{0}$

Again solve the acceleration equation for $\left[\ddot{\boldsymbol{q}} \;\; \boldsymbol{\lambda}\right]_{i+1}$ at predicted position $[\boldsymbol{q}]_{i+1}^P$ and velocity $[\dot{\boldsymbol{q}}]_{i+1}^P$.

- ➢ Corrector step

- Compute position $[\boldsymbol{q}]_{i+1}$ and velocity $[\dot{\boldsymbol{q}}]_{i+1}$ for accelerations $[\ddot{\boldsymbol{q}}]_i$ and $[\ddot{\boldsymbol{q}}]_{i+1}$
  - $[\dot{\boldsymbol{q}}]_{i+1}^c = [\dot{\boldsymbol{q}}]_{t_i} + h\left(\left[\ddot{\boldsymbol{q}}\right]_{i+1} - \frac{1}{2}\left(\left[\ddot{\boldsymbol{q}}\right]_{i+1} - \left[\ddot{\boldsymbol{q}}\right]_i\right)\right)$
  - $[\boldsymbol{q}]_{i+1}^c = [\boldsymbol{q}]_{t_i} + h\left(\left[\dot{\boldsymbol{q}}\right]_{i+1} - \frac{1}{2}\left(\left[\dot{\boldsymbol{q}}\right]_{i+1} - \left[\dot{\boldsymbol{q}}\right]_i\right)\right)$
- Update $[\boldsymbol{q}]_{i+1}^c$ to satisfy $\boldsymbol{\Phi}(\boldsymbol{q}_{i+1}^c, t_{i+1}) = \boldsymbol{0}$
- Update $[\dot{\boldsymbol{q}}]_{i+1}^c$ to satisfy $\boldsymbol{\Phi}_q \dot{\boldsymbol{q}}_{i+1}^c + \boldsymbol{\Phi}_t = \boldsymbol{0}$

<u>From time t_{i+1} to t_{i+2}</u>

Repeat the same procedure as from time t_i to t_{i+1}.

The procedure to update state and velocities to satisfy constraints can be done by identifying a set of dependent and independent coordinates and portion $\boldsymbol{\Phi}_q$ accordingly. One way to do that is from a triangulation of $\boldsymbol{\Phi}_q$, see [7].

3. A Generic Synchronizer

3.1 A general description and equations of motion

The generic synchronizer as depicted in *Figure 4* is a mechanical system that consists of 3 rigid bodies, the sleeve, the synchronizer ring and the gearwheel, denoted by subscripts s, r and g, respectively, below $\{RB_s, RB_r, RB_g\}$.

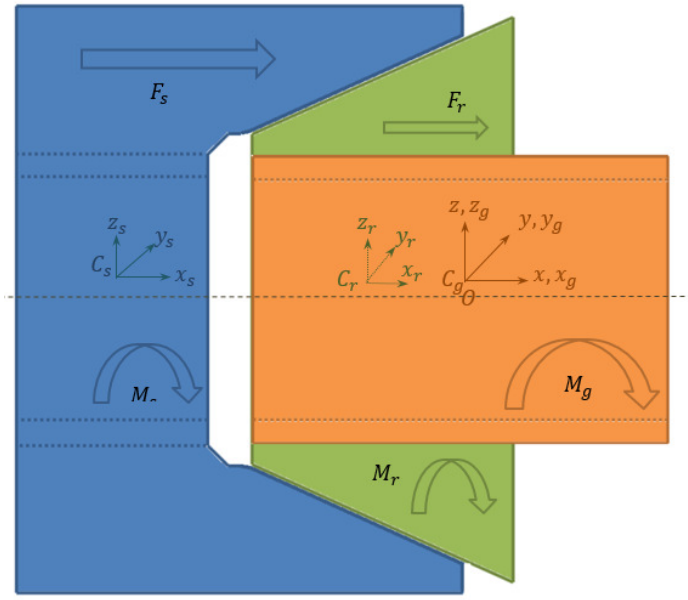

Figure 4: Synchronizer.

Letting $O(x, y, z)$ be the inertial reference frame and $C_g(x_g, y_g, z_g)$, $C_r(x_r, y_r, z_r)$ and $C_s(x_s, y_s, z_s)$ are the body fixed reference frames for RB_g, RB_r and RB_s with their origins at the centers of mass bodies, and

$$\left.\begin{aligned} \boldsymbol{q}_g &= [x_g, y_g, z_g, \theta_g, \psi_g, \varphi_g]^T \\ \boldsymbol{q}_r &= [x_r, y_r, z_r, \theta_r, \psi_r, \varphi_r]^T \\ \boldsymbol{q}_s &= [x_s, y_s, z_s, \theta_s, \psi_s, \varphi_s]^T \end{aligned}\right\} \tag{3.1}$$

are the vector of generalized coordinates of RB_g, RB_r and RB_s respectivley.

The sleeve RB_s is assumed to be ideally attached to the shaft such that it cannot translate or rotate perpendicular to the shaft, hence $[y_s, z_s, \emptyset_s, \varphi_s]^T = 0$. The ring RB_r will similarly constrained $[y_r, z_r, \emptyset_r, \varphi_r]^T = 0$. Finally, the gear RB_g is constrained in the same manner, but also fixed to the shaft hindering its axial motion such that $[x_g, y_g, z_g, \psi_g, \varphi_g]^T = 0$.

In summary, the vector of generalized coordinates of the considered MBS modelled the generic synchronizer is:

$$\begin{aligned} q_g &= [\,\theta_g] \\ \boldsymbol{q}_r &= [x_r, \theta_r]^T \\ \boldsymbol{q}_s &= [x_s, \theta_s]^T \end{aligned}$$

$$\boldsymbol{q} = \left[\boldsymbol{q}_s^T, \boldsymbol{q}_r^T, q_g\right]^T = \left[x_s, \theta_s, x_r, \theta_r, \theta_g\right]^T \tag{3.2}$$

The kinetic energy of the system is

$$T = T(\boldsymbol{q}, \dot{\boldsymbol{q}}) = \overbrace{\frac{1}{2}m_s\dot{x}_s^2 + \frac{1}{2}I_s\dot{\theta}_s^2}^{Sleeve} + \overbrace{\frac{1}{2}m_r\dot{x}_r^2 + \frac{1}{2}I_r\dot{\theta}_r^2}^{Synchronizer\ Ring} + \overbrace{\frac{1}{2}I_g\dot{\theta}_g^2}^{Gearwheel} \tag{3.3}$$

which can be written in matrix form as

$$T = \frac{1}{2}\begin{bmatrix}\dot{x}_s & \dot{\theta}_s & \dot{x}_r & \dot{\theta}_r & \dot{\theta}_g\end{bmatrix}\begin{bmatrix} m_s & 0 & 0 & 0 & 0 \\ 0 & I_s & 0 & 0 & 0 \\ 0 & 0 & m_r & 0 & 0 \\ 0 & 0 & 0 & I_r & 0 \\ 0 & 0 & 0 & 0 & I_g \end{bmatrix}\begin{bmatrix}\dot{x}_s \\ \dot{\theta}_s \\ \dot{x}_r \\ \dot{\theta}_r \\ \dot{\theta}_g\end{bmatrix} = \frac{1}{2}\dot{\boldsymbol{q}}^T\boldsymbol{M}\dot{\boldsymbol{q}} \tag{3.4}$$

The Lagrangian of the considered system in case of $U(\boldsymbol{q}_r) = 0$ will be

$$L = T(\boldsymbol{q}, \dot{\boldsymbol{q}}) - U(\boldsymbol{q}_r) = \frac{1}{2}\dot{\boldsymbol{q}}^T\boldsymbol{M}\dot{\boldsymbol{q}} \tag{3.5}$$

Next, $\boldsymbol{Q}^A$ is the vector of generalized forces due to non-conservative applied loads corresponding to generalized coordinate $\boldsymbol{q}$. Three contributions to $\boldsymbol{Q}^A$ are considered here, external applied force, friction and from splashing of the oil in the gearbox. A simple assumption is made here assuming that the losses are proportional to the rotational velocities, i.e. a Rayleigh type loss, which gives

$$\boldsymbol{Q}^A = \left[F_s, M_s, F_r, M_r, M_g\right]^T + \left[F_s, M_s, F_r, M_r, M_g\right]_{fric}^T + \left[F_s, M_s, F_r, M_r, M_g\right]_{oil,splash}^T \tag{3.6}$$

We consider the following dissipation function

$$R(\dot{\boldsymbol{q}}) = R_{splash}(\dot{\boldsymbol{q}}) + R_{fric}(\dot{\boldsymbol{q}}) \tag{3.7}$$

where

$$R_{splash}(\dot{\boldsymbol{q}}) = \frac{1}{2}\dot{\boldsymbol{q}}^T\boldsymbol{C}\dot{\boldsymbol{q}}, \ = \begin{bmatrix} 0 & 0 & 0 & 0 & 0 \\ 0 & C_s & 0 & 0 & 0 \\ 0 & 0 & 0 & 0 & 0 \\ 0 & 0 & 0 & C_r & 0 \\ 0 & 0 & 0 & 0 & C_g \end{bmatrix}$$

is a classical Rayleigh loss function, assuming that the rotation of sleeve, ring and gear give rise to a power loss proportional to the square of the each part. $R_{fric}(\dot{\boldsymbol{q}})$ is the dissipated function due to frictional sliding between the surfaces of two solid bodies. For each contact i, we have the contribution

$$N_i\mu_i|v_i|$$

where N_i is the normal force between the bodies, v_i is the sliding (relative tangential) velocity and μ_i is friction constant (a topic for future study is to consider how μ_i depends on e.g. v_i and N_i). There is also friction associated with the axial sliding of sleeve and synchronizer ring, giving the contribution $C_{s\alpha}|\dot{x}_s| + C_{r\beta}|\dot{x}_r|$ to the dissipation function. In summary, we consider the following frictional part of dissipation function

$$R_{fric} = N_{cone}\,\mu_\alpha\,\left|\dot{\theta}_s - \dot{\theta}_r\right| r_c + N_{cham}\,\mu_\beta\,|v_{cham}| + N_{eng}\mu_{eng}\left|v_{eng}\right| + C_{s\alpha}|\dot{x}_s| + C_{r\beta}|\dot{x}_r|$$

where N_{cone}, N_{cham}, N_{eng} are the contacting forces at cones, chamfers and engagement teeth, respectively, which are determined from its respective Lagrangian multiplier. The relative velocities v_{cham} and v_{eng} depend on the direction of contacting surfaces which change with the different phases of synchronization.

The system is assumed to be subject to a number of holonomic kinematic constraints. To distinguish between constraints associated with the arised motion of the system due to interaction between bodies, we split the constraint vector $\boldsymbol{\Phi}$ as

$$\boldsymbol{\Phi} = \begin{bmatrix} \boldsymbol{\Phi}^{external} \\ \boldsymbol{\Phi}^{internal} \end{bmatrix} = \mathbf{0} \tag{3.8}$$

where $\boldsymbol{\Phi}^{internal}$ will be defined for the different phases below.

The synchronizer motion can be imposed in different ways, either the sleeve motion is prescribed as $x_s = x_s^{pres}(t)$ which leads to the sleeve applied force is solved from Lagrangian multiplier. In this case, we have the constraint $\boldsymbol{\Phi}^{external} = x_s - x_s^{pres}(t) = 0$ and $F_s = 0$. Alternatively, the sleeve force is applied as given function $F_s = F_s^{pres}(t)$.

We may also consider the case that the force depends on the position of the sleeve for instance that $F_s = a\left(x_s - x_s^{pres}(t)\right)$, in which case we have no term in $\boldsymbol{\Phi}^{external}$ related to sleeve translation.

In the same manner, the angle θ_s can be described by the output shaft speed or the torque $T_s = T_s^{pres}(t)$. In the torque case $\theta_s = \omega_s t$ corresponds to constant vehicle speed during the synchronizing. Alternatively $T_s = k(\theta_s - \omega_s t)$ allows studying torsion vibration accounting fluctuations in the output shaft.

3.2 Models of Different Phases for the Generic Synchronizer

In the process of synchronization during gear shift, different parts interact with each other to assure the engagement or disengagement without clashing of the teeth. We consider four main phases; Pre-synchronization, Main synchronization, Blocker transition and Engagement as shown in Figure 5. These main phases are further divided in sub-phases, which are depicted in Figure 6. In this study division of the synchronization is not only based on relative position of the parts but also on interaction of the parts to capture the forces arising during synchronization. Although in real applications some phases overlap, these are restricted to follow the prescribed sequence. Each phase will be described in detail below.

In the following description of phases, the sleeve is taken as master and the gearwheel as slave. A downshift case is studied where the sleeve (master) has to increase the low rotational speed of the gearwheel (slave).

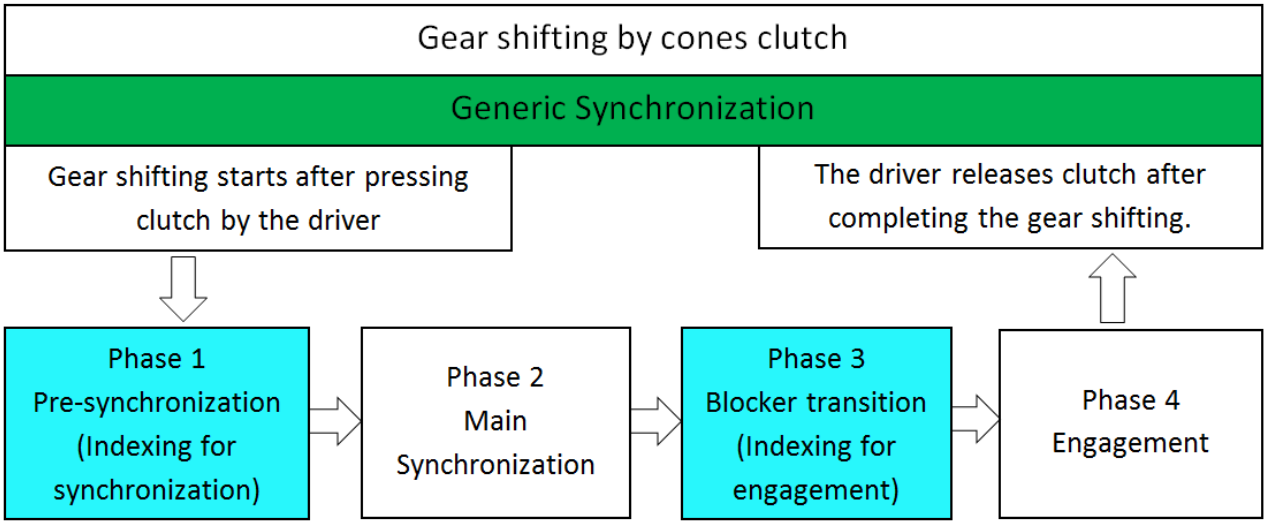

Figure 5: Division of the generic synchronization into phase events.

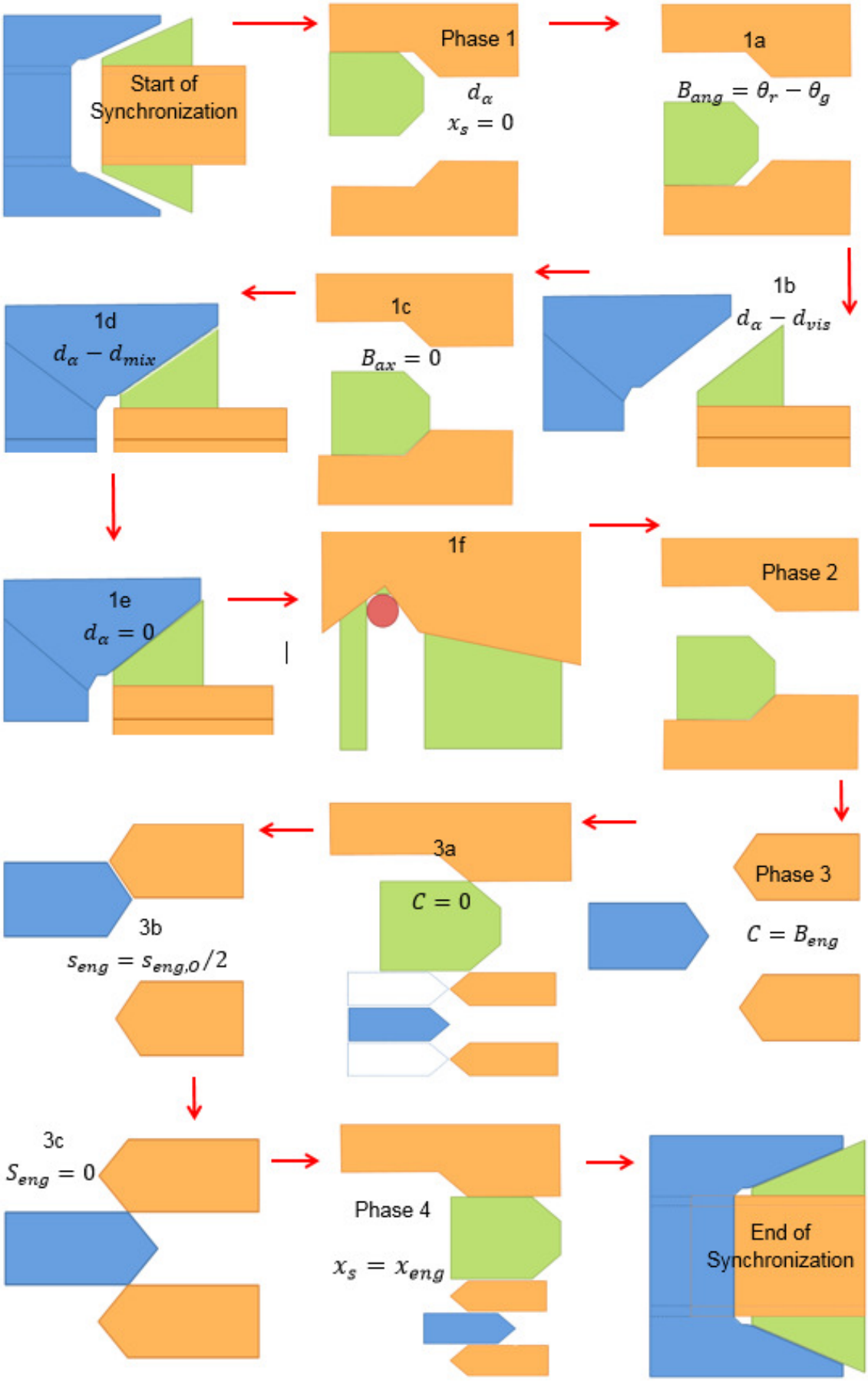

Figure 6: Division of synchronization in different phase events.

3.2.1 Phase 1-Pre-synchronization

Phase 1 has the purpose of indexing, i.e. move the synchronizer ring chamfer in contact of the gearwheel chamfer. The phase 1 starts from neutral position and ends where the axial force overcomes the axial resistance of the detent after contact of the blocker ring's chamfer with the gear's chamfer. It is assumed during the phase 1 that first the blocker ring gets indexed position and second the oil film squeezes out.

The nominal order of events concerning the ring relative movement is that first the ring spline comes in contact with gearwheel spline (angular indexing) and secondly chamfers of the ring and the gear come in contact (axial indexing).

Here phase 1 is further divided in different sub-phases based on the relative movement of the sleeve, the blocker ring and the gearwheel and varying oil film thickness to identify the viscous, mixed and solid friction. The phase 1 is divided into 1a, 1b, 1c, 1d, 1e and 1f.

The axial clearance between the cones at neutral is assumed to be d_α mm whereas the viscous friction will start from d_{vis}, the mixed friction will start from d_{min} and after the dry friction will start. d_{min} depends on surfaces roughness as

$$d_{min} = c_n\sqrt{R_{ss} + R_{rr}}/\sin(\alpha)$$

where d_{min} is normal distance between the cones when mixed friction will start, R_{ss} and R_{rr} are surface roughness of the sleeve and the blocker ring respectively, and c_n is a constant according to a lubricant theory [8].

Before the end of phase 1, if the sleeve force is higher than the force needed to flush out the oil between the cones, mixed surface contact is considered otherwise the cones must have mixed surface contact in start of the phase 2. In the case where the cones still have oil contact at start of the phase 2 and the oil flush out force is higher than the spring force (including the axial resistance offered by the blocker ring angle), there is a risk that the synchronizer ring chamfer will slip over the gear chamfer while speed difference between the sleeve and the gear does not decrease to desired level. In that case the ring and the sleeve together will continue to move axially and engaging teeth of the sleeve will strike with engaging teeth of the gear resulting in clashing.

The same kind of uncomfort shifting can be the result of higher axial speed of the sleeve than rotational speed of the gear and the shift force is higher than the spring force, because there will be no any event of phase 1a and the sleeve will pass quickly through the phases 1b-3 by flushing out the oil and the engaging teeth will strike with each other. There is a spring ring in the detent which is in contact with the gear and the blocker ring to control the sleeve axial speed relative to the gear rotational speed. Axial dimension of the blocker ring and the axial clearance between the blocker ring and the spring will control length of contact between the chamfers. Effect of varying oil flush out force and varying the detent angle with spring stiffness on the synchronization will also be analyzed through the CLF model.

According to starting and ending points of different events of the phase 1, the axial clearance between the ring slot and the spring must be zero before the viscous friction starts to decrease the speed difference.

Oil viscosity and density vary during the synchronization. The viscous and mixed friction models considered in the synchronizer model only takes into account the varying oil viscosity ρ with respect to the temperature T [8].

$$\rho(T) = 0.035989 \times 10^{-0.01554.T}$$

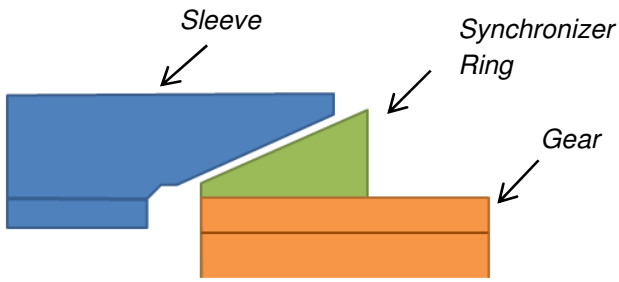

Figure 7: The synchronizer at neutral position.

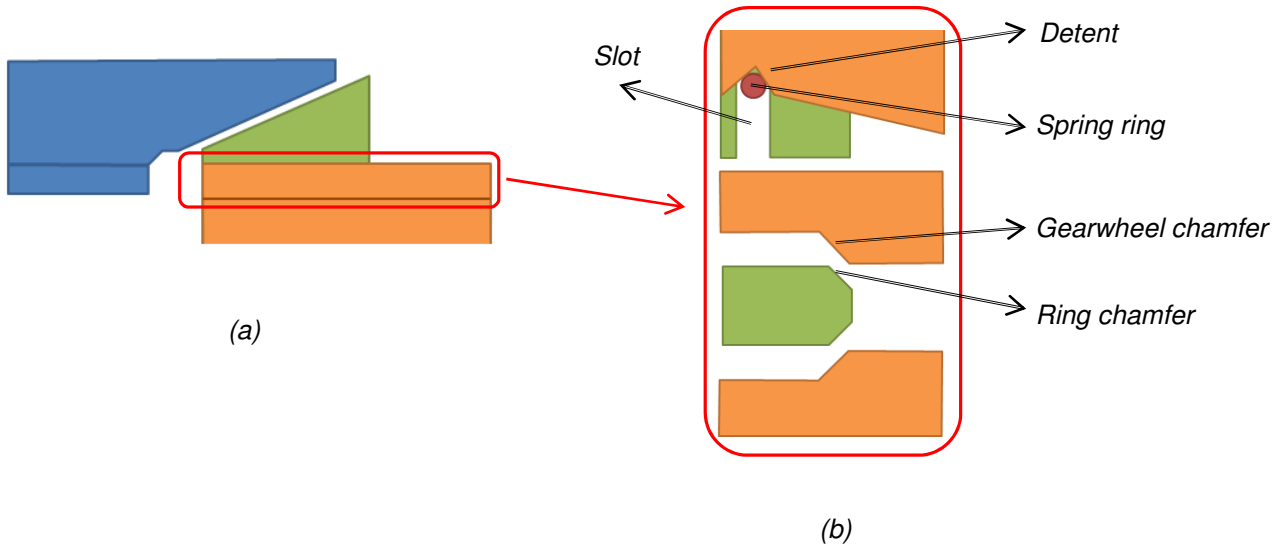

Figure 8: Position of detent, spring, slot, gear chamfer, ring chamfer before synchronization.

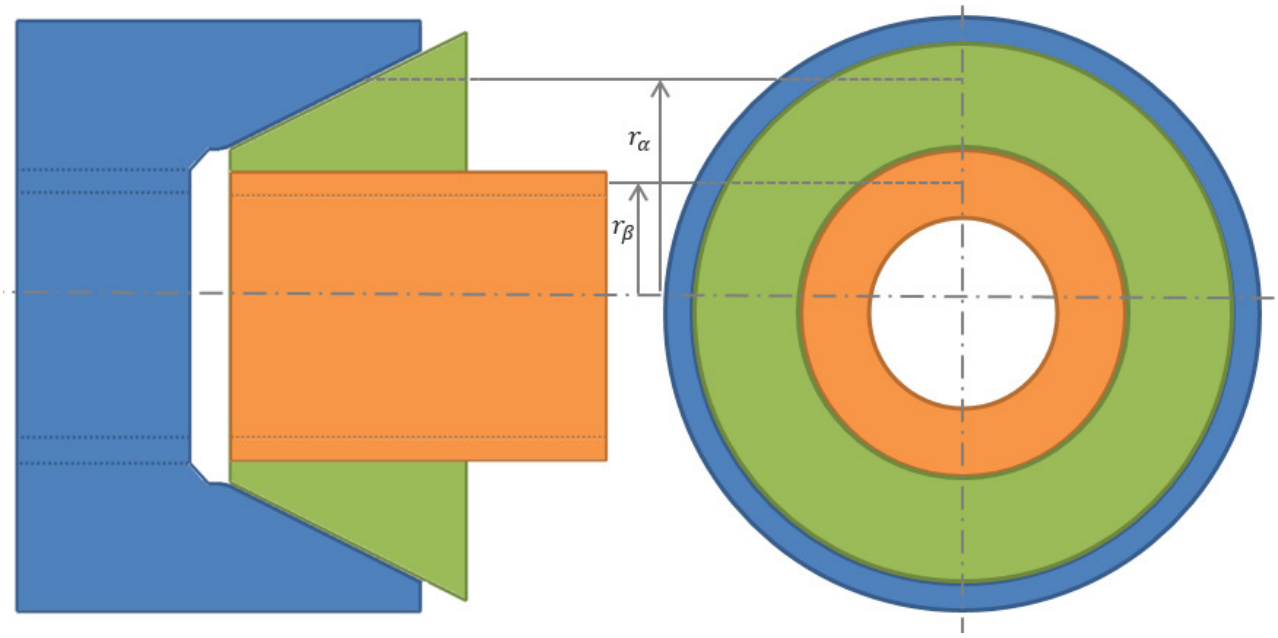

Figure 9: Synchronizer.

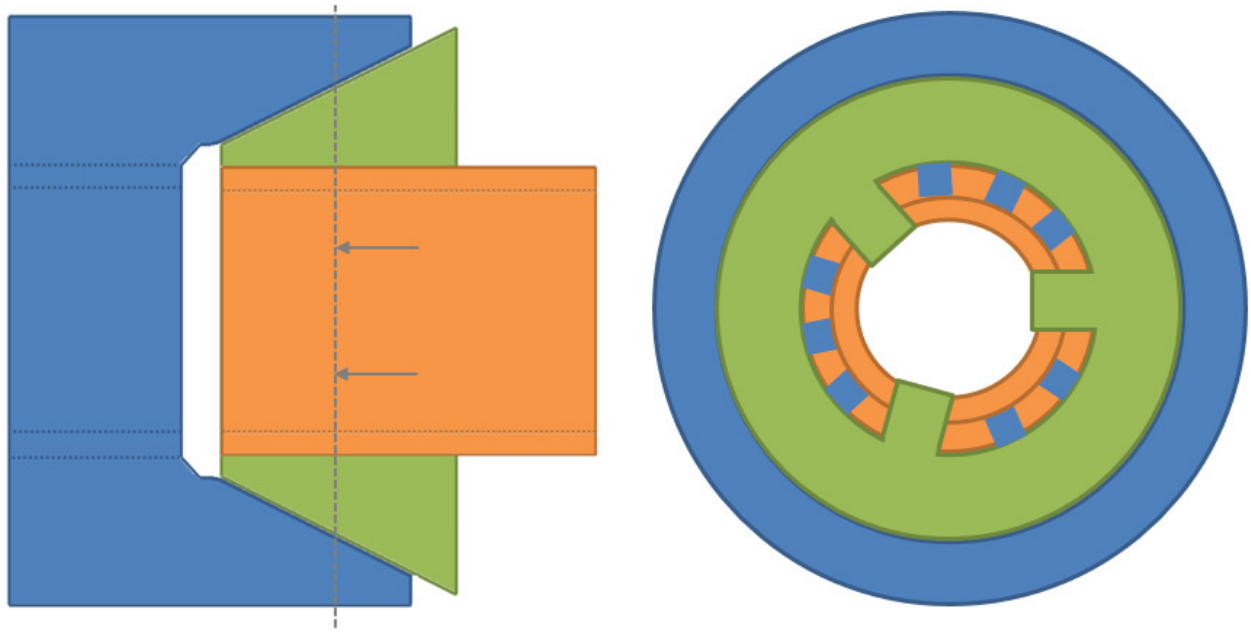

Figure 10: A cut view of Synchronizer.

In Figure 9 and Figure 10 r_α is the pitch radius of sleeve cone, and r_β is the pitch radius of ring cone, $F_{sh} = F_s$ is applied shift force.

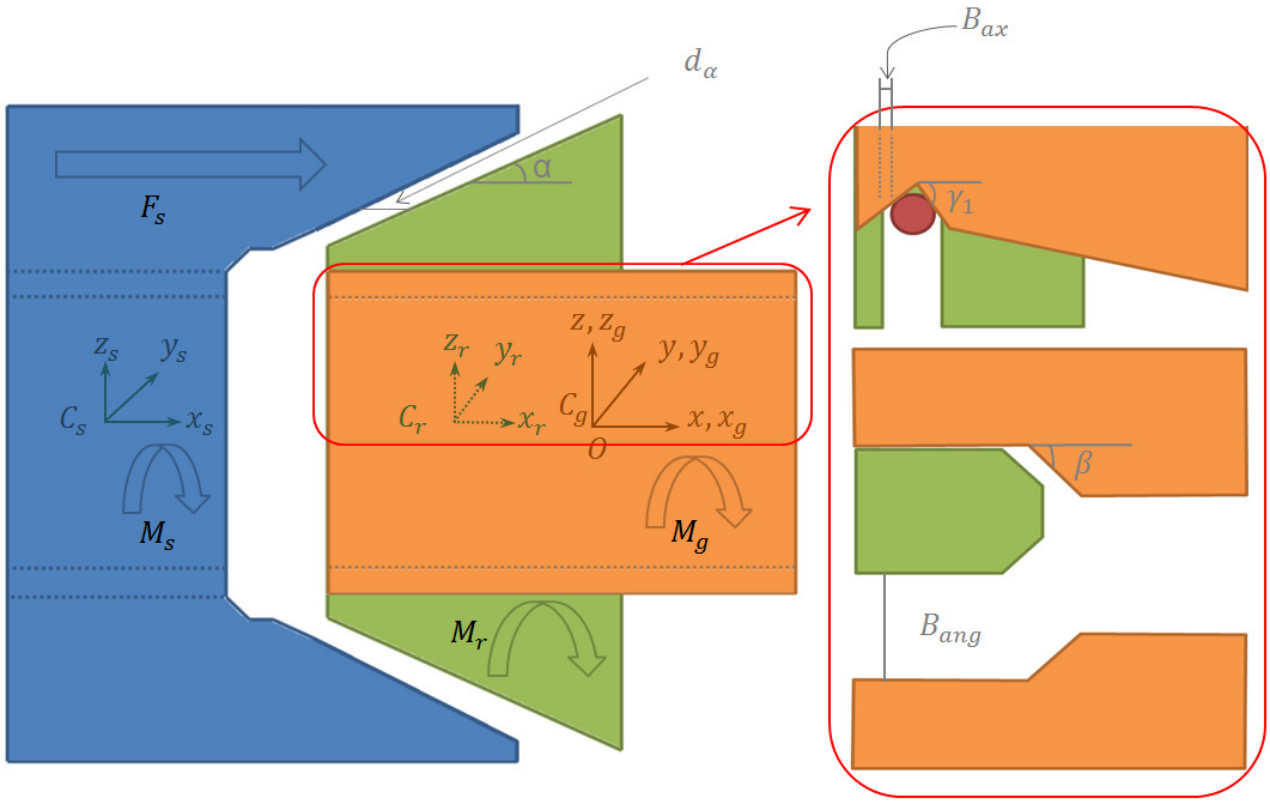

Figure 11: Neutral position at start of the phase 1a.

3.2.1.1 Phase 1a-Angular indexing of the ring

Because both the ring and the gear are subjected to oil splash losses, in this down shift case at neutral position, splines of the ring and the gear will be in contact at top as shown in *Figure 12*. At start of the phase 1a torque transfers from the sleeve to the ring through oil film and the ring will get angular rotation. After a while splines of the ring and the gear will come in contact at bottom as shown in *Figure 13* at end of the phase 1a.

In some conventional synchronizers an axial push is transferred from the sleeve to the detent and from the detent to the blocker ring. Because of the oil friction between the cones the blocker ring get relative movement and the splines of the gear and the blocker ring come in contact. But in the generic synchronizer in this study it is considered that the blocker ring will get relative rotation to gear because of the oil friction between the cones.

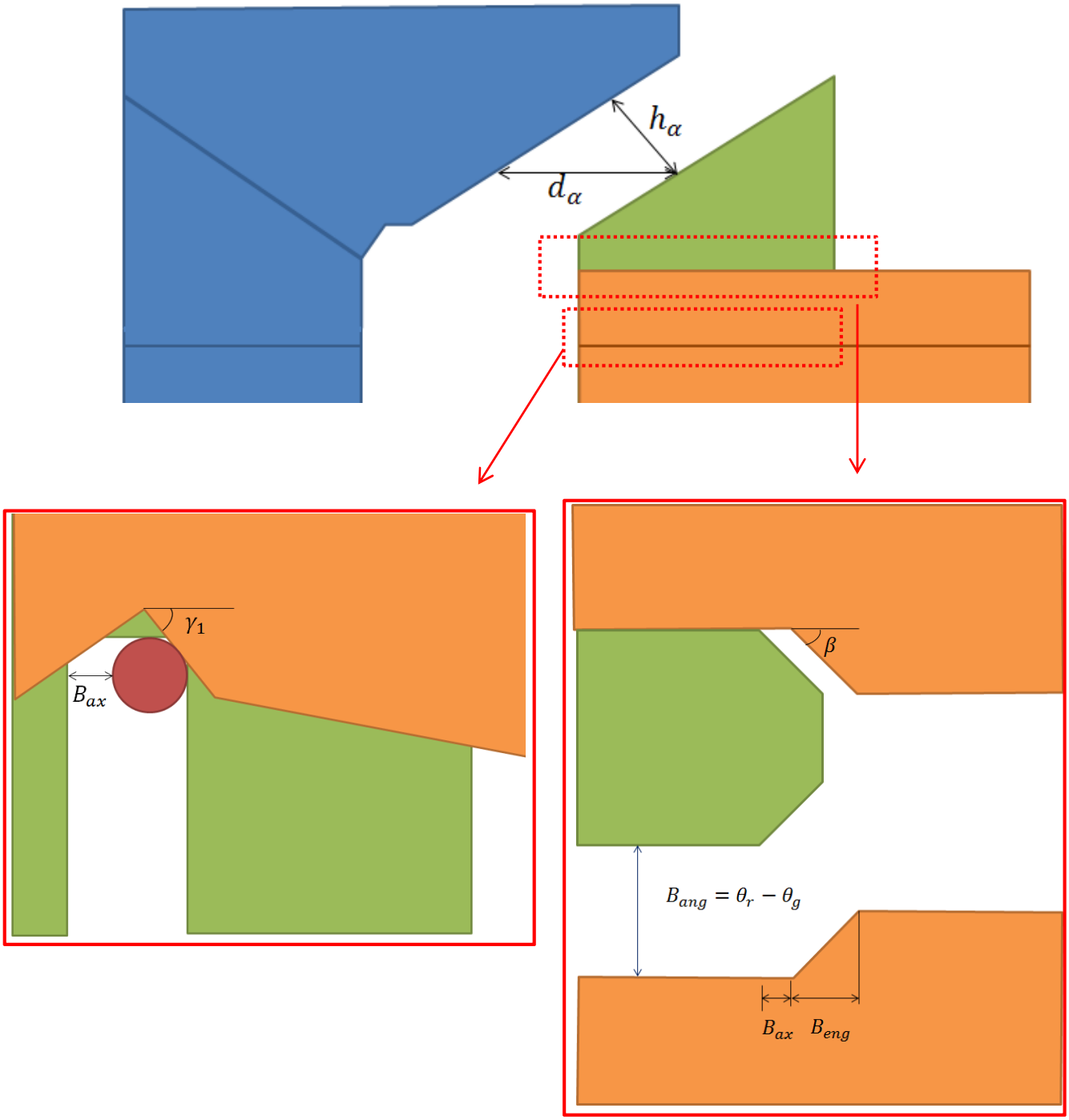

Figure 12: Neutral position at start of the phase 1a.

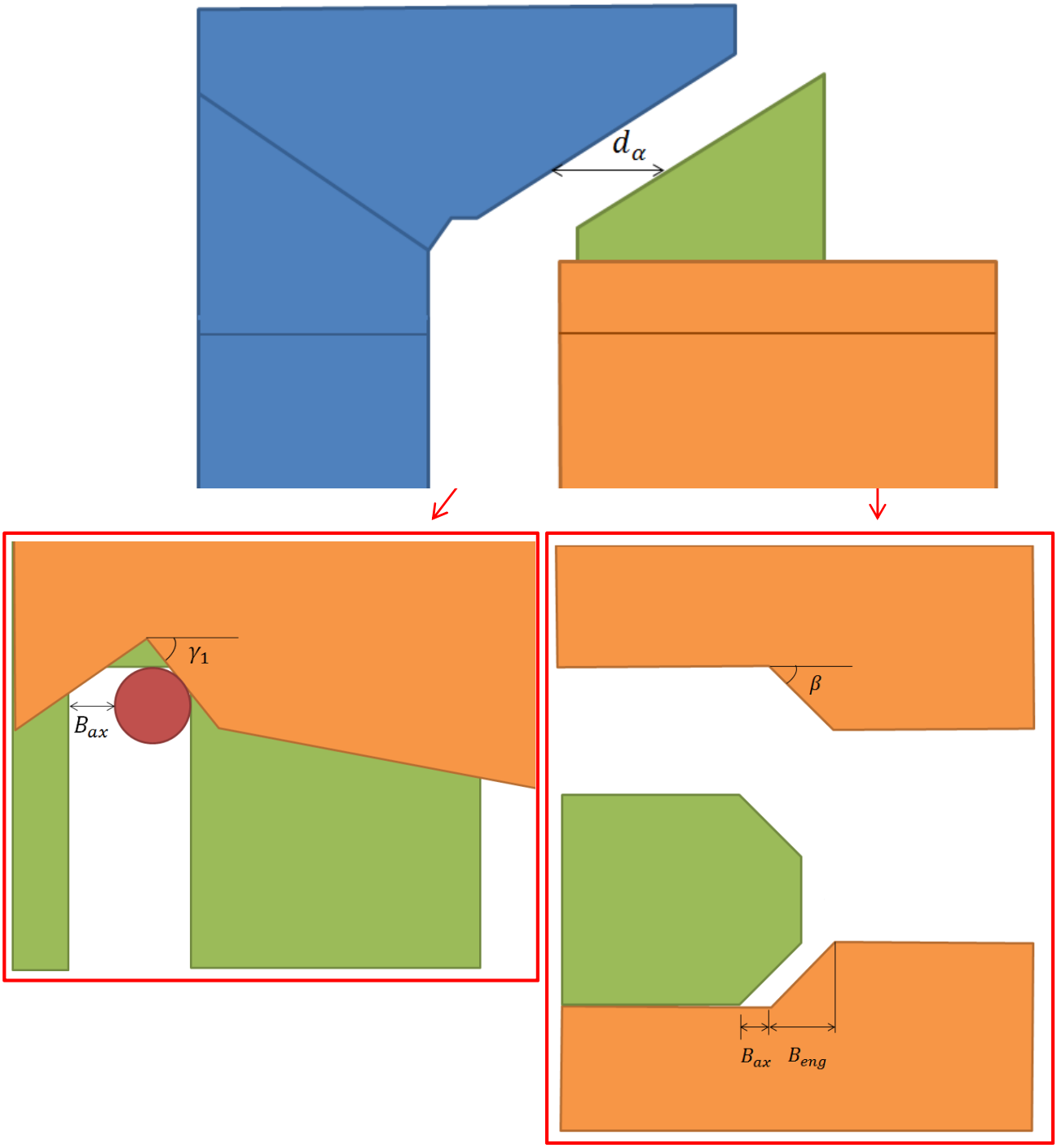

Figure 13: End position of the phase 1a.

3.2.1.2 Phase 1a-Equations

During phase 1a the splines of the gear and the blocker ring should come in contact on the side to ready for blocking the sleeve, which is called angular indexing of the ring.

For development of the model it is assumed that the spring ring sliding friction is such that axial displacement of the ring will be zero during phase 1a.

The set of active internal constraints for the phase 1a is

$$\boldsymbol{\Phi}(\boldsymbol{q},t)^{internal} = [x_r] = [0] \tag{3.9}$$

At start of the phase 1a, $x_{s_0} = \theta_{s_0} = \theta_{r_0} = \theta_{g_0} = 0$ and $x_r = 0$. It is assumed that $B_{ang} = 5^o$.

$$d_\alpha(t=0) = d_o = 2mm$$

The resulting applied forces are

$$\boldsymbol{Q}^A = \begin{bmatrix} F_s + F_{sq} + C_{s\alpha}\, sign(\dot{x}_s) \\ T_{sq} + C_s\dot{\theta}_s \\ -F_{sq} \\ -T_{sq} + C_r\,\dot{\theta}_r \\ C_g\;\dot{\theta}_g \end{bmatrix} \tag{3.10}$$

where F_{sq} and T_{sq} are viscous force and viscous torque transfered in cones until condition of mixed friction (phase 1e below). The expression for force and torque are derived in [8] from Reynold's equation.

$$\begin{aligned} F_{sq} &= K_{NC}\, 16\pi\rho\dot{d}_\alpha \sin(\alpha)\; r_c\left(\frac{b}{h_\alpha}\right)^3 \\ T_{sq} &= 4\pi\rho\dot{d}_\alpha r_c^3\;\dot{\theta}_s\frac{b}{h}\left(1-\frac{\dot{\theta}_r}{\dot{\theta}_s}\right) \end{aligned} \tag{3.11}$$

In case the cone surfaces have grooves, $K_{NC} = 0.1$ is suggested by [8].

3.2.2.1 Phase 1b-free flight

Phase 1b starts with axial movement of the sleeve and oil film thickness decreases. The phase 1b ends when viscous friction must be taken into account at particular oil film thickness. In this case it is considered the viscous friction will start to act at h_{vis} oil film thickness.

3.2.2.2 Phase 1b-Equations

Since angular indexing is complete, the gear and the ring will rotate together. During the phase 1b, torque transferred by cones is small but at least higher than the oil splashing losses to keep the splines in contact. The cone clearance decreases to 1mm.

It is assumed that $d_{vis} = 1\text{mm}$. The set of active constraint for the phase 1b is

$$\boldsymbol{\Phi}(\boldsymbol{q},\boldsymbol{t})^{internal} = \begin{bmatrix} x_r \\ \theta_r - \theta_g - B_{ang} \end{bmatrix} = \mathbf{0} \tag{3.12}$$

The resulting applied forces are

$$\boldsymbol{Q}^A = \begin{bmatrix} F_s + F_{sq} + C_{s\alpha}\, sign(\dot{x}_s) \\ T_{sq} + C_s\dot{\theta}_s \\ -F_{sq} \\ -T_{sq} + C_r\,\dot{\theta}_r \\ C_g\;\dot{\theta}_g \end{bmatrix} \tag{3.13}$$

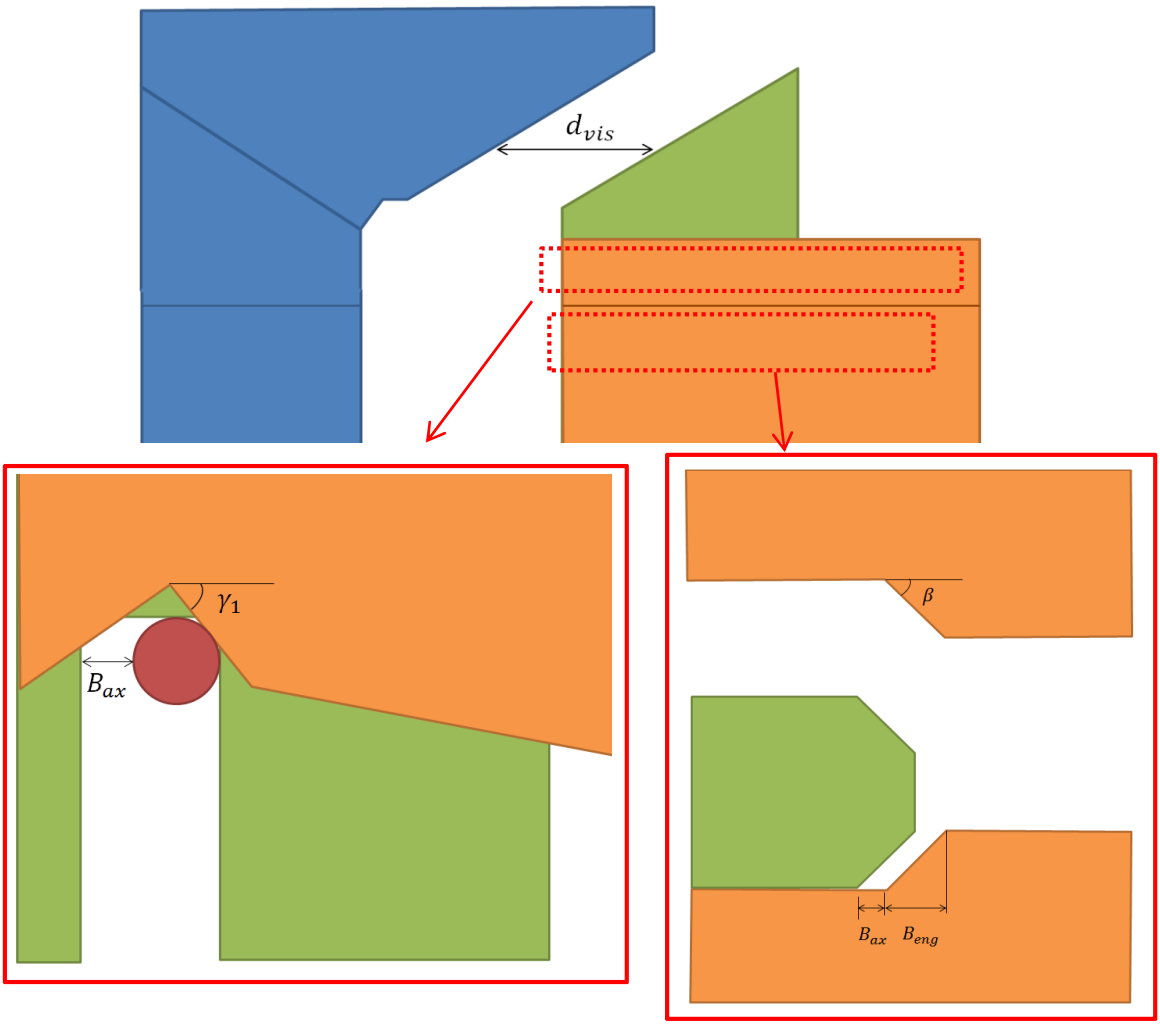

Figure 14: End position of the phase 1b.

3.2.3.1 Phase 1c-Axial indexing of the ring

When the axial clearance between the cones reaches at d_{vis}, the viscous friction starts to transfer higher torque and the force required to flush out the oil is much greater than the force needed to slide the ring axially to cover B_{ax}. During phase 1c, it is assumed that oil thickness will not decrease while the sleeve and the ring will move axially together with d_{vis} oil thickness until chamfers will come in contact and at the same time the ring and the spring will also come in contact because it is also assumed that after the phase 1a, the two clearances; between the ring slot and the spring and between the ring and the gear, will be same in axial dimension.

3.2.3.2 Phase 1c-Equations

The sleeve and the ring will move axially with same and constant axial speed. The gear and the ring will rotate with same rotational speed during the phase 1c. It is assumed that $B_{ax} = 1\ \mathrm{mm}$.

The set of active constraint for the phase 1c is

$$\boldsymbol{\Phi}(\boldsymbol{q}, t)^{internal} = \begin{bmatrix} x_s - x_r - d_{vis} \\ \theta_r - \theta_g - B_{ang} \end{bmatrix} = \mathbf{0} \tag{3.14}$$

The applied forces are

$$\boldsymbol{Q}^A = \begin{bmatrix} F_s + F_{sq} + C_{s\alpha}\, sign(\dot{x}_s) \\ T_{sq} + C_s \dot{\theta}_s \\ -F_{sq} \\ -T_{sq} + C_r\, \dot{\theta}_r \\ C_g\ \dot{\theta}_g \end{bmatrix} \tag{3.15}$$

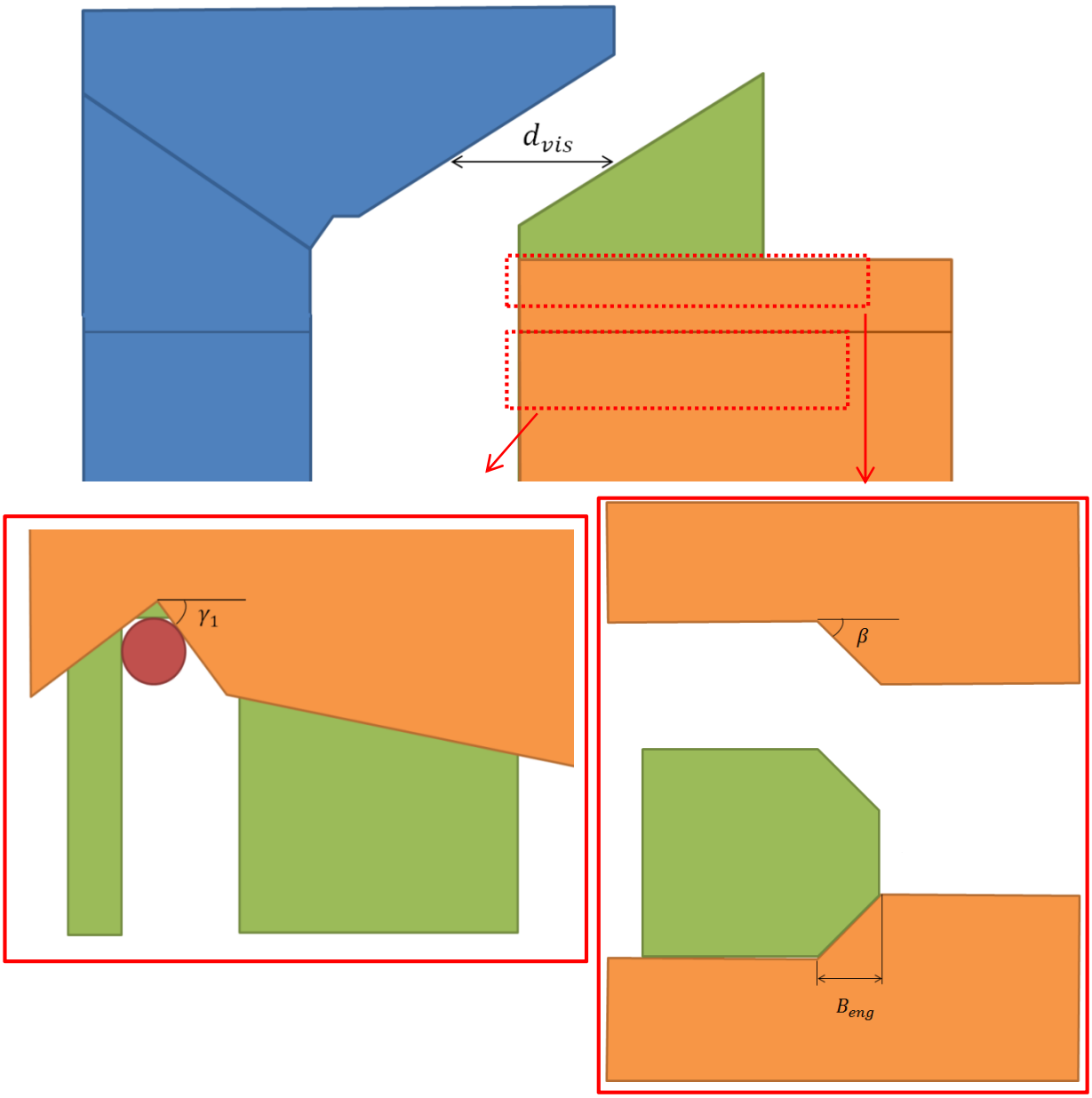

Figure 15: End position of the phase 1c.

3.2.4.1 Phase 1d-Viscous friction

From start of the phase 1d an increment in the shift force is required to break the oil film. The ring is blocked to move axially by the chamfers and the spring detent. At end of the phase 1d the viscous friction will transfer to mixed friction. The surface roughnesses of the cones is assumed such that $d_{min} = 0.1\mathrm{mm}$.

3.2.4.2 Phase 1d-Equations

The sleeve will move also when force is prescribed while the ring will not move axially further because of the chamfers blocking contact and the spring detent contact. The gearwheel and the ring will rotate with same rotational speed which is affected by the viscous friction torque.

The set of active constraint for the phase 1d is

$$\boldsymbol{\Phi}(\boldsymbol{q},t)^{internal} = \begin{bmatrix} x_r - B_{ax,N} \\ \theta_r - \theta_g - B_{ang} \end{bmatrix} = \mathbf{0} \tag{3.16}$$

The applied forces are

$$\boldsymbol{Q}^A = \begin{bmatrix} F_s + F_{sq} + C_{s\alpha}\, sign(\dot{x}_s) \\ T_{sq} + C_s\dot{\theta}_s \\ -F_{sq} \\ -T_{sq} + C_r\,\dot{\theta}_r \\ C_g\;\dot{\theta}_g \end{bmatrix} \tag{3.17}$$

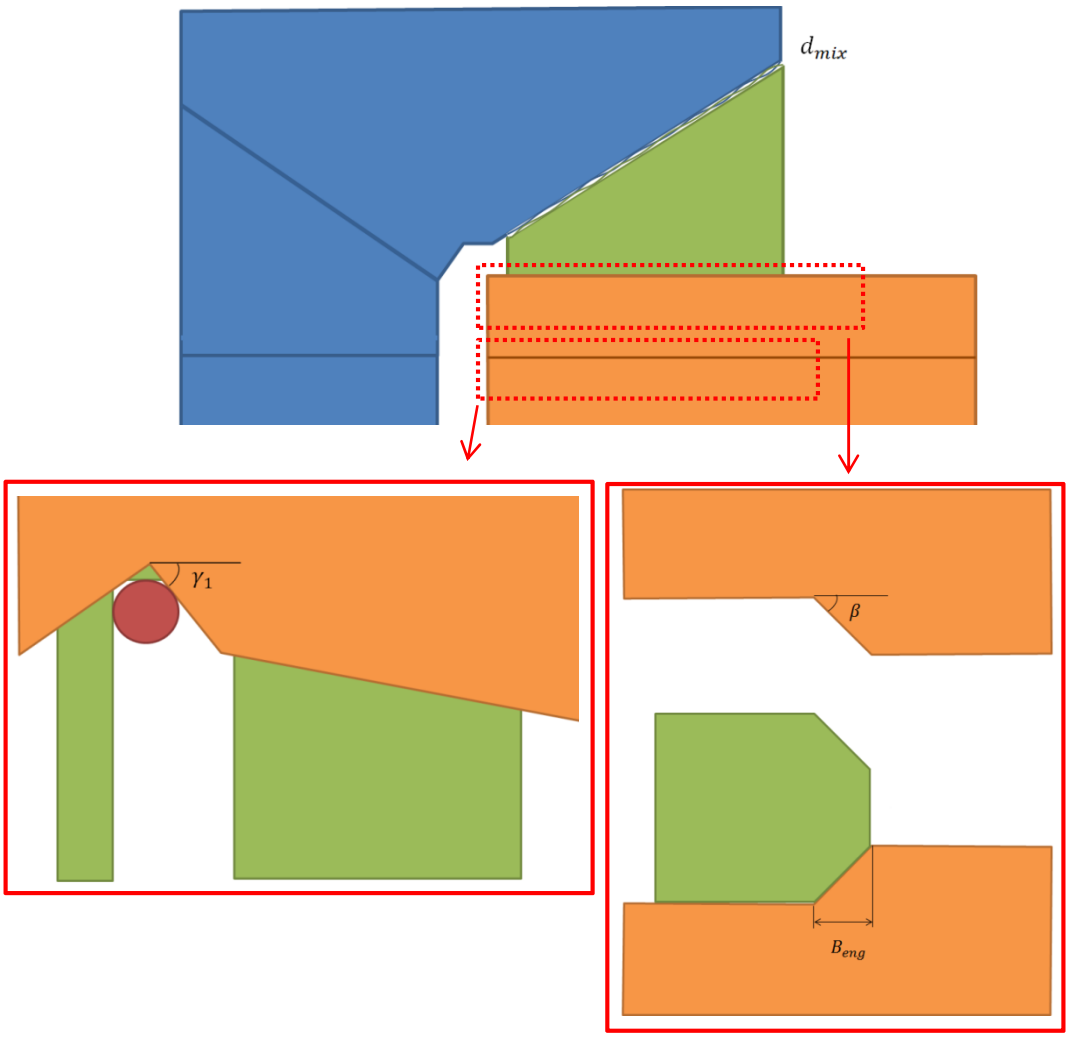

Figure 16: End position of the phase 1d.

3.2.5.1 Phase 1e-Mixed friction

When the oil is flushed out and the cones are near to come in contact mixed friction is present which is considered as phase 1e.

In reality the phase 1e and the phase 1f will be simultaneously but in this model two phases are divided into two events after each other to capture clearly the effect of the mixed friction and the spring detent force on the shift force. The division of the two phases will not affect the overall timing of the synchronization because the time duration of the shift force to overcome the double resistance at the same time will be equal to the time duration of the shift force to overcome the each resistance after one another.

Phase 1e ends when the mixed friction is replaced by dry (boundary) friction.

3.2.5.2 Phase 1e-Equations

Based on [8], the following relations are used for mixed friction phase

$$F_c = \left(\frac{F_{dry} - F_{sq}}{t_{dry} - t_{vis}}\right)(t - t_{vis}) \qquad (3.18)$$
$$T_c = \eta_1 F_c + \eta_2 + \eta_3 \omega_r$$

where $\eta_i = \lambda_{cons}\, \chi_{\,i}$, $\lambda_{cons} = \frac{r_c}{\sin(\alpha)}\left(1 + \frac{1}{3}\left(\frac{b}{r_c}\right)^2 \sin^2(\alpha)\right)$ and F_{sq} is at end of phase 1d.

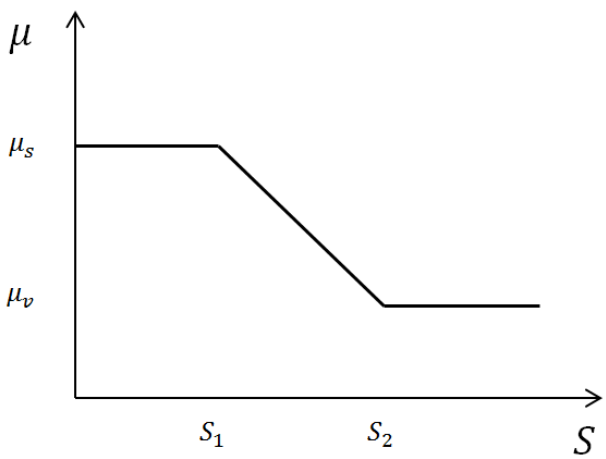

Figure 17: Stribeck diagram in case of linear mixed friction.

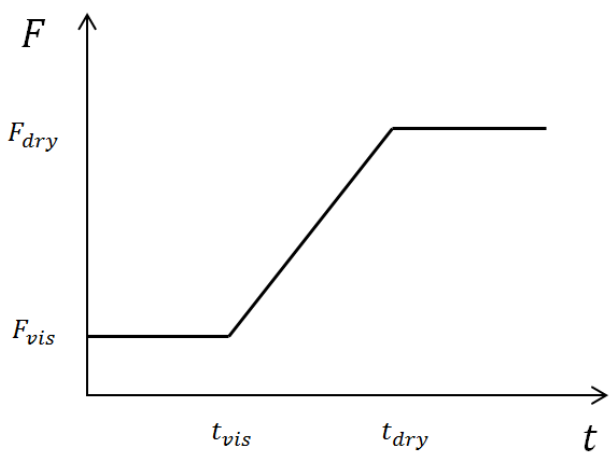

Figure 18: Linear increment of force from viscous friction to solid friction [8].

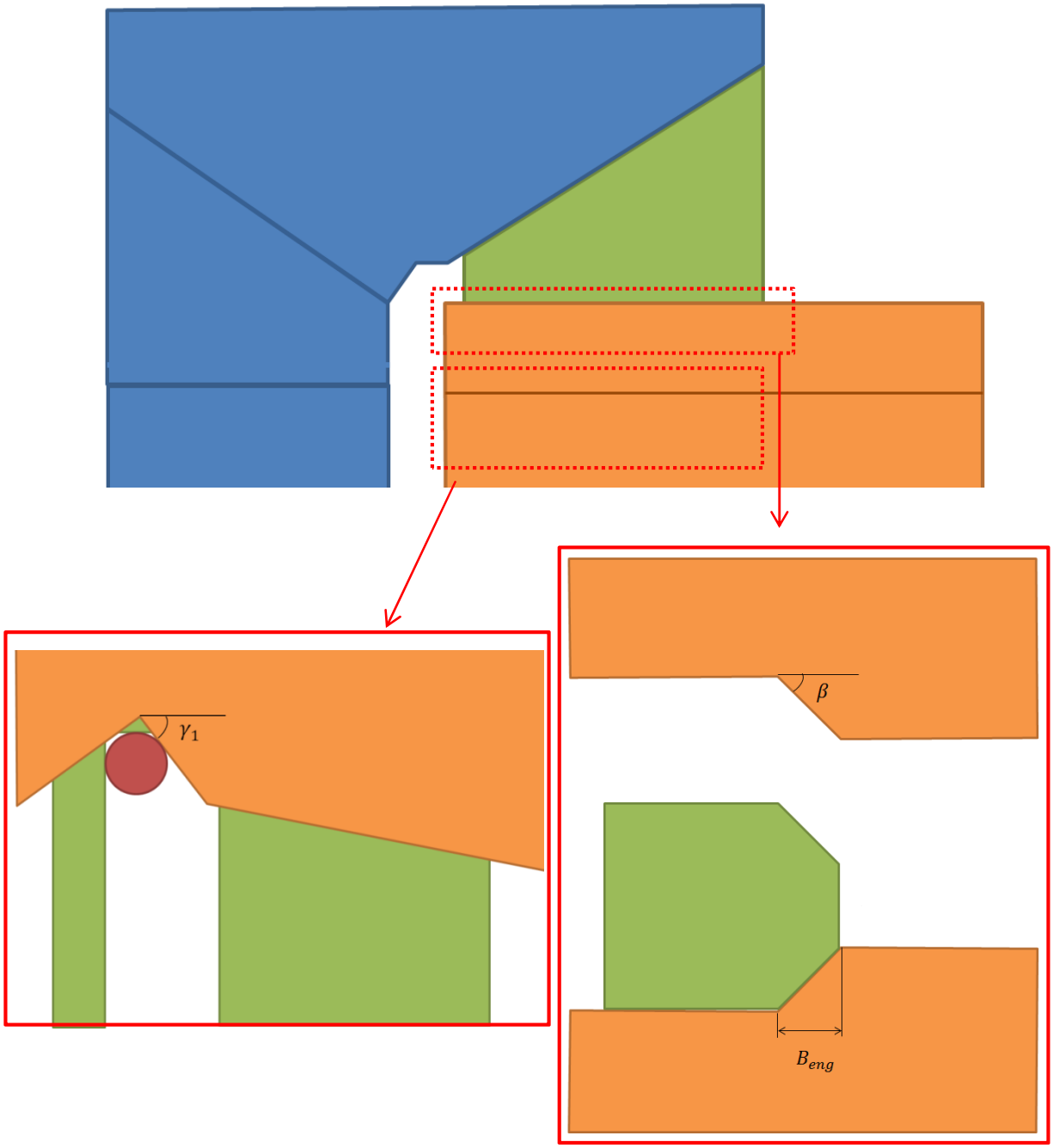

Figure 19: End position of the phase 1e.

The set of active constraint for the phase 1e is

$$\boldsymbol{\Phi}(\boldsymbol{q},t)^{internal} = \begin{bmatrix} x_r - B_{ax,N} \\ \theta_r - \theta_g - B_{ang} \end{bmatrix} = \mathbf{0} \tag{3.19}$$

The applied forces are

$$\boldsymbol{Q}^A = \begin{bmatrix} F_s + F_c + C_{s\alpha}\, sign(\dot{x}_s) \\ T_c + C_s\dot{\theta}_s \\ -F_c \\ -T_c + C_r\, \dot{\theta}_r \\ C_g\ \ \dot{\theta}_g \end{bmatrix} \tag{3.20}$$

3.2.6.1 Phase 1f-Force buildup

In the case with assumption of the synchronization model, amount of the shift force at start of the phase 1f can shift the mixed friction to the solid friction but it cannot further build up the pressure between the cones until the amount of shift force further exceeds the detent axial resistance together with spring stiffness. Because of division into phase 1e and phase 1f, the cone torque T_c is here omitted to not give extra acceleration of gearwheel.

As the spring force is less than the maximum acceptable shift force for synchronization, the shift force will first be resisted by the detent resistance during the present phase, before increasing the cone pressure and then the shift force will decrease the rpm rapidly in next phase. When the shift force becomes equal to the spring force F_{spr} the phase 1f will end.

3.2.6.2 Phase 1f-Equations

(3.21)

The set of active constraint for the phase 1f is

$$\boldsymbol{\Phi}(\boldsymbol{q}, t)^{internal} = \begin{bmatrix} x_r - x_s - d_\alpha \\ \theta_r - \theta_g - B_{ang} \\ x_r \end{bmatrix} = \boldsymbol{0} \tag{3.22}$$

The applied forces are

$$\boldsymbol{Q}^A = \begin{bmatrix} F_s + C_{s\alpha}\, sign(\dot{x}_s) \\ C_s\dot{\theta}_s \\ -F_{spr} \\ C_r\, \dot{\theta}_r \\ C_g\ \ \dot{\theta}_g \end{bmatrix} \tag{3.23}$$

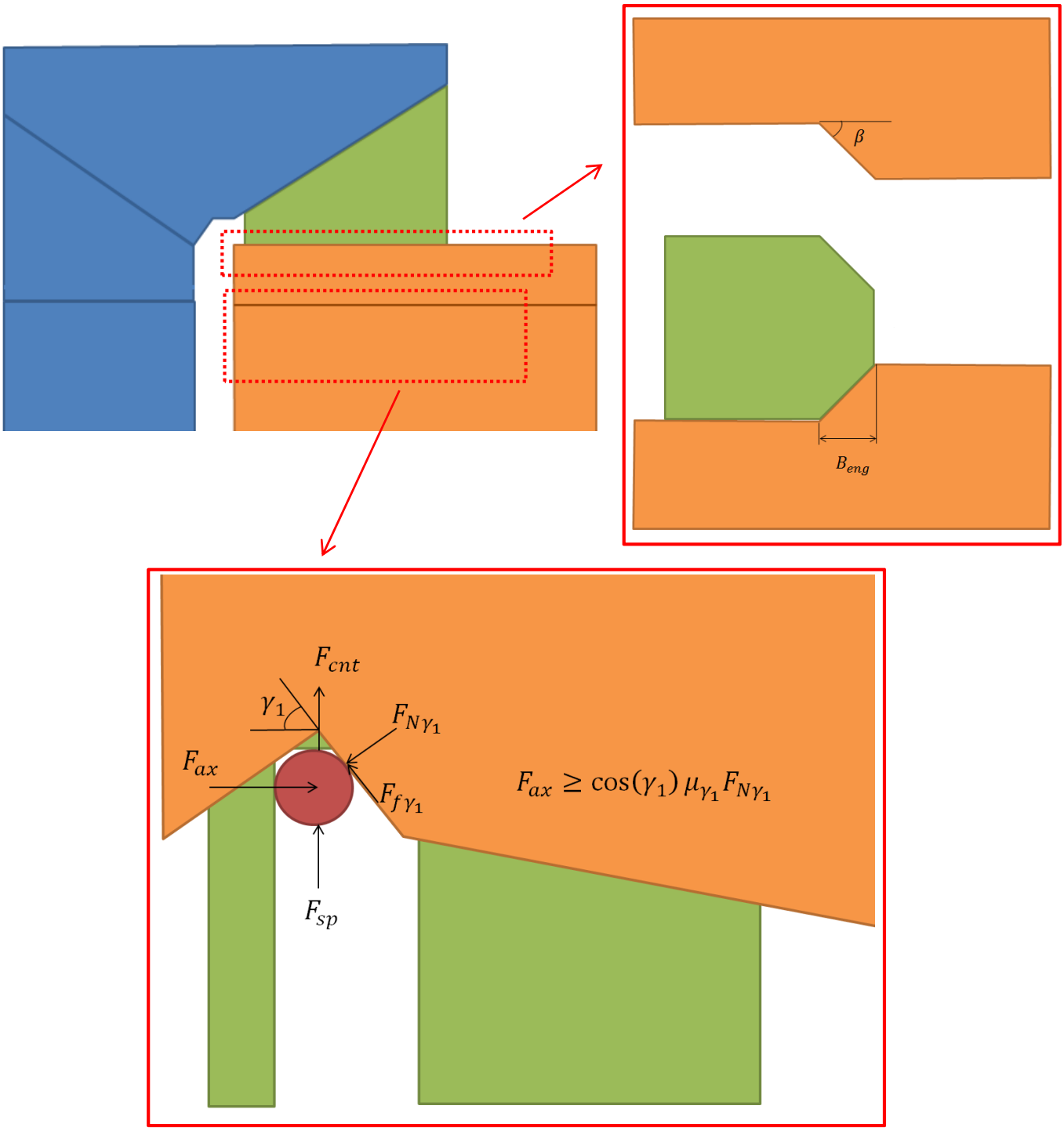

Figure 20: End position of the phase 1f.

3.2.7 Phase 2- Main synchronization

During main synchronization there is dry friction between cones. The shift force increases while there is no axial movement of the sleeve and the ring due to friction at chamfer contact. Phase 2 ends when the sleeve force is high enough to overcome chamfer friction limit and the sleeve starts to move axially.

In the chamfer contact, there will be a normal force $F_{N\beta_1}$ and a friction force $F_{f\beta_1}$, that are to balance the transferred sleeve force F_{ax} and force T_c/r_β associated with the transferred torque. When the cone torque comes to zero the friction force $F_{f\beta_1}$ will overcome the friction limit $F_{f\beta_1} \leq \mu\, F_{N\beta_1}$ and phase 2 will end, which normally occurs when the speed difference between cones are zero. Under assumption of solid friction in the chamfers and no axial motion of the sleeve, the end condition for Phase 2 can be derived as

$$T_c < \left(\frac{1 - \mu_\beta \tan(\beta)}{\mu_\beta + \tan(\beta)}\right) r_\beta\, F_{ax} = T_{index} \tag{3.24}$$

where T_{index} is sometimes referred to as index torque [9]. In this report the following condition based on the angular momentum is used

$$T_c > \frac{(I_g + I_r)(\dot{\theta}_s - \dot{\theta}_g)}{\Delta t} \tag{3.25}$$

meaning that the end of phase 2 occurs when cone torque is high enough and the speed difference is small enough to come to zero within the current time-step.

If the oil has high density and viscosity the oil might not be squeezed out properly during phase 1 and the cone torque may be low, that may result in a remaining speed difference at end of phase 2, with a high risk of clashing.

Also, if the shift force is very high when the speed difference between cones comes to zero, there is a risk that the cones will be stuck over each other because of wedging. Coefficient of friction between the cones must therefore be less than the tangent of the cones angles to reduce the risk of wedging.

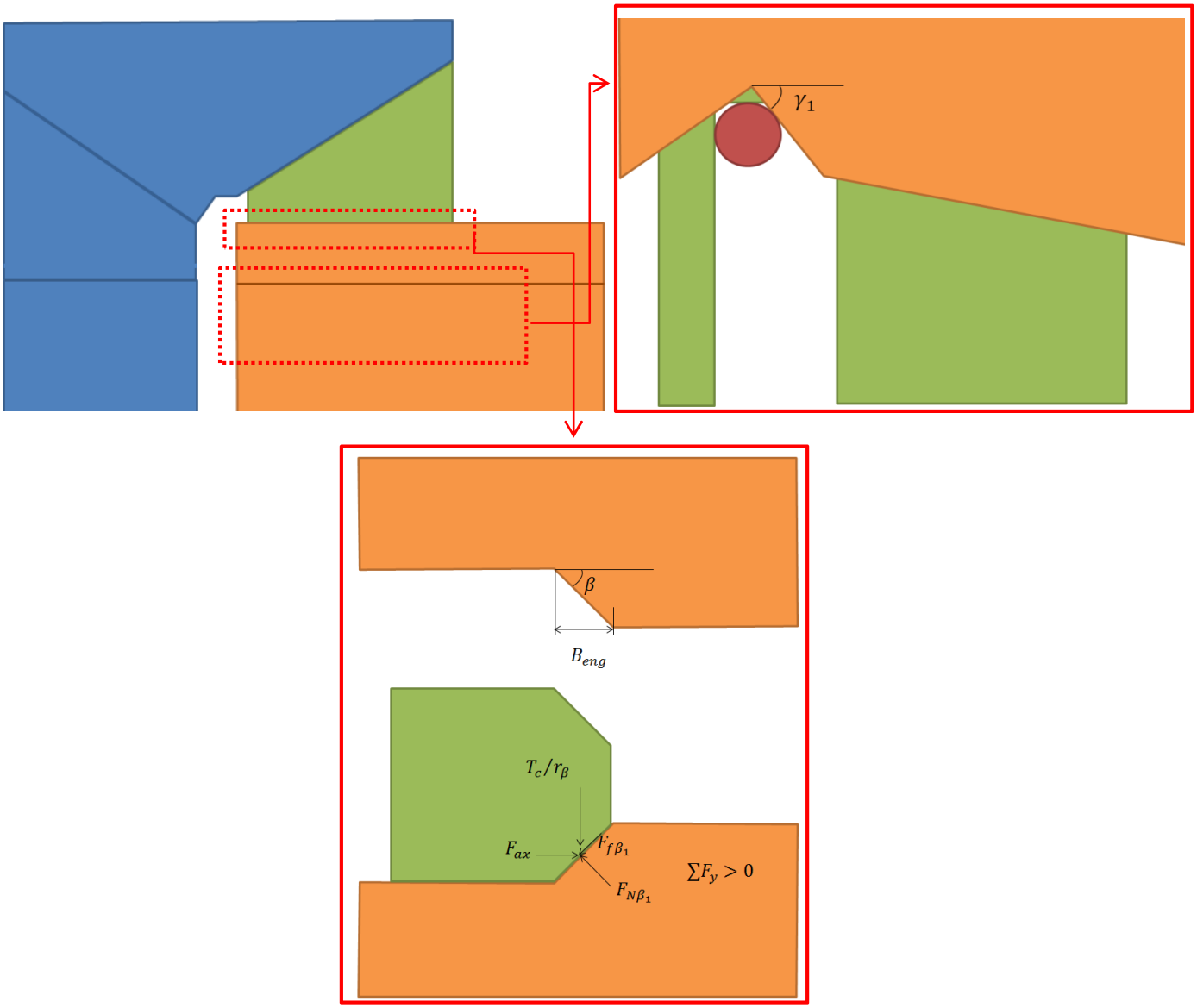

Figure 21: End position of the phase 2.

3.2.7.2 Phase 2-Equation

The cone torque is

$$T_c = \lambda_{cons}\, \mu_\alpha\, F_s \tag{3.26}$$

where $\lambda_{cons} = \frac{r_c}{\sin(\alpha)}\left(1 + \frac{1}{3}\left(\frac{b}{r_c}\right)^2 \sin^2(\alpha)\right)$ [8] and F_s is applied shift force.

The set of active constraint for the phase 2 is

$$\boldsymbol{\Phi}(\boldsymbol{q},t)^{internal} = \begin{bmatrix} x_r - x_s - d_\alpha \\ \theta_r - \theta_g - B_{ang} \\ x_r \end{bmatrix} = \mathbf{0} \tag{3.27}$$

The applied forces

$$\boldsymbol{Q}^A = \begin{bmatrix} F_s + C_{s\alpha}\, sign(\dot{x}_s) \\ T_c + C_s\dot{\theta}_s \\ C_{r\beta}\, sign(\dot{x}_r) \\ -T_c + C_r\, \dot{\theta}_r \\ C_g\ \dot{\theta}_g \end{bmatrix} \tag{3.28}$$

3.2.8 Phase 3-Blocker transition

At end of the phase 2 the sleeve axial force overcomes the axial component of the resistance at the chamfers (limited by friction) and also the spring force. The sleeve and the ring will move axially together. The shift force will drop down when the sleeve will move.

The speed difference at start of the phase 3 will also depend on the blocking chamfers angle since a smaller angle β will require a higher shift force and thus a higher torque is transmitted. Suitable range of degree of the blocking angle will depend on the cones angle and friction coefficients between the cones and between the blocking chamfers.

Depending on the shift force, initial conditions and geometry of the synchronizer the speed difference between the sleeve and the gearwheel may or may not come to zero at end of the phase 3a/3b. At the same time, the clearance C between sleeve and engaging teeth may or may not be finished. Possibilities of the phase 3 are given in *Figure 22*.

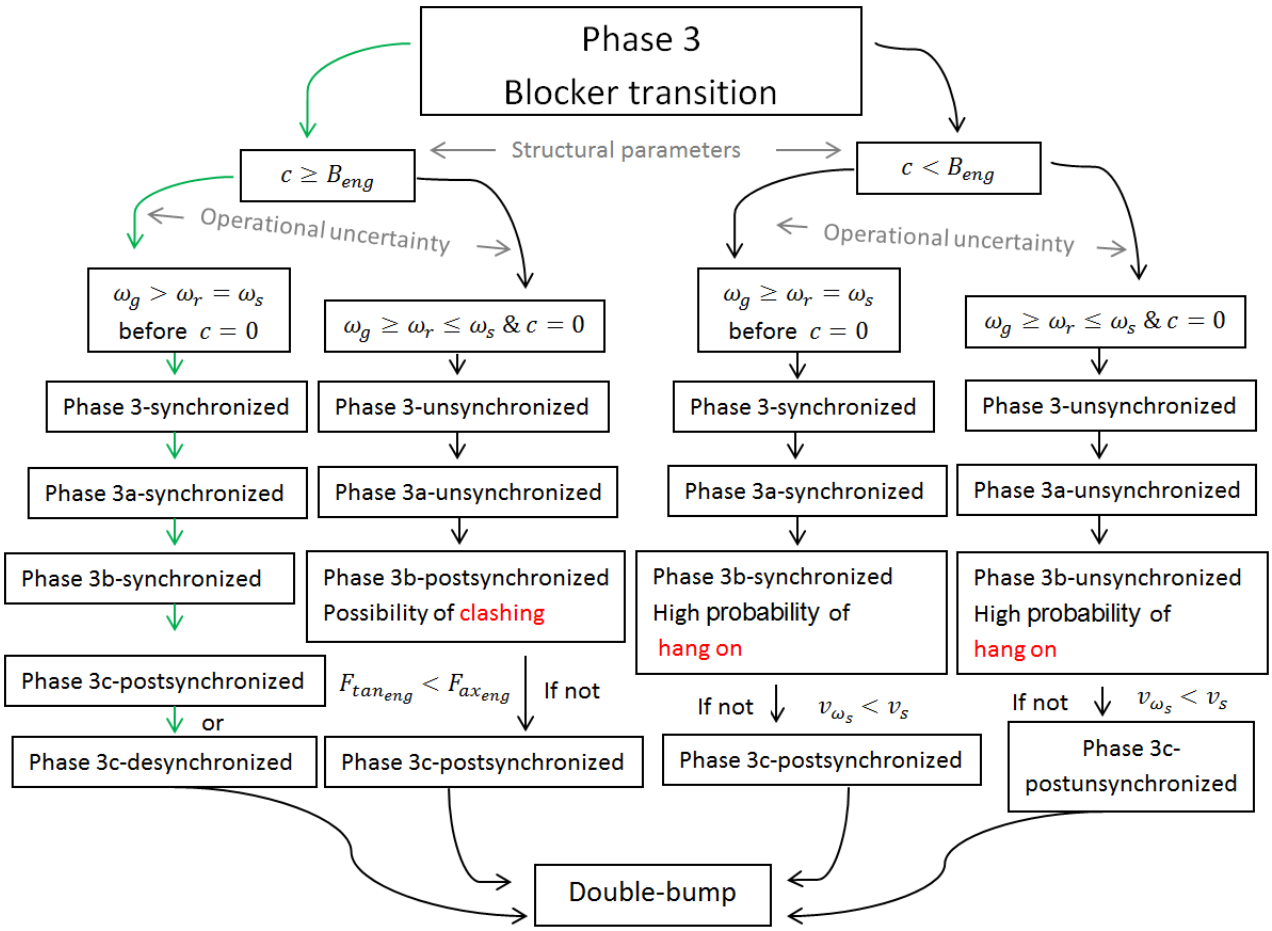

Figure 22: Possibility of the phase 3 based on dimensions of $\boldsymbol{c}$ and $\boldsymbol{B_{eng}}$.

In practice, the dimensions of the synchronizer's are such that the engaging teeth chamfers come in contact after the blocking teeth chamfers come out of contact, i.e $c \geq B_{eng}$. We shall therefore consider this case here. The case $c < B_{eng}$ is described in appendix A.2.

3.2.8.1 Phase 3a-Synchronized

The speed difference decreases to zero before the engaging teeth chamfers come in contact meanwhile the blocking chamfers slide over each other. Because of the sliding the gear relative rotational speed will be $\omega_{g_rel} = \frac{\dot{x}_r}{r_\beta} \tan \beta$.

The time duration of the phase 3a depends upon rate of the shift force with angle of the cones, maximum amount of the shift force at start of the phase 3a, the blocker chamfers angle and the friction at blocking chamfers contact.

Reason of the phase to exist is that during practical application variations in pressure buildup between the cones is quite possible because of the variations in oil properties and variations in applied load.

3.2.8.2 Phase 3a-Synchronized-Equations

The cone torque is

$$T_c = \lambda\, \mu_\alpha\, F_c \tag{3.29}$$

The set of active constraint for the phase 3a is

$$\boldsymbol{\Phi}(\boldsymbol{q}, t)^{internal} = \begin{bmatrix} x_r - x_s - d_\alpha \\ \theta_g - \theta_r + B_{ang} - \dfrac{x_r - B_{ax}}{r_\beta} \tan\beta \end{bmatrix} = \mathbf{0} \tag{3.30}$$

The applied forces are

$$\boldsymbol{Q}^A = \begin{bmatrix} F_s + C_{s\alpha}\, sign(\dot{x}_s) \\ T_c + C_s \dot{\theta}_s \\ C_{r\beta}\, sign(\dot{x}_r) \\ -T_c + C_r\, \dot{\theta}_r \\ C_g\ \dot{\theta}_g \end{bmatrix} \tag{3.31}$$

3.2.8.3 Phase 3b-Synchronized

The synchronizer proceed further in the same condition of motion until the clearance c between the engaging teeth decreases to zero. The gear will have same relative rotational speed as in the previous phase. If $c = B_{eng}$, contact positions of the engaging teeth chamfers and the blocking teeth chamfers at end of the phase are shown in *Figure 23*.

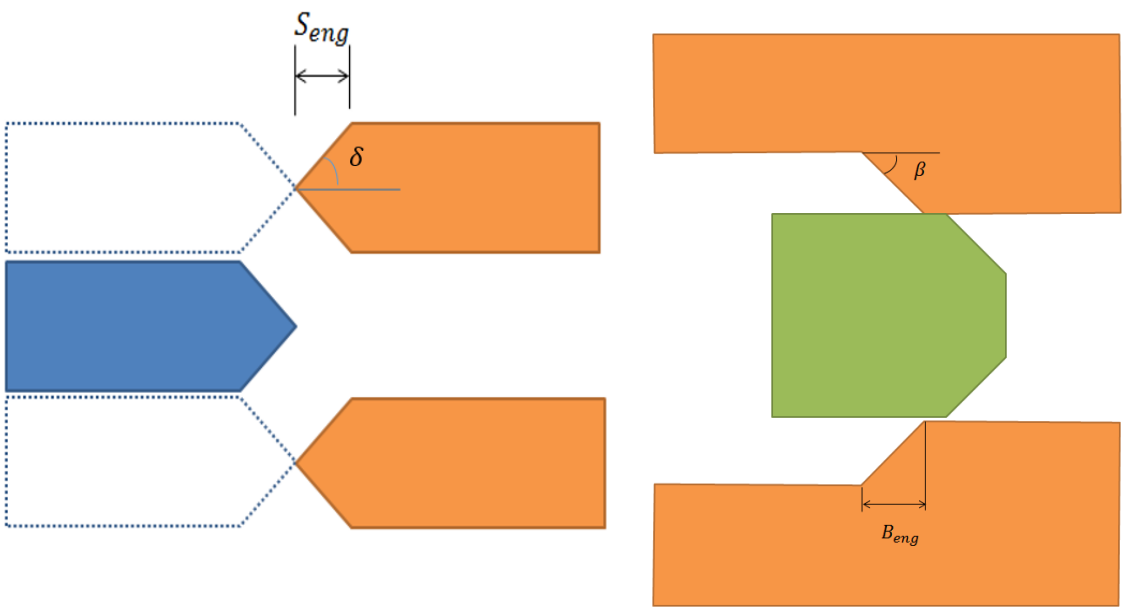

Figure 23: Engaging and blocking chamfers contact at end of the phase 3b.

3.2.8.4 Phase 3b-Synchronized-Equations

The set of active constraint for the phase 3b is

$$\boldsymbol{\Phi}(\boldsymbol{q},t)^{internal} = \begin{bmatrix} x_r - x_s - d_\alpha \\ \theta_r - \theta_s - \Delta\theta \\ \theta_g - \theta_r + B_{ang} - \dfrac{x_r - B_{ax}}{r_\beta}\tan\beta \end{bmatrix} = \mathbf{0} \tag{3.32}$$

$\Delta\theta$ is taken as $\theta_s - \theta_r$ at end of the phase 3a.

The applied forces are

$$\boldsymbol{Q}^A = \begin{bmatrix} F_s + C_{s\alpha}\, sign(\dot{x}_s) \\ T_c + C_s\dot{\theta}_s \\ C_{r\beta}\, sign(\dot{x}_r) \\ -T_c + C_r\,\dot{\theta}_r \\ C_g\;\dot{\theta}_g \end{bmatrix} \tag{3.33}$$

3.2.8.5 Phase 3c-Synchronized

The phase 3c will end when $2\,S_{eng}$ decreases to zero. After the clearance decreases to zero, to find the probability of relative position of the engaging teeth chamfers is quite hard. Two extreme positions which are called postsynchronization and desynchronization of the contact are considered as shown in Figure 24. The gear and the ring will rotate together. The gear relative rotational speed will be $\omega_g = \frac{\dot{x}_s}{r_\delta}\tan\delta$.

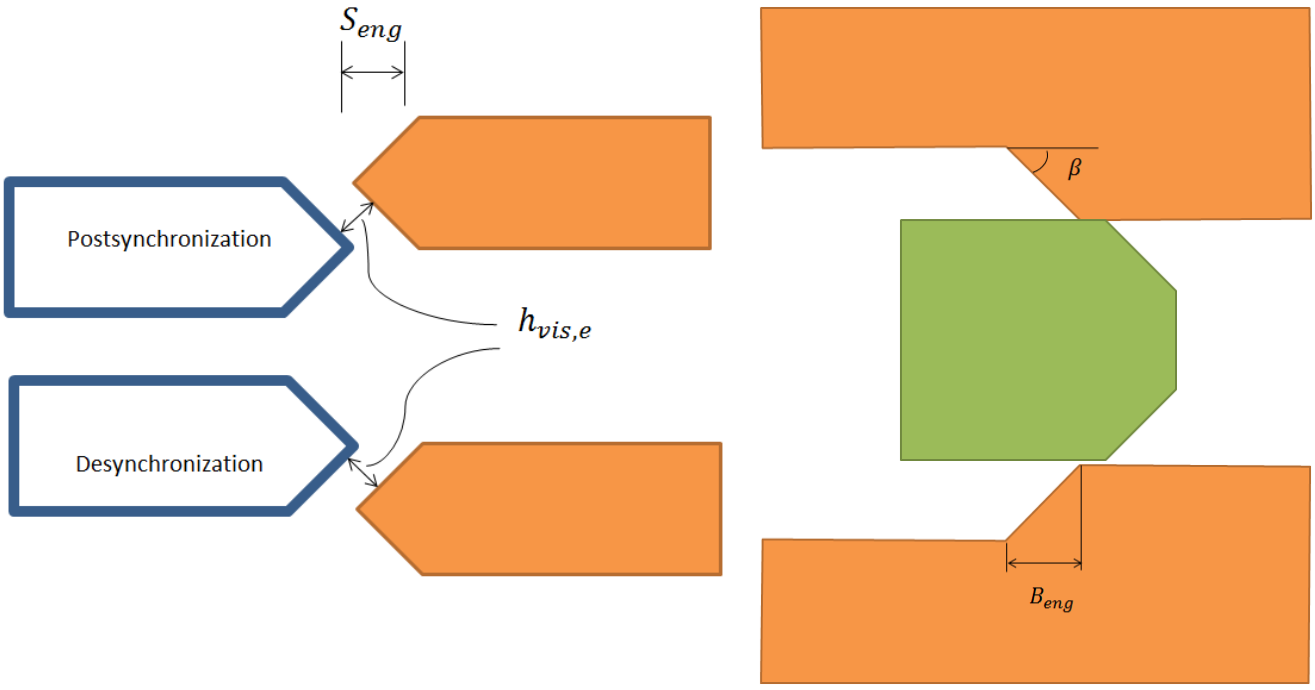

Figure 24: Postsynchronization or desynchronization during the phase 3c.

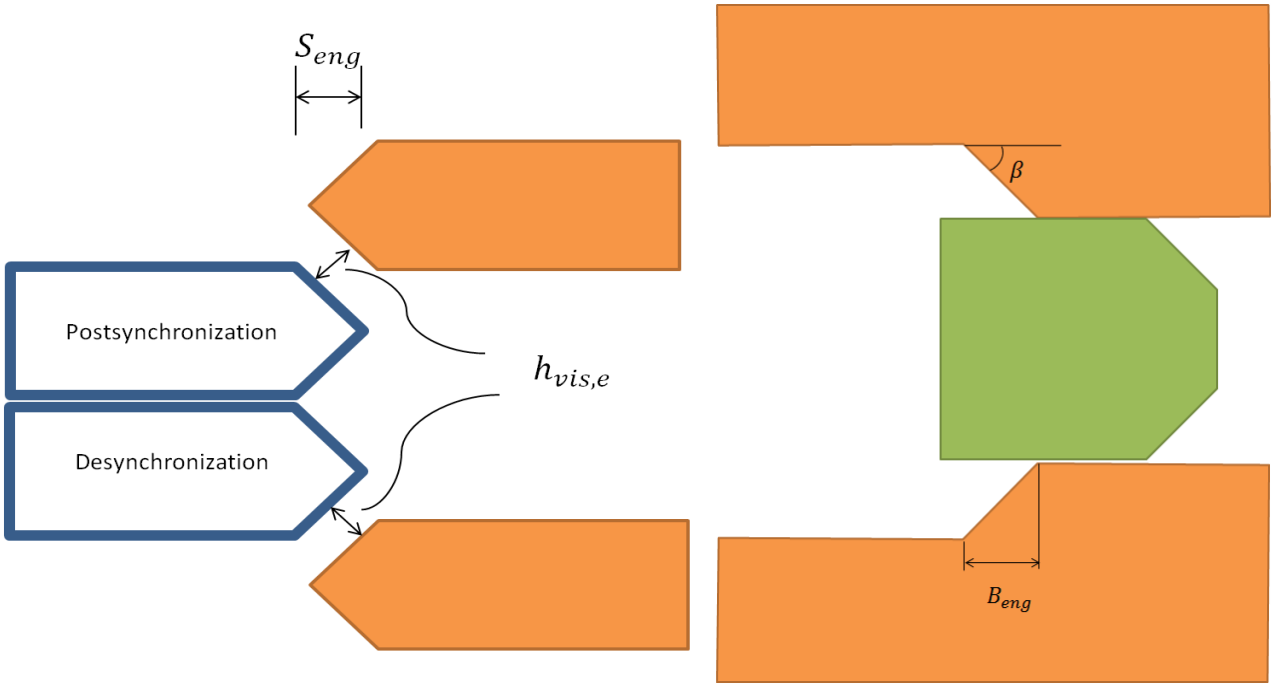

Figure 25: Postsynchronization or desynchronization at middle of the phase 3c.

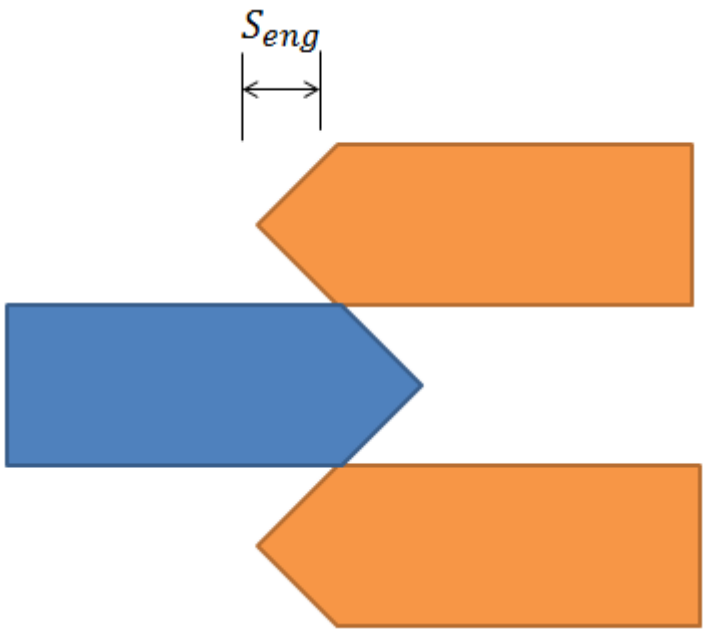

Figure 26: End of the phase 3c.

3.2.8.6 Phase 3c-Synchronized Postsynchronization-Equations

Oil splash losses will not support turning of the gear. The set of active constraint for the phase 3c is

$$\boldsymbol{\Phi}(\boldsymbol{q},t)^{internal} = \begin{bmatrix} x_r - x_s - d_\alpha \\ \theta_r - \theta_g - \dfrac{B_{ang}}{2} \\ \theta_s - \theta_g + S_{ang} - \dfrac{x_s - (c + B_{ax})}{r_\delta}\tan\delta \end{bmatrix} = \mathbf{0} \tag{3.34}$$

The applied forces are

$$\boldsymbol{Q}^A = \begin{bmatrix} F_s + C_{s\alpha}\, sign(\dot{x}_s) \\ T_c + C_s\dot{\theta}_s \\ C_{r\beta}\, sign(\dot{x}_r) \\ -T_c + C_r\,\dot{\theta}_r \\ C_g\;\dot{\theta}_g \end{bmatrix} \tag{3.35}$$

3.2.8.7 Phase 3c-Synchronized Desynchronization-Equations

Oil splash losses will support turning of the gear. The set of active constraint for the phase 3c is

$$\boldsymbol{\Phi}(\boldsymbol{q},t)^{internal} = \begin{bmatrix} x_r - x_s - d_\alpha \\ \theta_r - \theta_g - \dfrac{B_{ang}}{2} \\ \theta_s - \theta_g + S_{ang} + \dfrac{x_s - (c + B_{ax})}{r_\delta}\tan\delta \end{bmatrix} = \mathbf{0} \tag{3.36}$$

The applied forces are

$$\boldsymbol{Q}^A = \begin{bmatrix} F_s + C_{s\alpha}\, sign(\dot{x}_s) \\ T_c + C_s\dot{\theta}_s \\ C_{r\beta}\, sign(\dot{x}_r) \\ -T_c + C_r\,\dot{\theta}_r \\ C_g\;\dot{\theta}_g \end{bmatrix} \tag{3.37}$$

3.2.8.8 Phase 3a-Unsynchronized

Clearance between the engaging teeth decreases to zero and the engaging teeth chamfers come in contact with a rotational speed difference.

Depending on the oil properties, the cones angle, the blocking chamfers angle and the amount of maximum shift force at end of the phase 2, it is possible in reality that the sleeve has axial velocity such that the engaging teeth chamfers come in contact before the speed difference decreases to zero.

3.2.8.9 Phase 3b-Unsynchronized

During the phase 3b the engaging teeth chamfers come in full contact as shown in *Figure 27*. The oil film between the chamfers will also squeeze out that gives rise to the double bump. Relative rotational speed of the gear will be determined from the axial speed of the sleeve $\omega_g = \frac{\dot{x}_s}{r_\delta} \tan \delta$.

Just after contact of the engaging teeth chamfers there are two kind of possibility either clashing of the teeth either further engagement. If axial component of the resultant force acting at the contact is greater than the tangential component of the resultant force, the engagement will be done otherwise the clashing of the teeth will be produced.

During this phase postsynchronization or desynchronization which leads to double bump can also possibly but half of the bump will occur in this phase and other half will occur in next the phase.

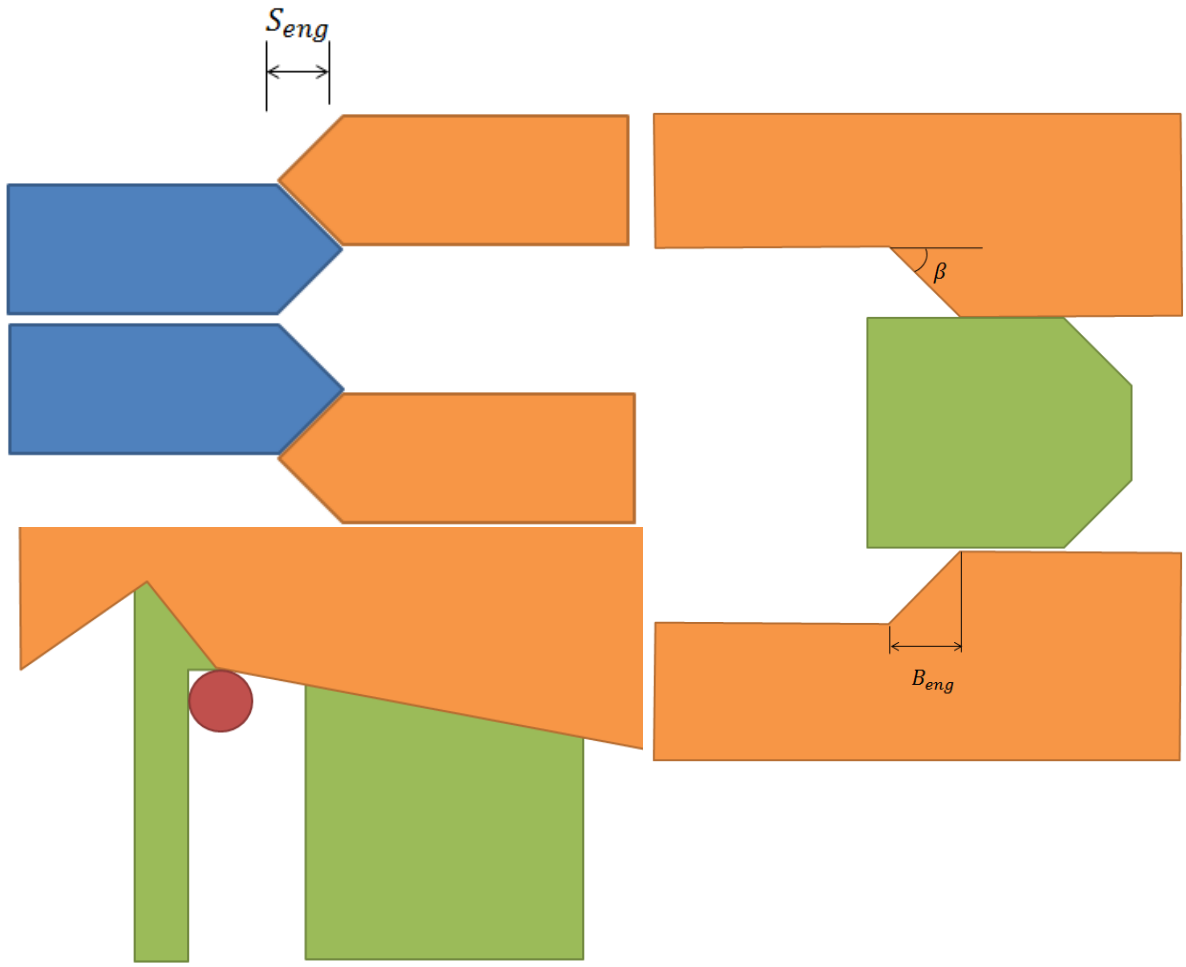

Figure 27: End position of the phase 3b.

3.2.8.10 Phase 3c-Unsynchronized

The phase 3c ends when the engaging teeth chamfers come out of contact and S_{eng} decreases to zero.

The force for the phase 3c can be the only force needed to turn the gear because it is possible that oil film squeeze out completely before the phase 3c.

3.2.8.11 Double bump

The shift force instantly drop down from the phase 3a but later on from a normal distance between the engaging teeth the shift force is needed again to keep continuous axial traveling of the sleeve for engagement which is called double bump. Because the shift force needed as a double bump depends mainly on the three factors; heating during dry friction, contact elasticity and turning of the gear wheel and these factors vary during shifting of the gear each time [8].

3.2.9 Phase 4-Engagement

This is last phase of the synchronization where the engaging teeth get the engagement for transmission of the torque.

This is the only phase where the sleeve, the ring and the gear have same rotational speed. The shift force is just needed to translate the sleeve and the ring for further engagement of the teeth. There is no resistance for the motion except the oil losses and the friction.

The shift force decreases from start of the phase but the sleeve is translating axially with an axial velocity. At end of the phase the sleeve can have an impact with the gear because of the axial velocity. But in the generic synchronizer because of the spring ring there will be less impact between the sleeve and the gear.

3.2.9.1 Phase 4-Engagement-Equations

The set of active constraint for the phase 4 is

$$\boldsymbol{\Phi}(\boldsymbol{q},\boldsymbol{t})^{internal} = \begin{bmatrix} x_r - x_s + d_\alpha \\ \theta_r - \theta_s + \Delta\theta_{r_s} \\ \theta_g - \theta_s + B_{ang} + \Delta\theta_{g_s} \end{bmatrix} = \mathbf{0} \tag{3.38}$$

$\Delta\theta_{r_s} = \theta_r - \theta_s$ and $\Delta\theta_{g_s} = \theta_g - \theta_s$ at end of phase 3c.

The applied forces are

$$\boldsymbol{Q}^A = \begin{bmatrix} F_s + C_{s\alpha}\, sign(\dot{x}_s) \\ T_c + C_s\dot{\theta}_s \\ C_{r\beta}\, sign(\dot{x}_r) \\ -T_c + C_r\, \dot{\theta}_r \\ C_g\ \dot{\theta}_g \end{bmatrix} \tag{3.39}$$

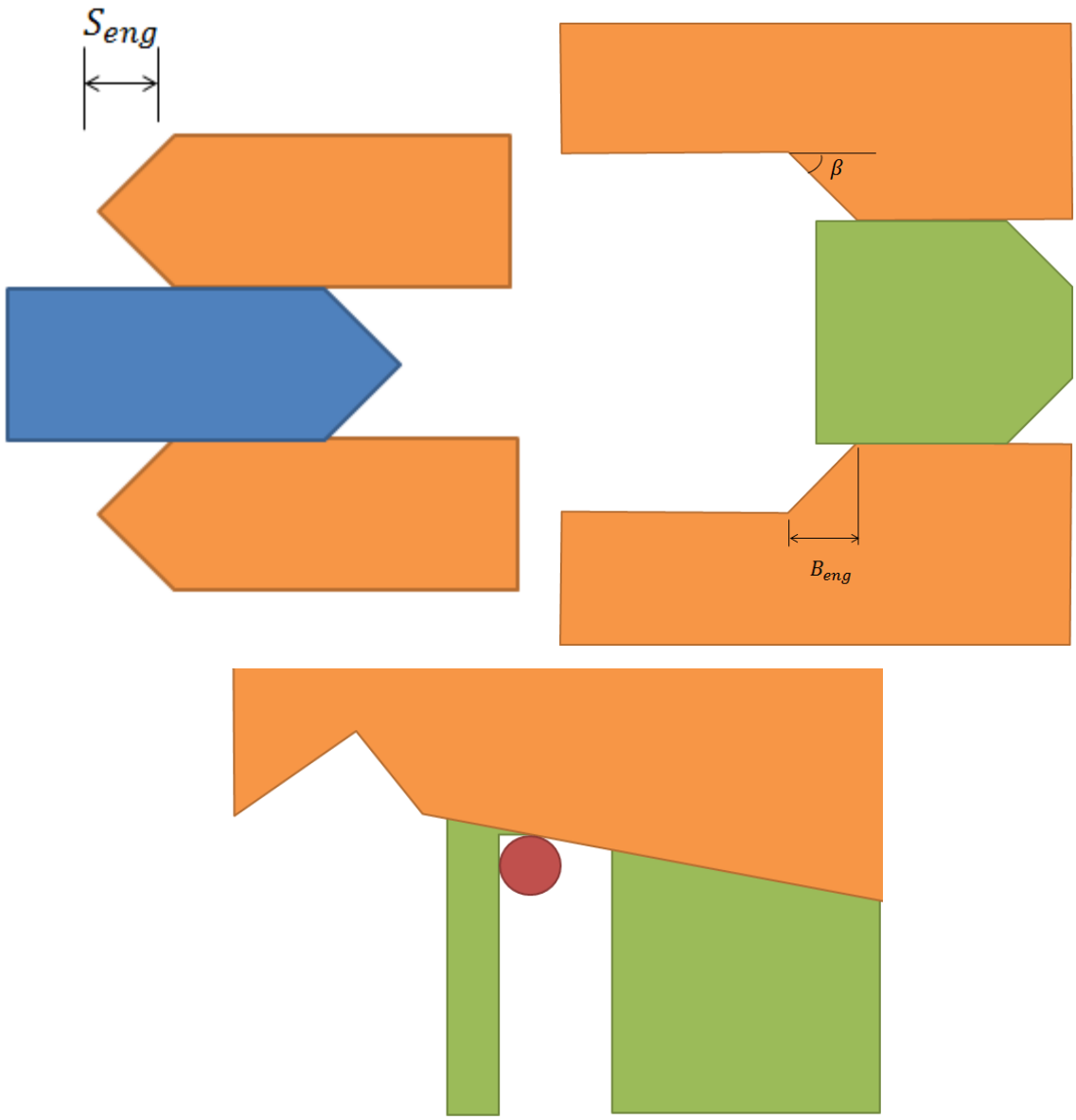

Figure 28: End position of the phase 4.

4. Problem Formulation

Problem A. Given the axial force acting on the sleeve, $F_s(t)$ (shift force), and the sleeve rotational speed, $\dot{\theta}_s(t)$, during the synchronization process, i.e. for all $t \in [0, t_s]$.

It is required to determine motion of the sleeve, the ring and the gearwheel as well as contact forces between the sleeve and the ring and between the gearwheel and the ring that all together satisfy the differential-algebric equations of motion (2.8) (2.9), the initial conditions

$$\begin{cases} x_s(0) = x_s^0 & \dot{x}_s(0) = 0 & x_r(0) = x_r^0 & \dot{x}_r(0) = 0 \\ \theta_s(0) = \theta_s^0 & \dot{\theta}_s(0) = \dot{\theta}_s^0 & \theta_r(0) = \theta_r^0 & \dot{\theta}_r(0) = \dot{\theta}_r^0 \end{cases} \quad \theta_g(0) = \theta_g^0 \quad \dot{\theta}_g(0) = \dot{\theta}_g^0 \tag{4.1}$$

and the final conditions

$$\begin{cases} x_s(t_s) = x_s^s & \dot{x}_s(t_s) = \dot{x}_s^s & x_r(t_s) = x_r^s & \dot{x}_r(t_s) = \dot{x}_r^s \\ \theta_s(t_s) = \theta_s^s & \dot{\theta}_s(t_s) = \dot{\theta}_s^s & \theta_r(t_s) = \theta_r^s & \dot{\theta}_r(t_s) = \dot{\theta}_r^s \end{cases} \quad \theta_g(t_s) = \theta_g^s \quad \dot{\theta}_g(t_s) = \dot{\theta}_g^s$$
$$\dot{\theta}_s(t_s) = \dot{\theta}_r(t_s) = \dot{\theta}_g(t_s) = \omega \tag{4.2}$$

Here in Eqs. (4.1) and (4.2): x_s^0, θ_s^0, θ_r^0, $\dot{\theta}_s^0$, $\dot{\theta}_r^0$, θ_g^0 and $\dot{\theta}_g^0$ are arbitrary prescribed parameters; the synchronization time t_s to be determined; x_s^s, $\dot{x}_s^s$, x_r^s, $\dot{x}_r^s$, θ_r^s and θ_g^s are determined at the end of the synchronization process. The Eqs. (4.2) expresses the synchronization conditions.

Problem B. Same as problem A, but here the motion of the sleeve, $x_s = x_s^{pres}(t)$, $x_s^{pres} = x_s\, t$ during phase 1, 3 and 4 while F_s during phase 2, and the sleeve rotational speed $\dot{\theta}_s(t)$ are given during the synchronization process, i.e. for all $t \in [0, t_s]$.

Problem C. Same as problem A, but here the motion of the sleeve, $x_s = x_s^{pres}(t)$, $x_s^{pres} = x_s\, t$ during phase 1, 3 and 4 while $\theta_g = \theta_g^{pres}(t)$, $\theta_g^{pres} = \omega_g\, t$ during phase 2, and the sleeve rotational speed $\dot{\theta}_s(t)$ are given during the synchronization process, i.e. for all $t \in [0, t_s]$.

To solve the Problems A, B and C a computational model of the dynamics of the synchronizer mechanism in question was developed in MATLAB. The core of the computational model is implementation of predictor-corrector type algorithm [6, 7] to solve the system of DAE (2.8) (2.9) with initial and boundary conditions given by Eqs. (4.1) and (4.2).

Input Parameters

Variable	Name	Variable	Name
$m_s = 1.5\ \mathrm{kg}$	Sleeve mass	$I_r = 0.004\ \mathrm{kgm}^2$	Ring moment of inertia
$m_{spr} = 0.2\ \mathrm{kg}$	Spring ring mass	$I_s = 0.01\ \mathrm{kgm}^2$	Sleeve moment of inertia
$m_r = 0.5\ \mathrm{kg}$	Ring mass	$I_g = 0.2\ \mathrm{kgm}^2$	Gear moment of inertia
$r_\alpha = 0.1\ \mathrm{m}$	Cones mean radius	$r_\beta = 0.07\ \mathrm{m}$	Chamfers mean radius
$r_{spr} = 0.04\ \mathrm{m}$	Spring mean radius	$F_{spr} = 50\ \mathrm{N}$	Spring force
$b = 5\ \mathrm{mm}$	Cones contact length	$d_\alpha = 2\ \mathrm{mm}$	Cones Initial clearance
$d_{vis} = 1\ \mathrm{mm}$	Viscous clearance	$h_{min} = 0.1\ \mathrm{mm}$	Mixed friction clearance
$T_{oil} = 90^o\ \mathrm{C}$	Temperature at start	$\Delta T_{oil} = 20^o\ \mathrm{C}$	Temperature change
$\alpha = 7^o$	Cone angle	$B_{ang} = 5^o$	Angular clearance
$\beta = 60^o$	Chamfer angle	$\gamma = 5^o$	Detent angle
$\rho = 15\ \mathrm{mm}^2/\mathrm{s}$	Oil viscosity [8]	$\mu_\alpha = 0.17$	Cones friction coefficient
$C_g = 5$	Gear oil splash losses	$C_s = 1$	Sleeve oil splash losses
$C_r = 0.003$	Ring sliding friction	$C_{s\alpha} = 0.02$	Sleeve sliding friction
$\omega_{s_o} = 1000\ \mathrm{rpm}$	Sleeve rotational speed	$\omega_{g_o} = 700\ \mathrm{rpm}$	Initial gear rotational speed
$\mu_{spr} = 0.12$	Spring friction coefficient	$\mu_\beta = 0.09$	Chamfer friction coefficient
$C_{r\alpha} = 0.002$	Ring sliding friction	$T_c = \lambda_{cons}\,\mu_\alpha F_s$	Cone Torque [8]
$F_{sf} = 16\pi\rho\dot{x}_s \sin(\alpha)\ r_c \left(\frac{b}{h}\right)^3$		Axial force transferred during viscous friction [8]	
$M_{sf} = 4\pi\rho\dot{x}_s r_c^3\ \omega_s \frac{b}{h}\left(1 - \frac{\omega_g}{\omega_s}\right)$		Torque transfer in viscous friction [8]	
$F_{s,max}$		Maximum acceptable applied shift force	

Table 1: Input parameters for the generic synchronization process.

The applied shift force during the synchronization process is described as follows

$$F_s(t) = \begin{cases} \dot{F}_s t & t_0 \le t_{F_{s,max}} \\ F_{s,max} & t_{F_{s,max}} \le t_{phase,2} \\ 300 + \dot{F}_{s,3} t & t_{phase,2} \le t_{phase,3a} \\ F_{bumb} + \dot{F}_{s,3} t & t_{phase,3a} \le t_{end} \end{cases}$$

where $\dot{F}_{s,3}$ is decreasing force rate and F_{bumb} is double bump force. The clearance is equal to the axial length of the blocking chamfers, i.e $C_o = B_{eng}$.

5. Simulation Results

5.1 Force Control

Some results from the simulation of synchronization of the generic synchronizer are shown in *Figure* 29. When the sleeve moves during the phase 1a and phase 1b with constant axial and rotational speed and with an amount of the shift force, the gear will lose its rotational speed because of the oil splash losses. During the phase 1c the oil thickness between the cones is also not sufficient to transfer the torque from the sleeve to the gear. From the phase 1d to start of the phase 2 the gear almost retain its speed but the shift force increases to break the oil film thickness between the cones. The shift force shown in the results is the minimum force needed to squeeze out the oil with particular oil properties and working conditions. The higher shift decreases the time for shifting the synchronization from viscous friction to dry friction.

From the phase 2 increase of shift force increases the torque transferred via cones which is the main cause to increase gear speed. The constant applied shift force causes a linear increase in the gear speed.

From the phase 3 the shift force can be decreased because the speed difference is small and now the shift force is only needed to translate the sleeve with the ring and to turn the gear. It is also implemented that decreasing rate of the shift force is such that at end of the synchronization it should be near to zero as shown in *Figure* 29.

Rotational speed of the gear during the phase 3 is higher than the speed of the sleeve in *Figure* 29 that shows when the gear turns, it will have additional speed increment by the sleeve or the ring.

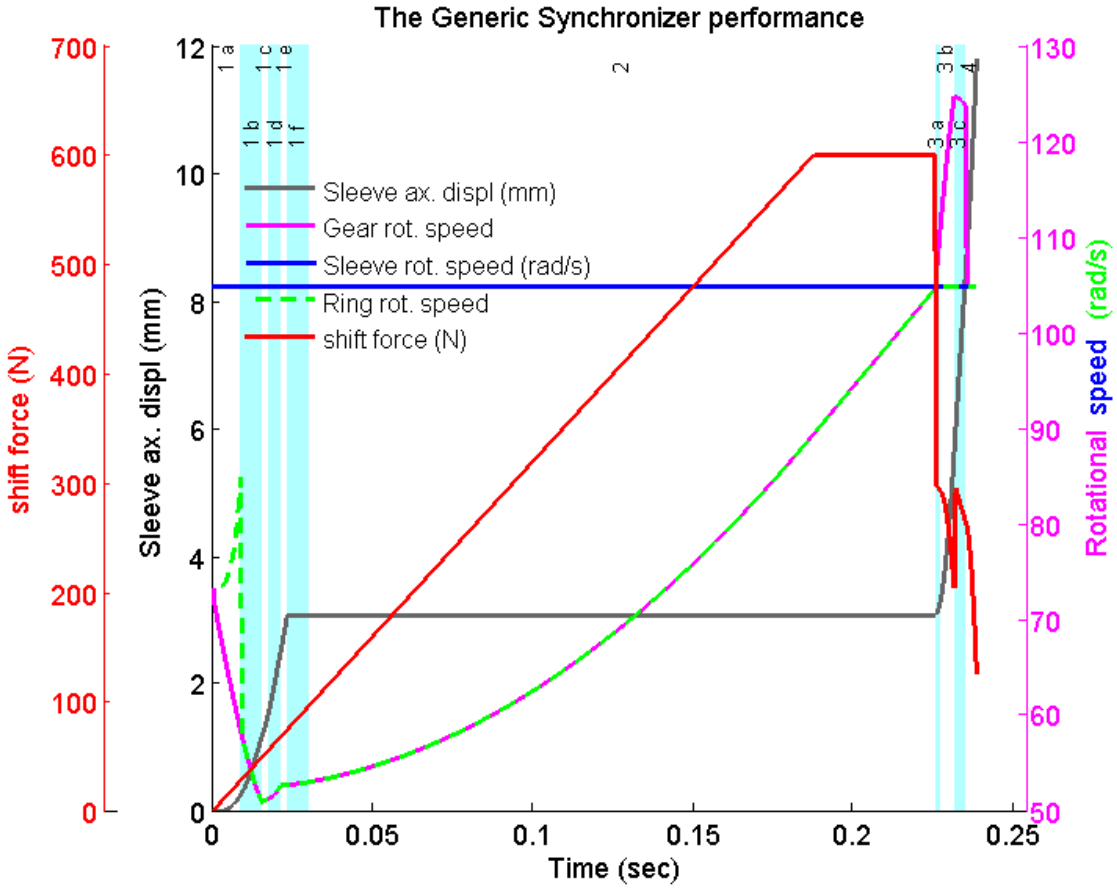

Figure 29: The generic synchronizer performance diagram of the synchronization with variations of the axial and rotational speeds and the shift force.

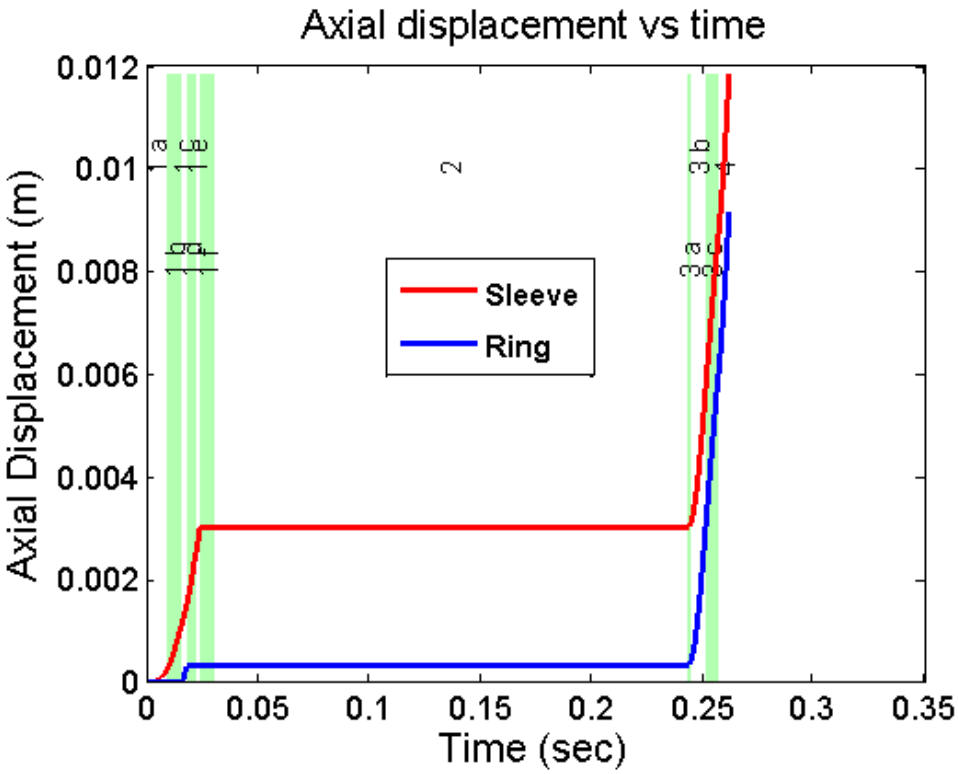

Figure 30: Axial displacement phase diagram of the synchronization of the generic synchronizer.

As shown in *Figure 30,* the sleeve has linear axial movement except during the phase 2 while the ring covered B_{ax} axial displacement together with the sleeve before the phase 1d and after the phase 2 it moves with the sleeve.

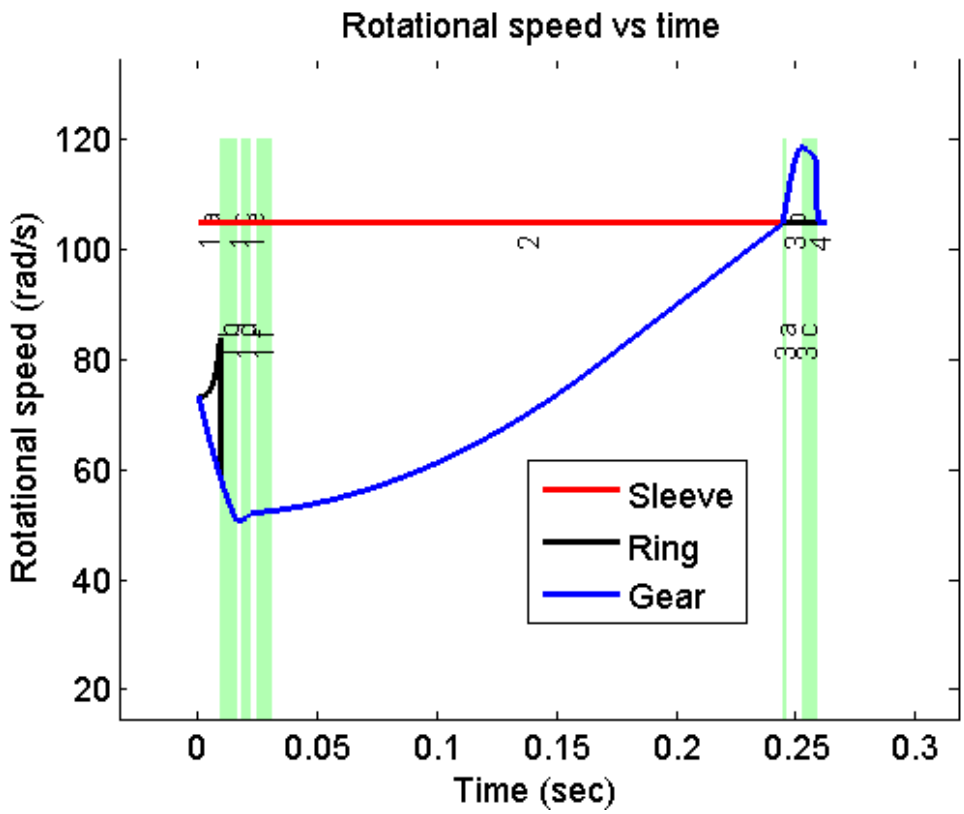

Figure 31: Rotational speed phase diagram of the synchronization of the generic synchronizer.

During the phase 1a rotational speed of the ring increases to cover the rotational displacement B_{ang} while the gear loses its speed. After both have same rotational speed till the end of phase 2. Because the sleeve has constant axial velocity, the gear rotational speed will also be constant during the phase 3. All three bodies have same rotational speed during the phase 4 and also afterwards during transmission.

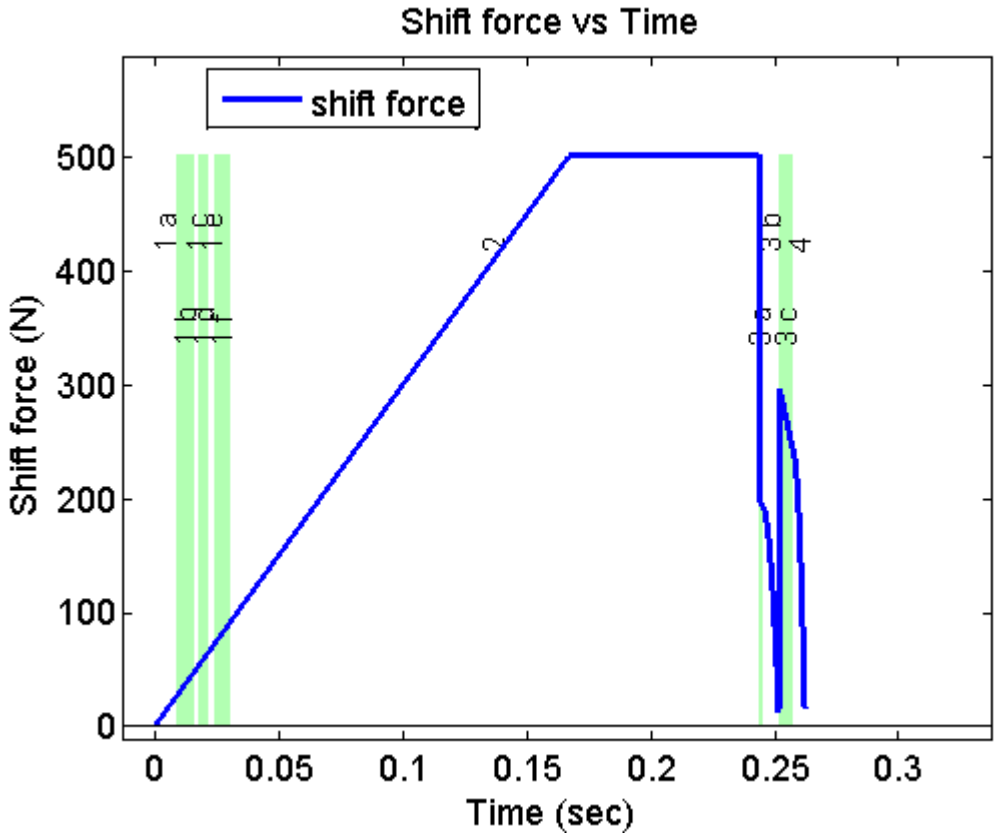

Figure 32: Shift force phase diagram of the synchronization of the generic synchronizer.

In *Figure 32* up to the phase 1f the shift force is the minimum required shift force with particular oil properties and working conditions to flush out the oil between the cones and to bring the synchronizer in indexing position before the main synchronization. The shift force during the phase 2 is the applied external force and variations in the applied force and varying maximum limit will vary the time to decrease the speed difference.

The shift force decreases with such a high rate during the phase 3a and 3b that the force needs to increase again to turn the gear during the phase 3c. The shift force during the phase 4 is also the minimum shift force required to translate the sleeve and the ring to complete the engagement.

In the scenario of results equations of motion of a dynamic system can be modelled by using Constrained Lagrangian Formulism. Mechanical model is developed for the generic synchronizer. Design parameters; cone angle, chamfer angle, spring ring stiffness and dynamic parameters; shift force, frictional model and the sleeve axial speed will be facilitated by the mechanical model.

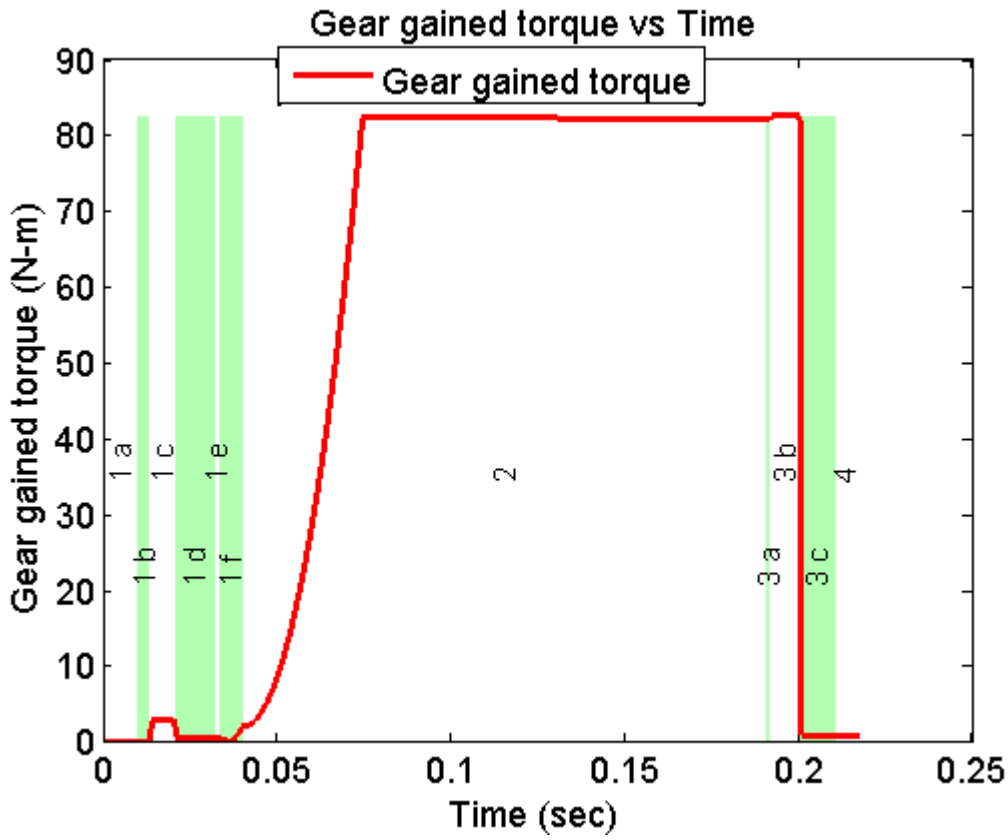

Figure 33: Gear gained torque phase diagram of the synchronization of the generic synchronizer.

Duration of phases as output from simulation are

Time step is 0.000500 sec
Time of the phase 1a is 0.009500 sec and no.of iterations are 19.
Time of the phase 1b is 0.004000 sec and no.of iterations are 8.
Time of the phase 1c is 0.007000 sec and no.of iterations are 14.
Time of the phase 1d is 0.011500 sec and no.of iterations are 23.
Time of the phase 1e is 0.001500 sec and no.of iterations are 3.
Time of the phase 1f is 0.006500 sec and no.of iterations are 13.
Time of the phase 2 is 0.150000 sec and no.of iterations are 300.
Time of the phase 3a is 0.001000 sec and no.of iterations are 2.
Time of the phase 3b is 0.008500 sec and no.of iterations are 17.
Time of the phase 3c is 0.010500 sec and no.of iterations are 21.
Time of the phase 4 is 0.006500 sec and no.of iterations are 13.
Total time up to phase 4 is 0.216500 sec.

5.2 Kinematic control

The generic synchronizer performance diagram of the problem B (semi-inverse) is given in Figure 34.

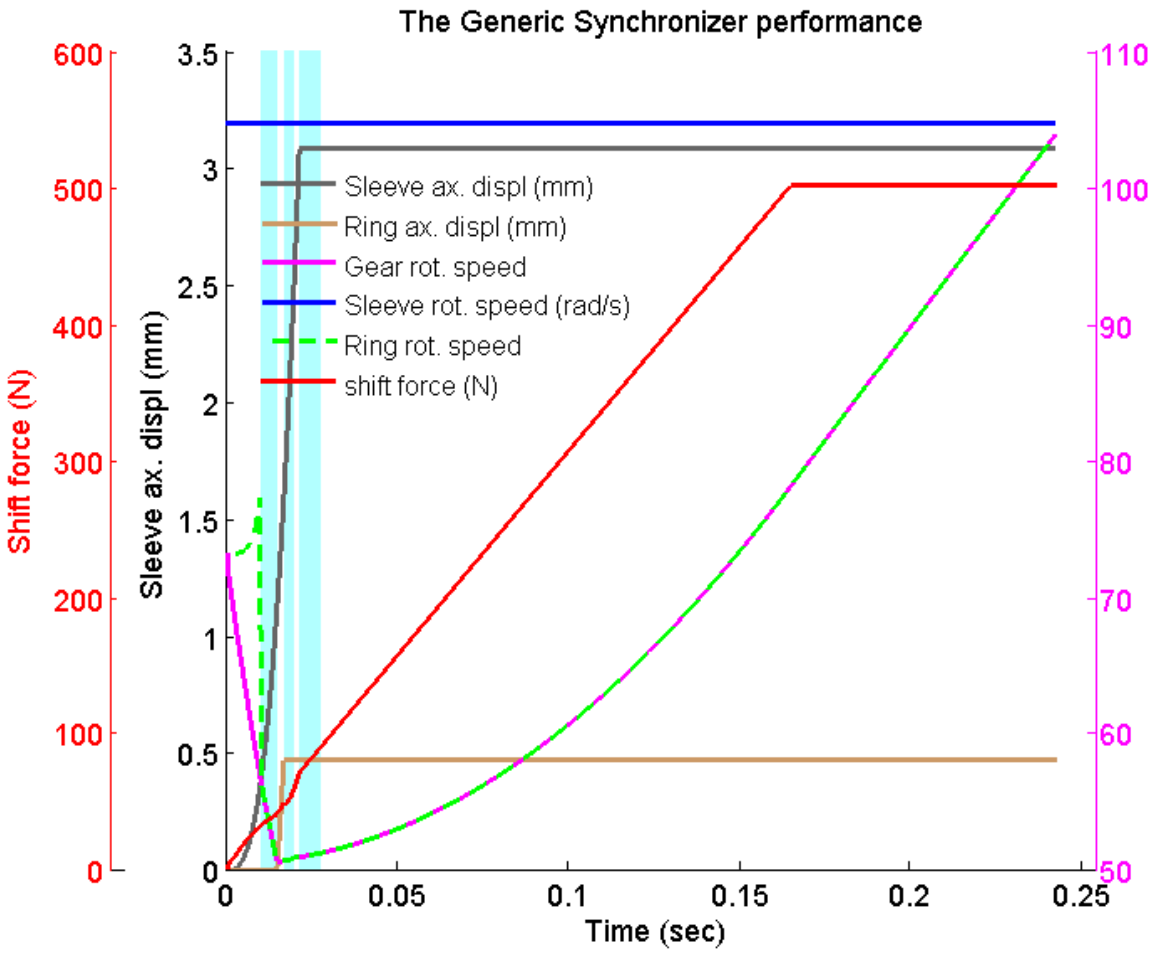

Figure 34: The generic synchronizer performance diagram for the semi-inverse case.

The generic synchronizer performance diagram of the problem C (inverse) is given in *Figure 35.*

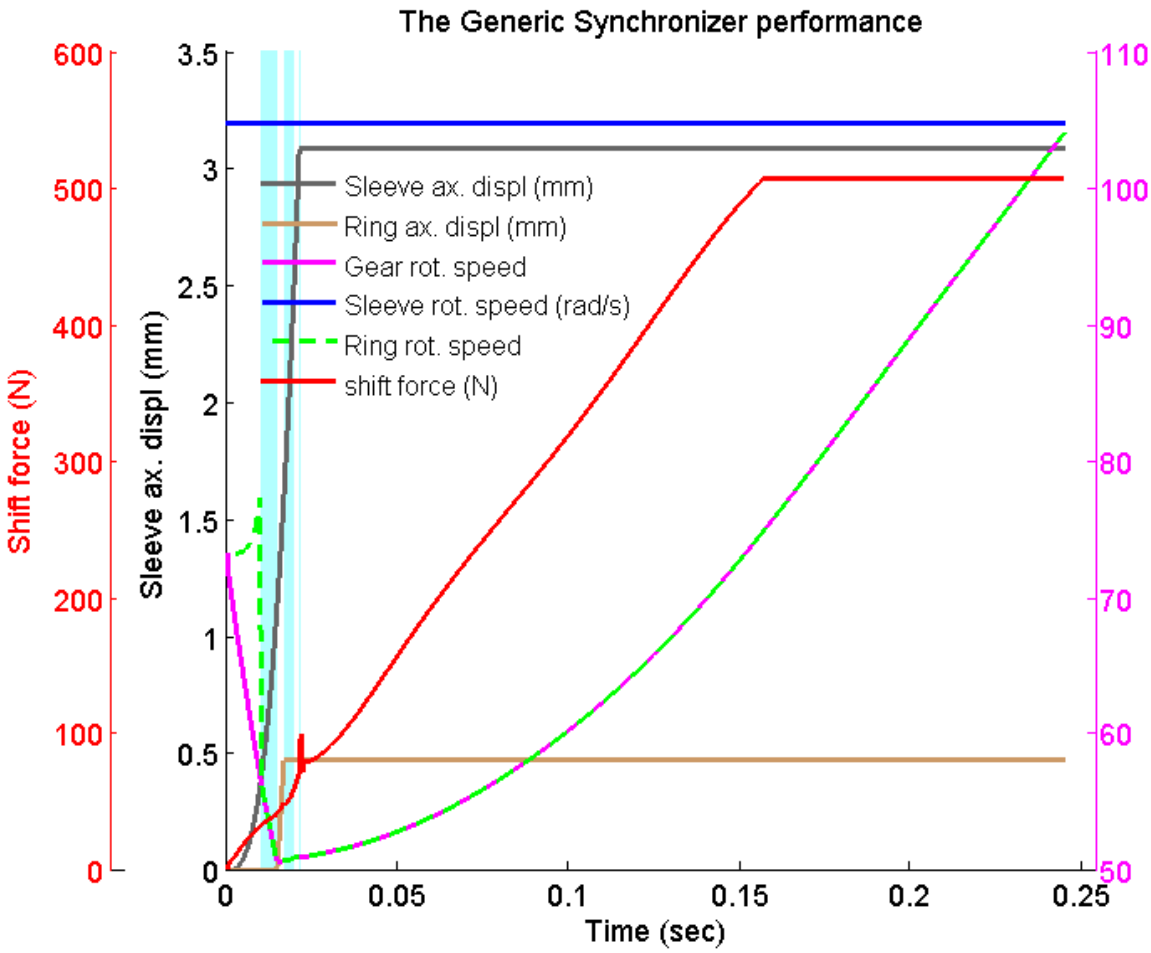

Figure 35: The generic synchronizer performance diagram of for the problem c.

5.3 Sensitivity Analysis

A sensitivity analysis is done in order to see how cone angle, coefficient of friction and how the sleeve force affect the predicted synchronization time (See *Figures 36-41)*. In Figure 42 synchronization time is depicted for different cone angles and coefficient of friction. The synchronization time decreases with decreasing cone angle α and with increasing coefficient of friction μ. The Figure 43 shows that the synchronization time decreases with increasing $F_{s,max}$ and $\dot{F}_s$. For higher values of the $F_{s,max}$ and $\dot{F}_s$ the synchronization time decreases rapidly than at lower values.

One problem of synchronizer design is its sensitivity to driveline vibrations. Here, the prescribed output shaft speed is modelled as $\omega_s = A\sin(2\pi f t + \vartheta)$ with frequency f and amplitude A. The generic synchronizer performance diagram with driveline vibrations is presented in Figure 44. The sensitivity of synchronization time with respect to amplitude and frequency is shown in Figure 45 and Figure 46. Since the phase shift is a random parameter $\vartheta \in [0, 2\pi]$, the mean synchronization time for 200 different values of ϑ is depicted.

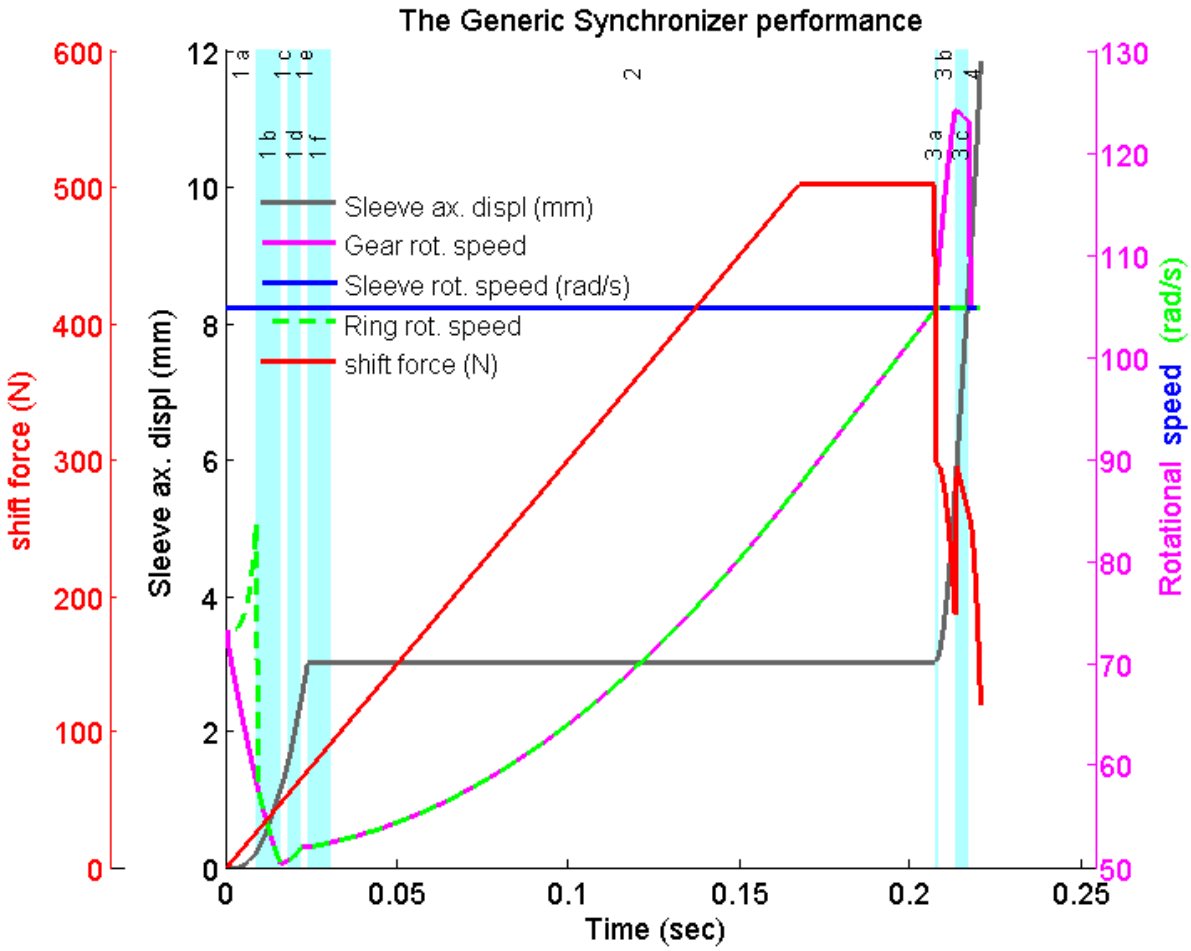

Figure 36: The generic synchronizer performance diagram at $\boldsymbol{\mu_s = 0.22}$.

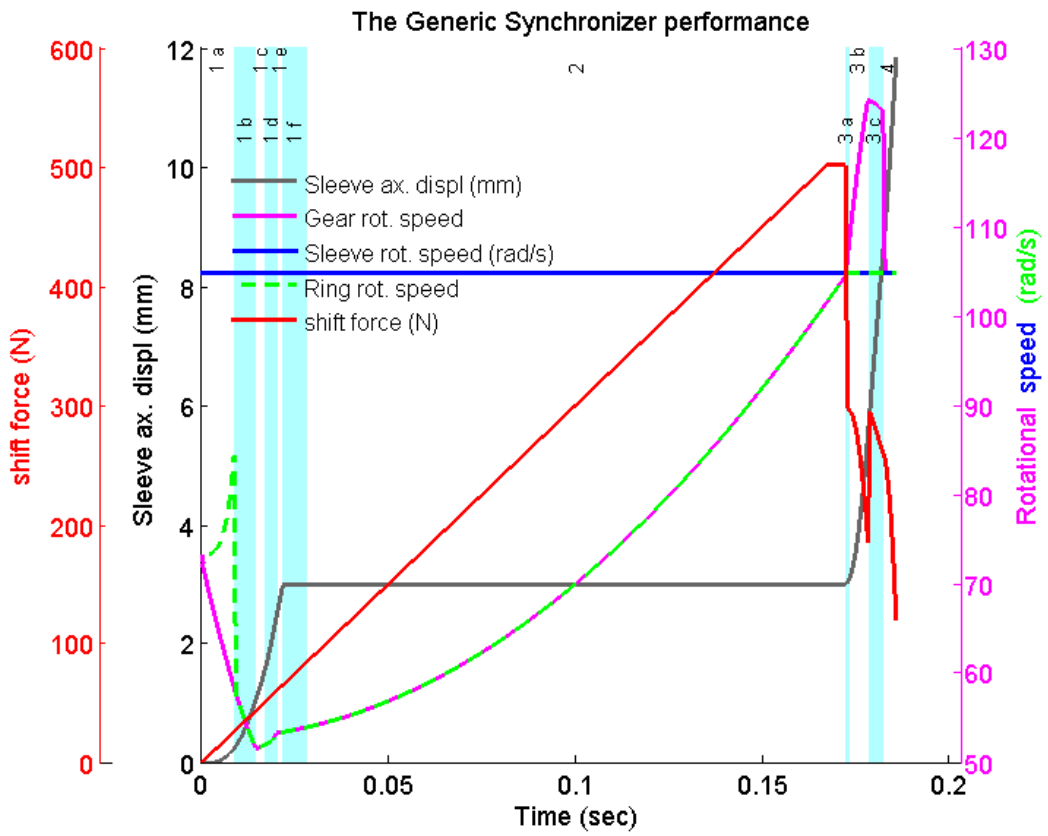

Figure 37: The generic synchronizer performance diagram at $\alpha = 4^o$

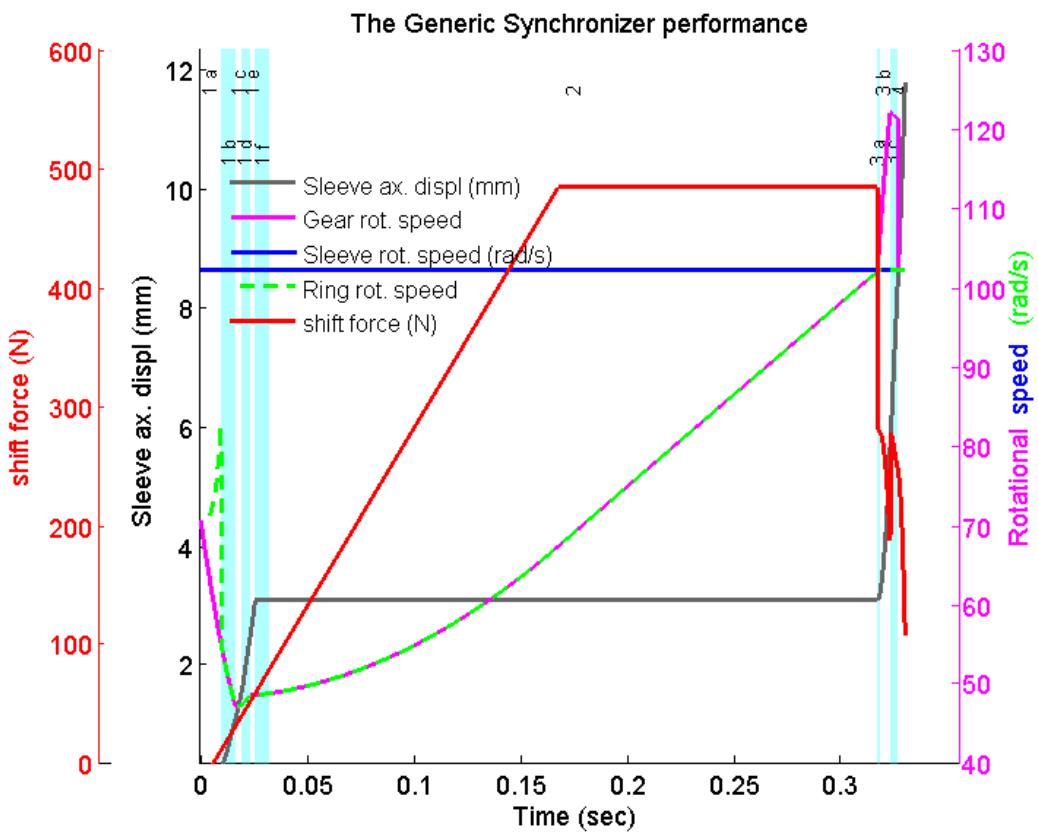

Figure 38: The generic synchronizer performance diagram at $\alpha = 10^o$.

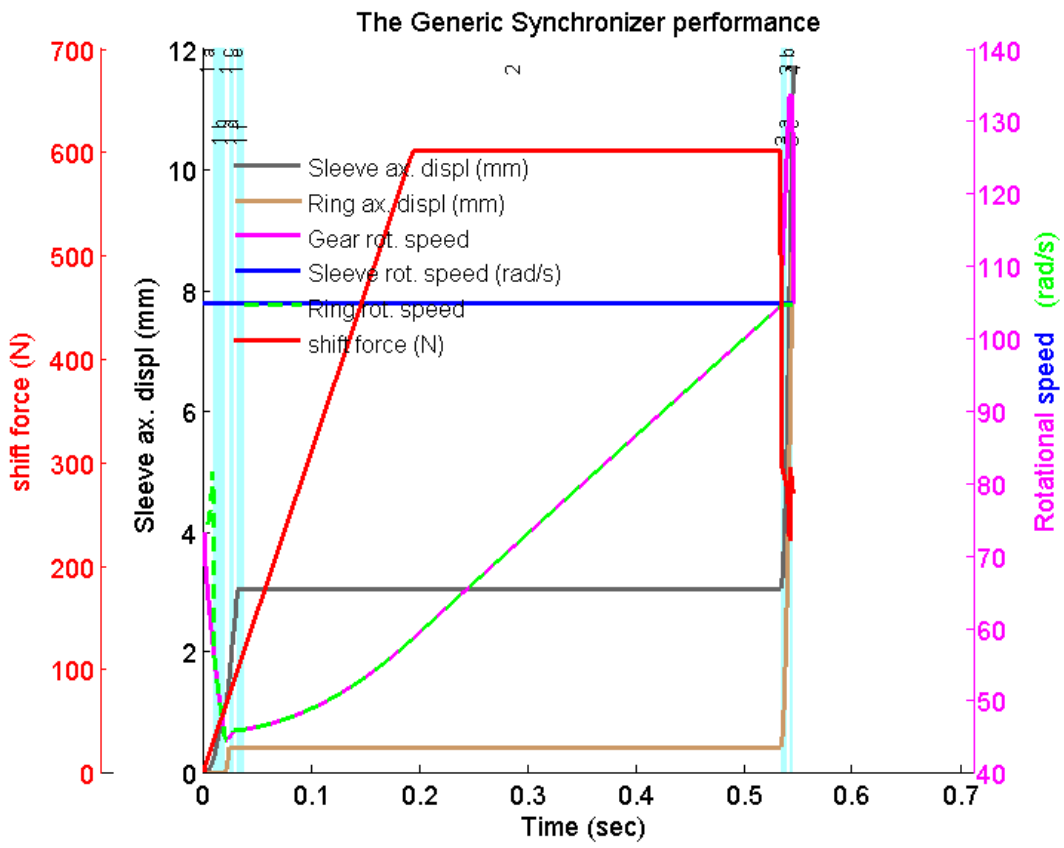

Figure 39: The generic synchronizer performance diagram at $\boldsymbol{\alpha = 24.7^o}$.

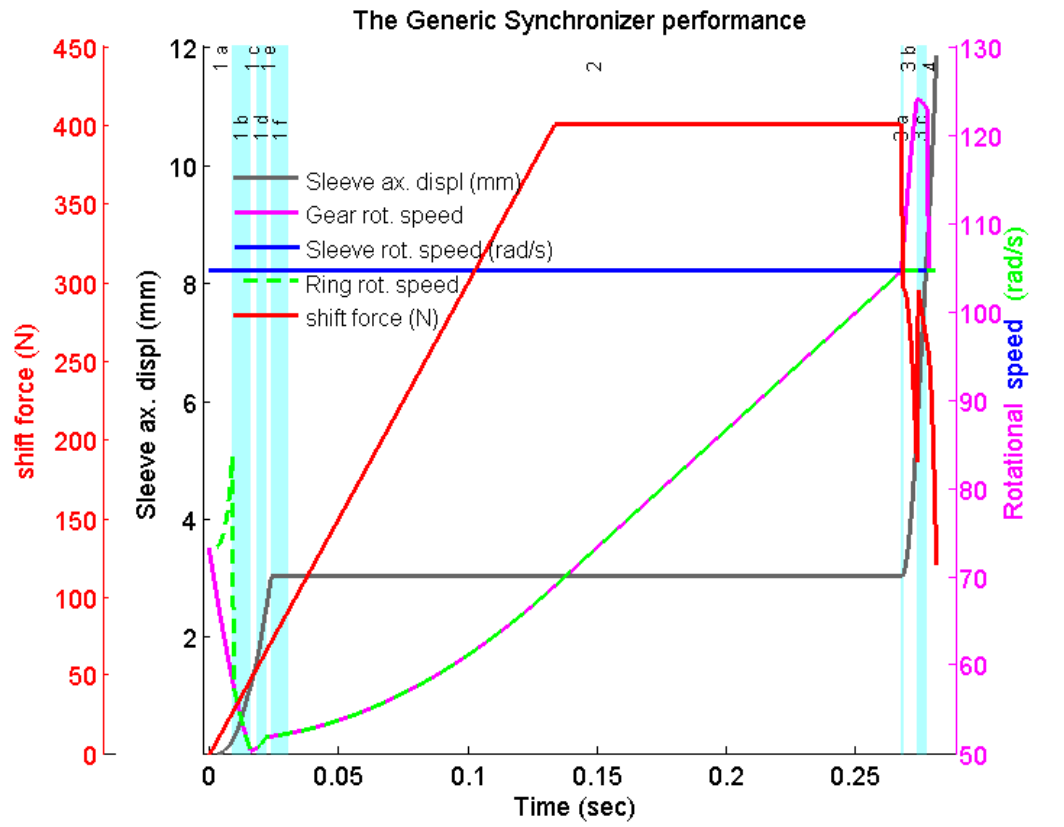

Figure 40: The generic synchronizer performance diagram at $\boldsymbol{max(F_s) = 400N}$.

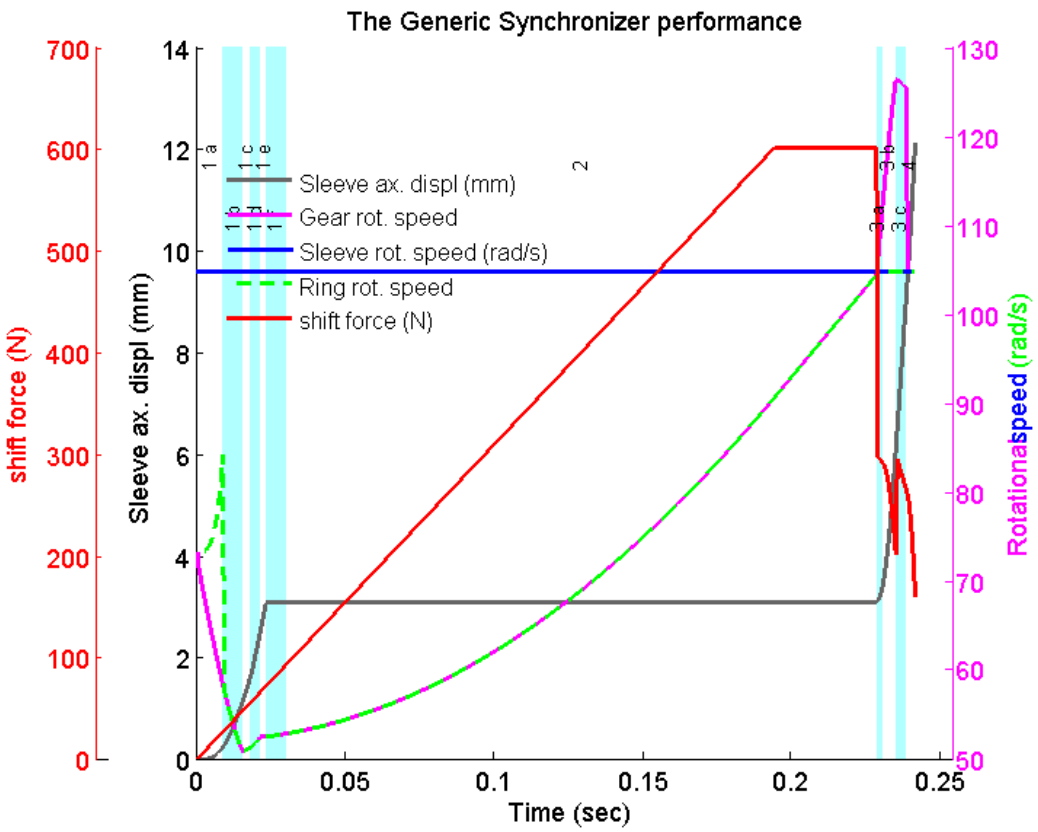

Figure 41: The generic synchronizer performance diagram at $\boldsymbol{max(F_s) = 600N}$.

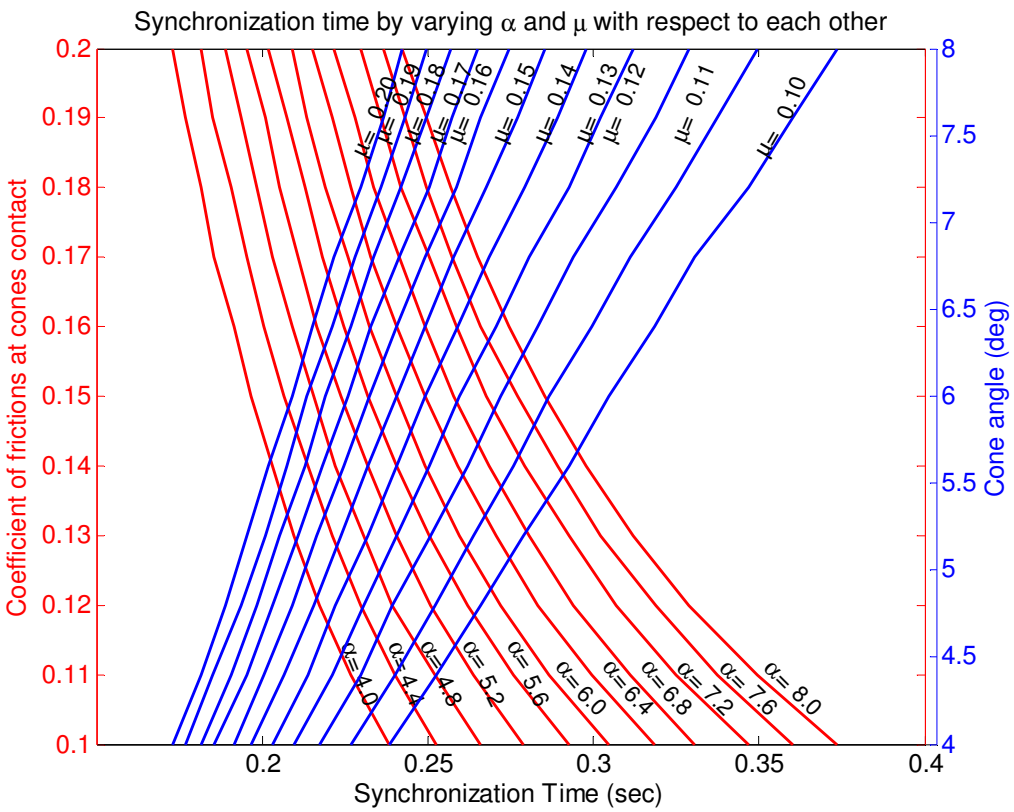

Figure 42: Synchronization time at varying cone angle and coefficient of friction.

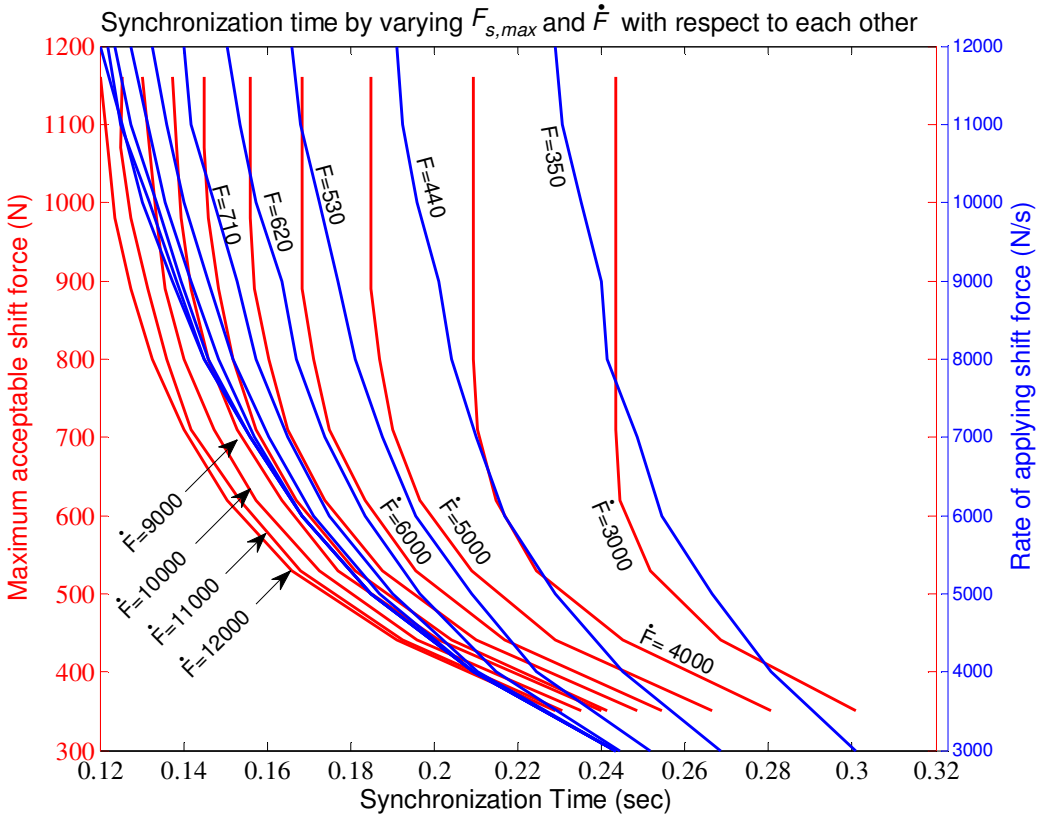

Figure 43: Synchronization time at varying $F_{s,max}$ and $\dot{F}_s$.

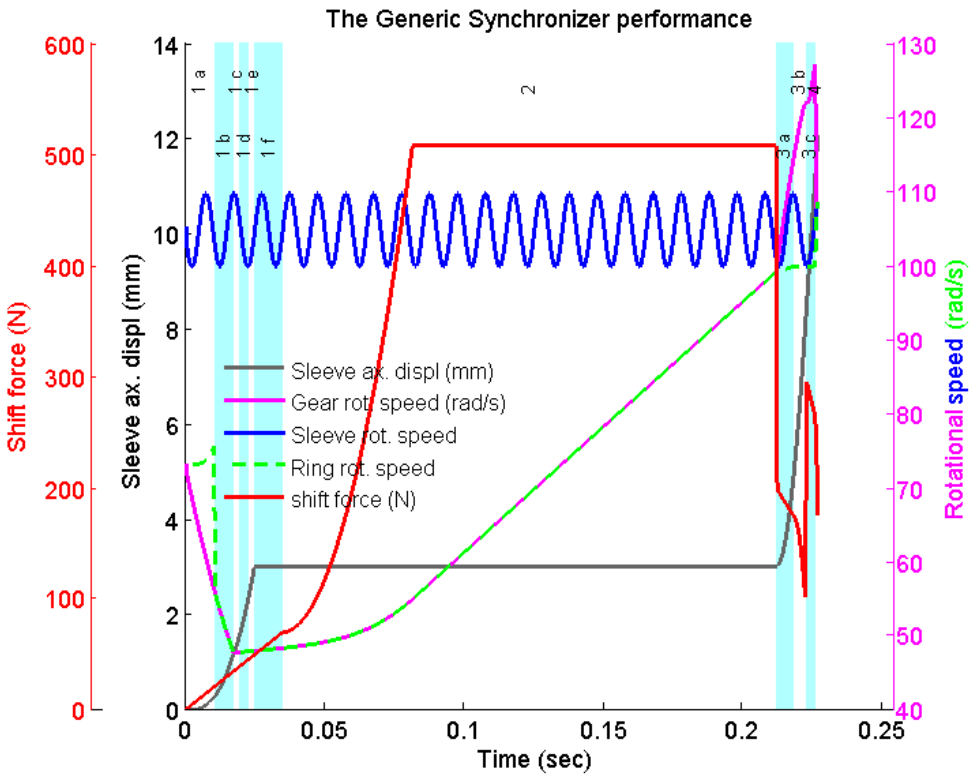

Figure 44: The generic synchronizer performance diagram with driveline vibrations.

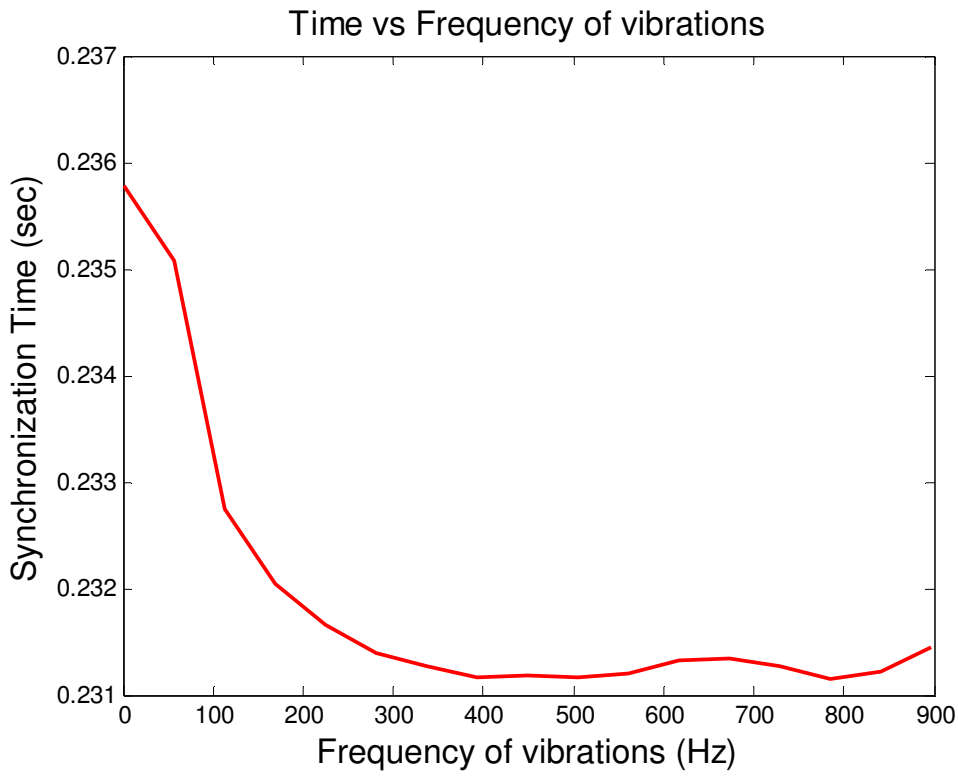

Figure 45: Variation of synchronization time with varying frequency of vibrations.

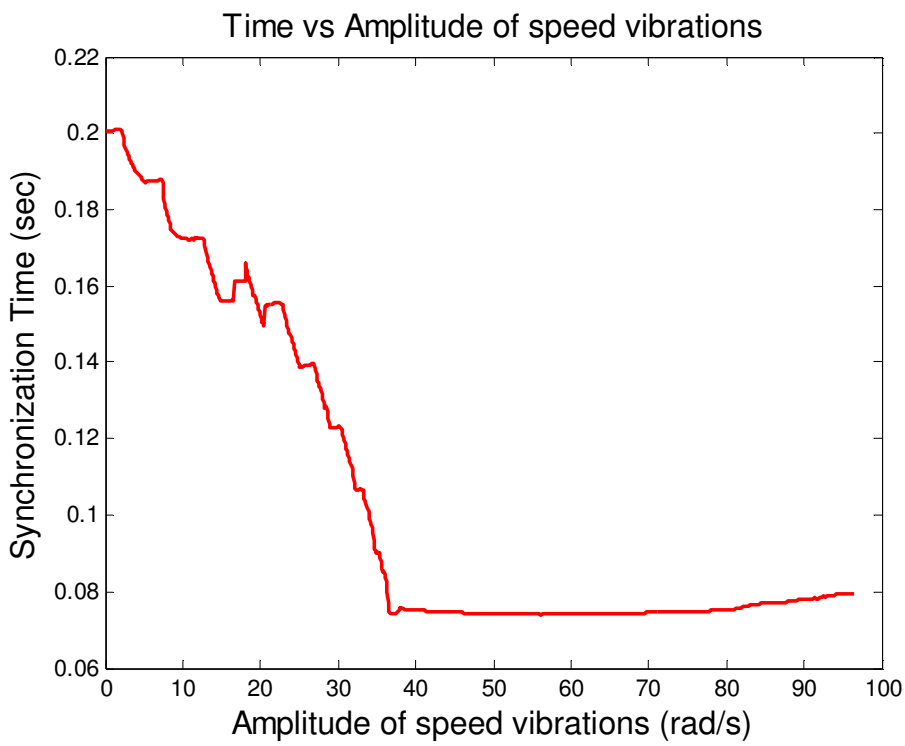

Figure 46: Variation of synchronization time with varying amplitude of vibrations.

5.4 Validation: Modified Generic Synchronizer to validate with the Scania Test Rig

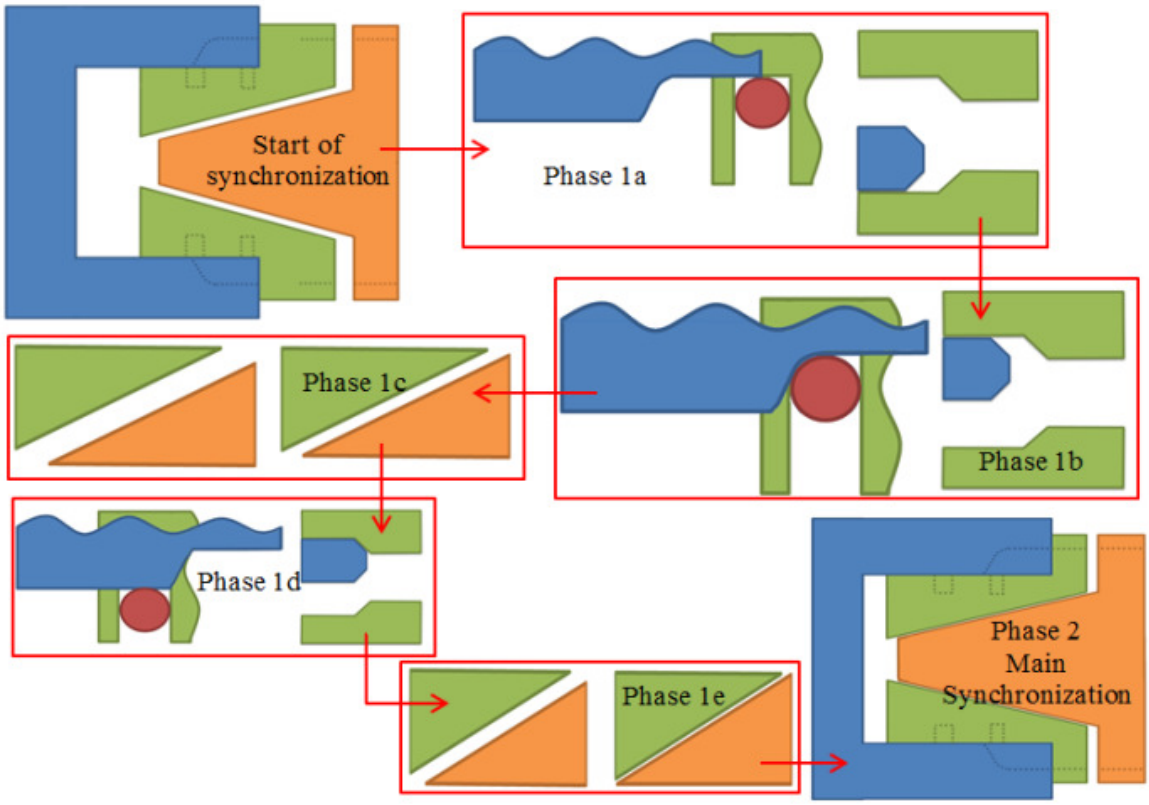

Figure 47: The modified generic synchronizer.

To validate the generic synchronization model against available rig measurements at Scania, the structure of the generic synchronizer needs to be modified. In the generic model described above the cones contact is between the sleeve and the ring but in test rig the cones contact is between the gearwheel and the ring.

The model of the generic synchronizer has been modified was validated up to the main synchronization phase (phase 2). Phase 1 is pre-synchronization phase and further divided into sub-phases 1a, 1b, 1c, 1d and 1e. Throughout the process a constraint will be active to keep the sleeve rotational speed at constant level and the bodies will not experience the oil splash losses. The specifics are given in appendix A.3.

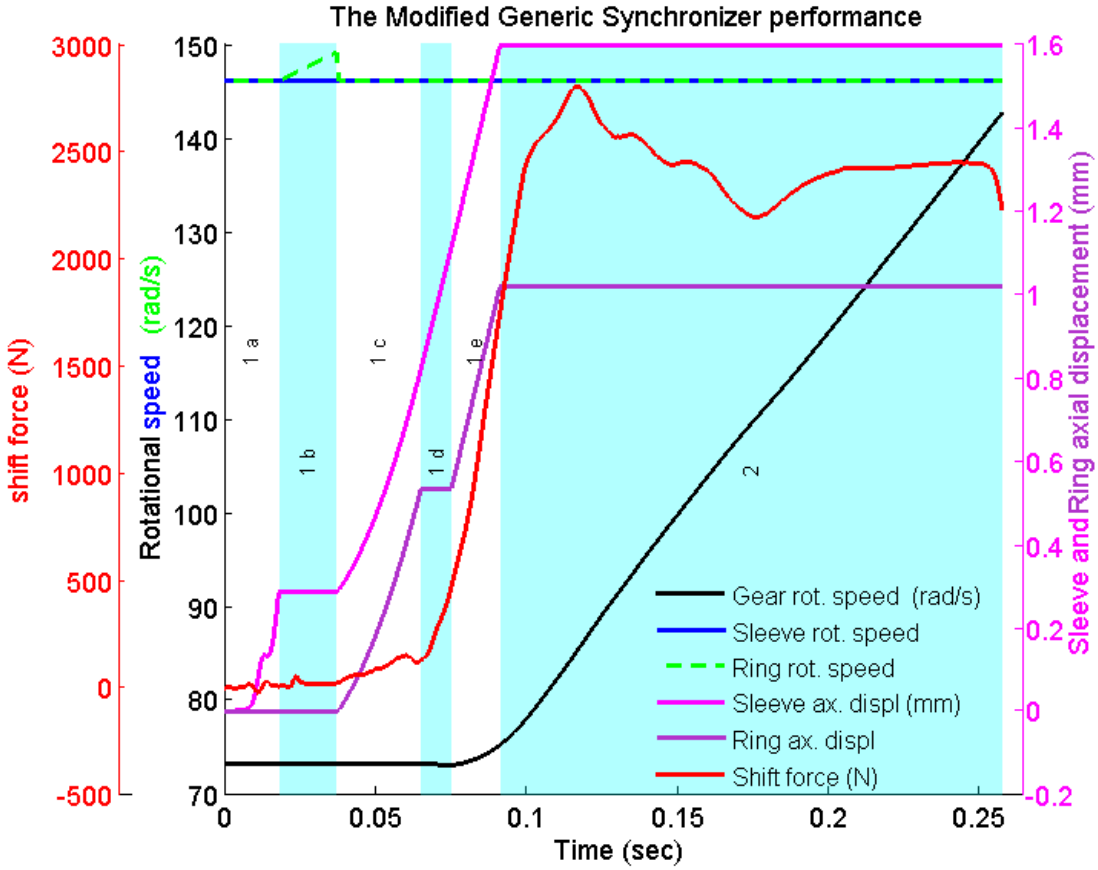

Figure 48: The modified generic synchronizer performance diagram.

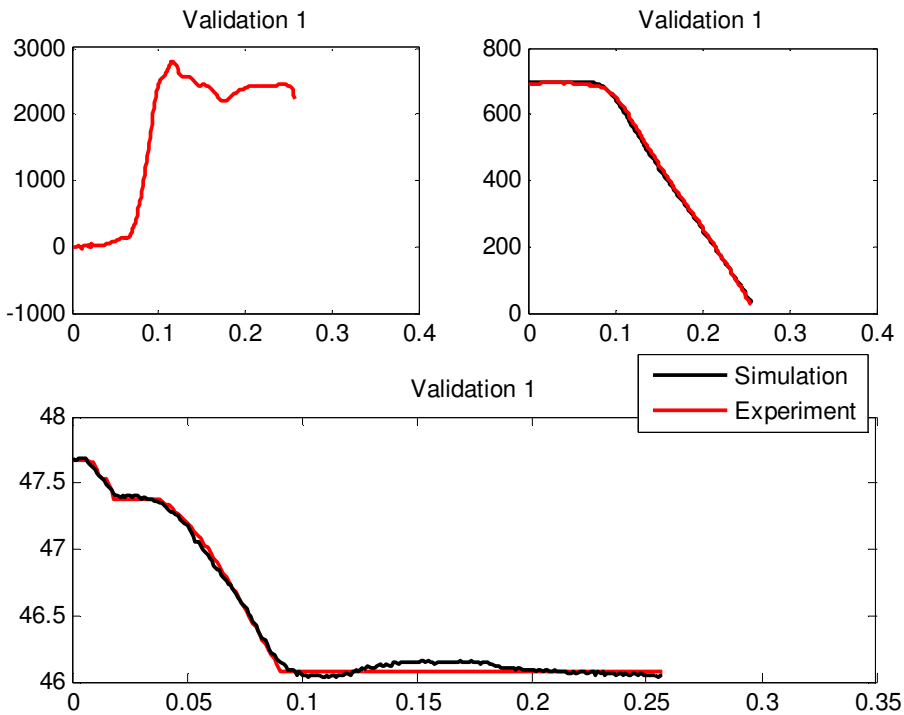

Figure 49: Comparison of the shift force, speed difference and sleeve axial displacement obtained from the model and Scania test rig.

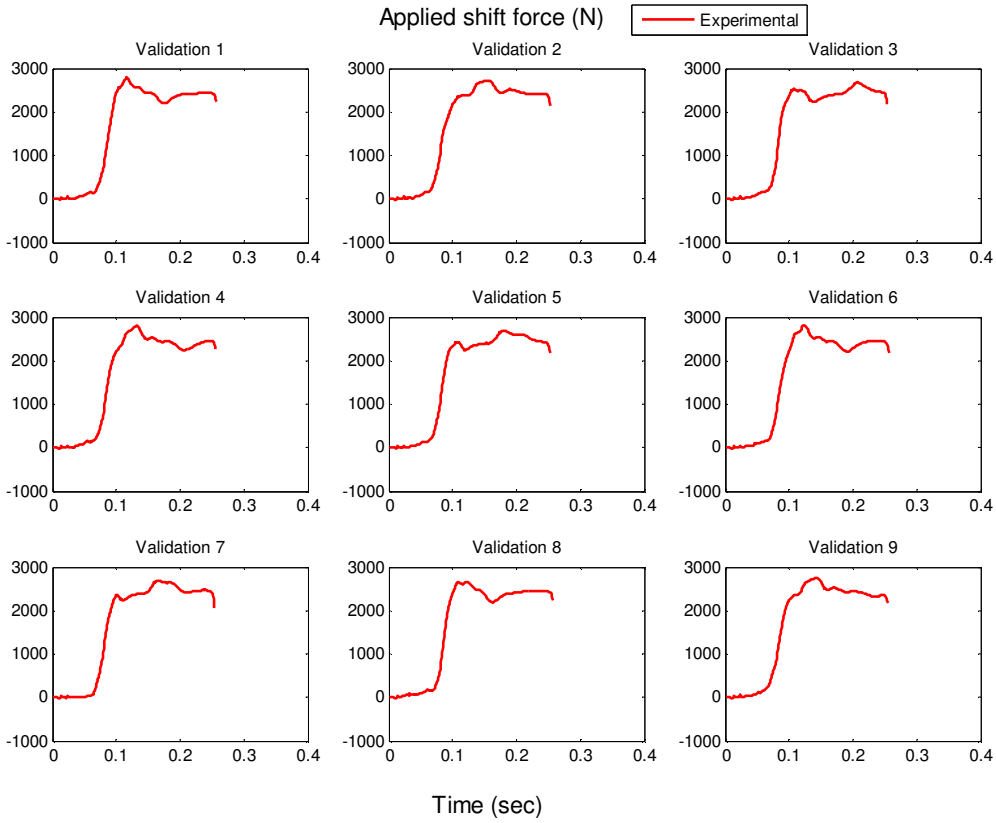

Figure 50: Applied shift force during experiments and simulations.

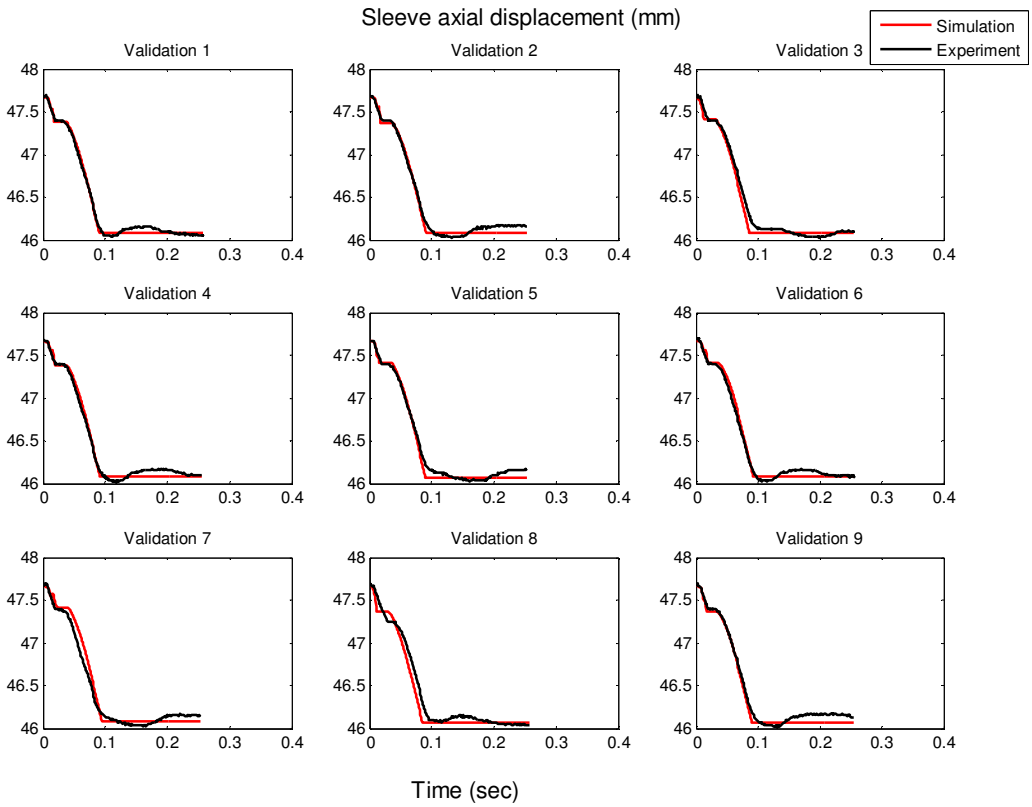

Figure 51: Obtained sleeve axial displacement during experiments.

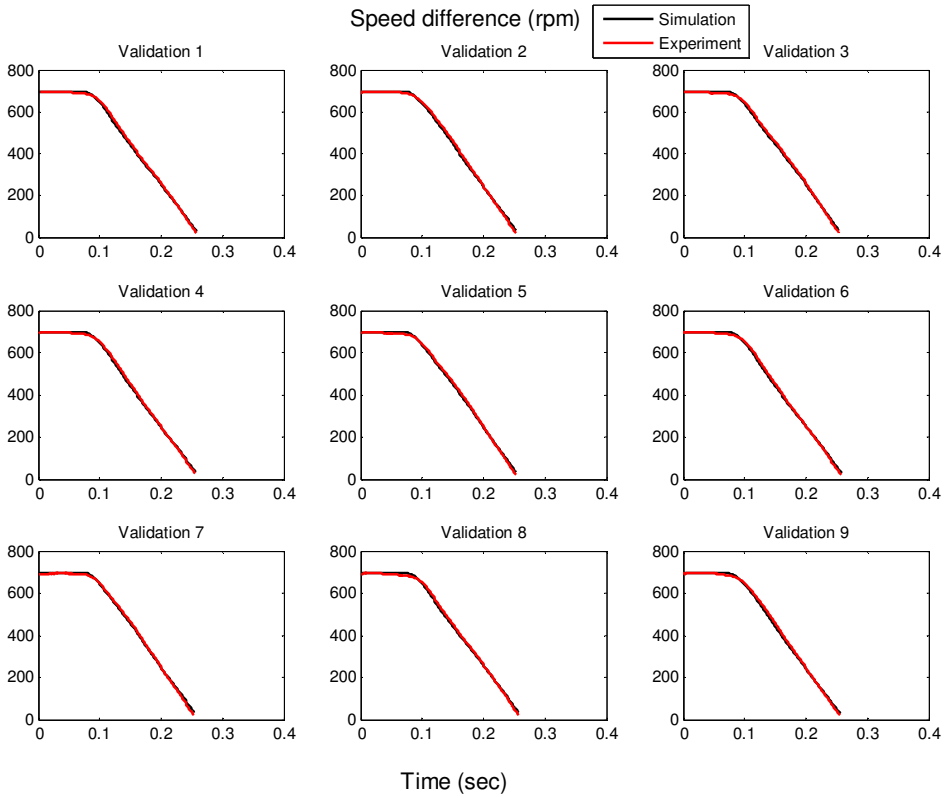

Figure 52: Obtained speed difference during experiments.

The results of validation are depicted in *Figures 48-52.* The results are closely matched as shown in Figure 49 except some small noticeable variations in the sleeve axial displacement.

In validation 8 (see *Figure* 52) the phase 1a takes longer time that means the sleeve has to travel more axial displacement than the expected designed displacement to come in contact with the spring. That kind of variation can be expected from the practical application that the ring has already travelled some axial displacement with spring before starting the synchronization and that's why the sleeve also has to travel longer displacement than usual to complete the phase 1a. The similar kind of reason is expected in validation 7 of the phase 1b but with angular indexing. It seems from the experimental data that the ring has already got some angular displacement before start of the phase 1b and that's why the ring takes shorter time to complete its angular indexing position.

Except the phase 2, there can be different reasons for the small variations between the experimental data and the simulation: experimental error, unexpected or unobserved or un-control resisting agents in the test rig/real application which are still did not implement in the simulation. Variation during the phase 2 in axial displacement shows that the three bodies are moving together axially that means the gearwheel has a flexible axial support instead of fixed axial support assumed in model. When the force decreases at end of phase 2, the bodies move back axially towards original position.

6. Conclusions and Future Work

In the present report mathematical and computational models of a generic synchronizer with five degrees of freedom have been developed using CLF. Application of CLF on the modelling of the synchronization process gives system of differential-algebraic equations (DAE). Adams-Bashforth predictor corrector method is used to solve the obtained system of DAE. Direct dynamics, semi-inverse dynamics and inverse dynamics problems have been formulated and solved numerically. Analysis of the generic synchronizer performance diagrams has shown that the CLF based model is able to predict the synchronization process characteristics reasonably well. The developed model has been validated by using measurement data from test rig at Scania CV AB. Performance of the generic synchronizer is also analyzed in case of driveline vibrations. Sensitivity analysis of the synchronizer mechanism performance with respect to cone angle, coefficient of friction, maximum value of shift force and rate of applying shift force has been done.

Next, the developed models will be used to get further insight into synchronizer design and its performance diagrams with aid of global sensitivity analysis and Pareto optimization.

ACKNOWLEDGMENTS

Scania CV AB, Volvo GTT and the Sweden's Innovation Agency, VINNOVA are gratefully acknowledged for financially supporting the presented research, (project No: 2012-04619). The authors wish to thank Magnus Andersson for suggesting the engineering model of a generic synchronizer and Daniel Häggström and Kenth Hellström for experimental data and fruitful discussions.

References

[1] A. Bedmar, "Synchronization processes and synchronizer mechanisms" ,Diploma work no. 2013:20, Department of Applied Mechanics, Chalmers University of Technology, Göteborg, Sweden 2013.

[2] V. Berbyuk, "Towards Pareto optimization of performance of a generic synchronizer of transmission systems", in *In proceedings of IDETC/CIE 2015 ASME Conference*, Boston, USA, August 2-5, 2015 paper DETC 2015-46773, doi:10.1115/DETC 2015-46773.

[3] H. Hoshino, "Analysis on Synchronization Mechanism of Transmission", International Congress and Exposition, Detroit, Michigan, March 1-4, 1999.

[4] D. Kelly and C. Kent, "Gear Shift Quality Improvement In Manual Transmissions Using Dynamic Modelling", FISITA World Automotive Congress, Seoul, Korea, June 12-15, 2000.

[5] D. Häggström and M. Nordlander, "Development of a Program for Calculating Gearbox Synchronization", Master thesis, Department of Engineering Sciences and Mathematics, Luleå University of Technology, Södertälje, Luleå, 2011.

[6] E. J. Haug, "Intermediate Dynamics", Prentice Hall Englewood Cliffs, New Jersey, 1992.

[7] A. A. Shabana, "Dynamics of multibody systems", Cambridge: Cambridge university press, 1998, Second edition.

[8] L. Lovas, "Etude des relations entre le comportment et la fabrication des synchronisateurs des synchronisateurs des", National Institute of Applied Sciences, Lyon, PhD Thesis, 2004.

[9] R. Socin and L. Walters, "Manual Transmission Synchronizers", *SAE Technical Paper 680008,* 1968, doi:10.4271/680008.

Appendix

A.1 Constraints and equations of motion for generic synchronizer

The explicit expressions pertinent to problem B are given here.

A.1.1 Phase 1a-Equations

F_{sq} and T_{sq} are given in [8]. In case of constant with groves on the cones $K_{NC} = 0.1$ is assumed.

$$F_{sq} = K_{NC}\, 16\pi\rho\dot{d}_{\alpha} \sin(\alpha)\; r_c \left(\frac{b}{h_{\alpha}}\right)^3$$
$$T_{sq} = 4\pi\rho\dot{d}_{\alpha} r_c^3\, \dot{\theta}_s \frac{b}{h}\left(1 - \frac{\dot{\theta}_r}{\dot{\theta}_s}\right) \tag{A.1.1}$$

The set of active constraint for the phase 1a is

$$\boldsymbol{\Phi}(\boldsymbol{q}, t) = \begin{bmatrix} \boldsymbol{\Phi}^{external} \\ \boldsymbol{\Phi}^{internal} \end{bmatrix} = \begin{bmatrix} x_s - v_s t \\ \theta_s - \omega_s t \\ x_r \end{bmatrix} = \mathbf{0} \tag{A.1.2}$$

with

$$\frac{\partial \boldsymbol{\Phi}}{\partial \boldsymbol{q}} = \begin{bmatrix} 1 & 0 & 0 & 0 & 0 \\ 0 & 1 & 0 & 0 & 0 \\ 0 & 0 & 1 & 0 & 0 \end{bmatrix}, \quad \frac{\partial \boldsymbol{\Phi}}{\partial t} = \begin{bmatrix} -v_s \\ -\omega_s \\ 0 \end{bmatrix}$$

At start of the phase 1a, $x_{s_0} = \theta_{s_0} = \theta_{r_0} = \theta_{g_0} = 0$ and $x_r = 0$. It is assumed that $d_{\alpha} = 2mm$ and $B_{ang} = 5^o$.

The equations of motion are

$$\begin{bmatrix} m_s & 0 & 0 & 0 & 0 \\ 0 & I_s & 0 & 0 & 0 \\ 0 & 0 & m_r & 0 & 0 \\ 0 & 0 & 0 & I_r & 0 \\ 0 & 0 & 0 & 0 & I_g \end{bmatrix} \begin{bmatrix} \ddot{x}_s \\ \ddot{\theta}_s \\ \ddot{x}_r \\ \ddot{\theta}_r \\ \ddot{\theta}_g \end{bmatrix} - \begin{bmatrix} 1 & 0 & 0 \\ 0 & 1 & 0 \\ 0 & 0 & 1 \\ 0 & 0 & 0 \\ 0 & 0 & 0 \end{bmatrix} \begin{bmatrix} \lambda_1 \\ \lambda_2 \\ \lambda_3 \end{bmatrix} = \begin{bmatrix} F_s \\ 0 \\ 0 \\ 0 \\ 0 \end{bmatrix}^{app} - \begin{bmatrix} F_{sf} \\ M_{sf} \\ F_{rf} \\ M_{rf} \\ M_{gf} \end{bmatrix}^{fric} \tag{A.1.3}$$

where $F_{sf} = F_{sq} + C_{s\alpha}\, sign(\dot{x}_s)$, $M_{sf} = T_{sq} + C_s\dot{\theta}_s$, $F_{rf} = -F_{sq}$, $M_{rf} = -T_{sq} + C_r\, \dot{\theta}_r$, $M_{gf} = C_g\ \dot{\theta}_g$. F_{sq} and T_{sq} are viscous force and viscous torque which will transfer during the phase. Q^A is equal to the frictional forces $\left[F_{sf}, M_{sf}, F_{rf}, M_{rf}, M_{gf}\right]^{fric}$.

The acceleration equation becomes

$$\begin{bmatrix} m_s & 0 & 0 & 0 & 0 & 1 & 0 & 0 \\ 0 & I_s & 0 & 0 & 0 & 0 & 1 & 0 \\ 0 & 0 & m_r & 0 & 0 & 0 & 0 & 1 \\ 0 & 0 & 0 & I_r & 0 & 0 & 0 & 0 \\ 0 & 0 & 0 & 0 & I_g & 0 & 0 & 0 \\ 1 & 0 & 0 & 0 & 0 & 0 & 0 & 0 \\ 0 & 1 & 0 & 0 & 0 & 0 & 0 & 0 \\ 0 & 0 & 1 & 0 & 0 & 0 & 0 & 0 \end{bmatrix} \begin{bmatrix} \ddot{x}_s \\ \ddot{\theta}_s \\ \ddot{x}_r \\ \ddot{\theta}_r \\ \ddot{\theta}_g \\ \lambda_1 \\ \lambda_2 \\ \lambda_3 \end{bmatrix} = \begin{bmatrix} F_s - F_{sf} \\ -M_{sf} \\ -F_{rf} \\ -M_{rf} \\ -M_{gf} \\ 0 \\ 0 \\ 0 \end{bmatrix} \tag{A.1.4}$$

and

$$\boldsymbol{\gamma} = -\left[\frac{\partial}{\partial \boldsymbol{q}}\left(\frac{\partial \boldsymbol{\Phi}}{\partial \boldsymbol{q}}\dot{\boldsymbol{q}}\right)\right]\dot{\boldsymbol{q}} - 2\frac{\partial}{\partial \boldsymbol{q}}\left(\frac{\partial \boldsymbol{\Phi}}{\partial t}\right)\dot{\boldsymbol{q}} - \frac{\partial}{\partial t}\left(\frac{\partial \boldsymbol{\Phi}}{\partial t}\right) \Rightarrow \boldsymbol{\gamma} = \begin{bmatrix} 0 \\ 0 \\ 0 \end{bmatrix} \tag{A.1.5}$$

The end condition is $\theta_r - \theta_g = B_{ang}$.

A.1.2 Phase 1b-Equations

Since angular indexing is complete. The gear and the ring will rotate together. During the phase 1b, torque transferred by cones is small but at least higher than the oil splashing losses to keep the splines in contact. The cone clearance decreases to 1mm.

It is assumed that $d_{vis} = 1\text{mm}$. The set of active constraint for the phase 1b is

$$\boldsymbol{\Phi}(\boldsymbol{q}, t) = \begin{bmatrix} \boldsymbol{\Phi}^{external} \\ \boldsymbol{\Phi}^{internal} \end{bmatrix} = \begin{bmatrix} x_s - v_s t \\ \theta_s - \omega_s t \\ x_r \\ \theta_r - \theta_g - B_{ang} \end{bmatrix} = \mathbf{0} \tag{A.1.6}$$

with

$$\frac{\partial \boldsymbol{\Phi}}{\partial \boldsymbol{q}} = \begin{bmatrix} 1 & 0 & 0 & 0 & 0 \\ 0 & 1 & 0 & 0 & 0 \\ 0 & 0 & 1 & 0 & 0 \\ 0 & 0 & 0 & 1 & -1 \end{bmatrix}, \qquad \frac{\partial \boldsymbol{\Phi}}{\partial t} = \begin{bmatrix} -v_s \\ -\omega_s \\ 0 \\ 0 \end{bmatrix}$$

The equations of motion are

$$\begin{bmatrix} m_s & 0 & 0 & 0 & 0 \\ 0 & I_s & 0 & 0 & 0 \\ 0 & 0 & m_r & 0 & 0 \\ 0 & 0 & 0 & I_r & 0 \\ 0 & 0 & 0 & 0 & I_g \end{bmatrix} \begin{bmatrix} \ddot{x}_s \\ \ddot{\theta}_s \\ \ddot{x}_r \\ \ddot{\theta}_r \\ \ddot{\theta}_g \end{bmatrix} - \begin{bmatrix} 1 & 0 & 0 & 0 \\ 0 & 1 & 0 & 0 \\ 0 & 0 & 1 & 0 \\ 0 & 0 & 0 & 1 \\ 0 & 0 & 0 & -1 \end{bmatrix} \begin{bmatrix} \lambda_1 \\ \lambda_2 \\ \lambda_3 \\ \lambda_4 \end{bmatrix} = \begin{bmatrix} F_s \\ 0 \\ 0 \\ 0 \\ 0 \end{bmatrix}^{app} - \begin{bmatrix} F_{sf} \\ M_{sf} \\ F_{rf} \\ M_{rf} \\ M_{gf} \end{bmatrix}^{fric} \tag{A.1.7}$$

where $F_{sf} = F_{sq} + C_{s\alpha}\, sign(\dot{x}_s)$, $M_{sf} = T_{sq} + C_s\, sign(\dot{\theta}_s)$, $F_{rf} = -F_{sq}$, $M_{rf} = -T_{sq} + C_r sign(\dot{\theta}_r)$, $M_{gf} = C_g\, sign(\dot{\theta}_g)$. Q^A is equal to the frictional forces $[F_{sf}, M_{sf}, F_{rf}, M_{rf}, M_{gf}]^{fric}$.

$$\begin{bmatrix} m_s & 0 & 0 & 0 & 0 & 1 & 0 & 0 & 0 \\ 0 & I_s & 0 & 0 & 0 & 0 & 1 & 0 & 0 \\ 0 & 0 & m_r & 0 & 0 & 0 & 0 & 1 & 0 \\ 0 & 0 & 0 & I_r & 0 & 0 & 0 & 0 & 1 \\ 0 & 0 & 0 & 0 & I_g & 0 & 0 & 0 & -1 \\ 1 & 0 & 0 & 0 & 0 & 0 & 0 & 0 & 0 \\ 0 & 1 & 0 & 0 & 0 & 0 & 0 & 0 & 0 \\ 0 & 0 & 1 & 0 & 0 & 0 & 0 & 0 & 0 \\ 0 & 0 & 0 & 1 & -1 & 0 & 0 & 0 & 0 \end{bmatrix} \begin{bmatrix} \ddot{x}_s \\ \ddot{\theta}_s \\ \ddot{x}_r \\ \ddot{\theta}_r \\ \ddot{\theta}_g \\ \lambda_1 \\ \lambda_2 \\ \lambda_3 \\ \lambda_4 \end{bmatrix} = \begin{bmatrix} F_s - F_{sf} \\ -M_{sf} \\ -F_{rf} \\ -M_{rf} \\ -M_{gf} \\ 0 \\ 0 \\ 0 \\ 0 \end{bmatrix} \tag{A.1.8}$$

and $\boldsymbol{\gamma} = [0\ 0\ 0\ 0]^T$. The phase ends when $d_\alpha = d_{vis}$.

A.1.3 Phase 1c-Equations

The sleeve and the ring will move axially with same and constant axial speed. The gear and the ring will rotate with same rotational speed during the phase 1c. It is assumed that $B_{ax} = 1\ \mathrm{mm}$.

The set of active constraint for the phase 1c is

$$\boldsymbol{\Phi}(\boldsymbol{q}, t) = \begin{bmatrix} \boldsymbol{\Phi}^{external} \\ \boldsymbol{\Phi}^{internal} \end{bmatrix} = \begin{bmatrix} x_s - v_s t \\ \theta_s - \omega_s t \\ x_s - x_r - d_{vis} \\ \theta_r - \theta_g - B_{ang} \end{bmatrix} = \mathbf{0} \tag{A.1.9}$$

with

$$\frac{\partial \boldsymbol{\Phi}}{\partial \boldsymbol{q}} = \begin{bmatrix} 1 & 0 & 0 & 0 & 0 \\ 0 & 1 & 0 & 0 & 0 \\ 1 & 0 & -1 & 0 & 0 \\ 0 & 0 & 0 & 1 & -1 \end{bmatrix}, \qquad \frac{\partial \boldsymbol{\Phi}}{\partial t} = \begin{bmatrix} -v_s \\ -\omega_s \\ 0 \\ 0 \end{bmatrix}$$

The equations of motion are

$$\begin{bmatrix} m_s & 0 & 0 & 0 & 0 \\ 0 & I_s & 0 & 0 & 0 \\ 0 & 0 & m_r & 0 & 0 \\ 0 & 0 & 0 & I_r & 0 \\ 0 & 0 & 0 & 0 & I_g \end{bmatrix} \begin{bmatrix} \ddot{x}_s \\ \ddot{\theta}_s \\ \ddot{x}_r \\ \ddot{\theta}_r \\ \ddot{\theta}_g \end{bmatrix} - \begin{bmatrix} 1 & 0 & 1 & 0 \\ 0 & 1 & 0 & 0 \\ 0 & 0 & -1 & 0 \\ 0 & 0 & 0 & 1 \\ 0 & 0 & 0 & -1 \end{bmatrix} \begin{bmatrix} \lambda_1 \\ \lambda_2 \\ \lambda_3 \\ \lambda_4 \end{bmatrix} = \begin{bmatrix} F_s \\ 0 \\ 0 \\ 0 \\ 0 \end{bmatrix}^{app} - \begin{bmatrix} F_{sf} \\ M_{sf} \\ F_{rf} \\ M_{rf} \\ M_{gf} \end{bmatrix}^{fric} \tag{A.1.10}$$

where $F_{sf} = F_{sq} + C_{s\alpha}\, sign(\dot{x}_s)$, $M_{sf} = T_{sq} + C_s\dot{\theta}_s$, $F_{rf} = -F_{sq} + C_{r\beta}\, sign(\dot{x}_r)$, $M_{rf} = -T_{sq} + C_r\, \dot{\theta}_r$, $M_{gf} = C_g\ \dot{\theta}_g$. Q^A is equal to the frictional forces $\left[F_{sf}, M_{sf}, F_{rf}, M_{rf}, M_{gf}\right]^{fric}$.

$$\begin{bmatrix} m_s & 0 & 0 & 0 & 0 & 1 & 0 & 1 & 0 \\ 0 & I_s & 0 & 0 & 0 & 0 & 1 & 0 & 0 \\ 0 & 0 & m_r & 0 & 0 & 0 & 0 & -1 & 0 \\ 0 & 0 & 0 & I_r & 0 & 0 & 0 & 0 & 1 \\ 0 & 0 & 0 & 0 & I_g & 0 & 0 & 0 & -1 \\ 1 & 0 & 0 & 0 & 0 & 0 & 0 & 0 & 0 \\ 0 & 1 & 0 & 0 & 0 & 0 & 0 & 0 & 0 \\ 1 & 0 & 1 & 0 & 0 & 0 & 0 & 0 & 0 \\ 0 & 0 & 0 & 1 & -1 & 0 & 0 & 0 & 0 \end{bmatrix} \begin{bmatrix} \ddot{x}_s \\ \ddot{\theta}_s \\ \ddot{x}_r \\ \ddot{\theta}_r \\ \ddot{\theta}_g \\ \lambda_1 \\ \lambda_2 \\ \lambda_3 \\ \lambda_4 \end{bmatrix} = \begin{bmatrix} F_s - F_{sf} \\ -M_{sf} \\ -F_{rf} \\ -M_{rf} \\ -M_{gf} \\ 0 \\ 0 \\ 0 \\ 0 \end{bmatrix} \tag{A.1.11}$$

and $\boldsymbol{\gamma} = [0\ 0\ 0\ 0]^T$.
The end condition is $x_r = B_{ax,N} = B_{ax}(t = 0)$.

A.1.4 Phase 1d-Equations

The sleeve will move with constant axial speed while the ring will not move axially further because of the chamfers blocking contact and the spring detent contact. The gearwheel and the ring will rotate with same rotational speed which is affected by the viscous friction torque.

$$\boldsymbol{\Phi}(\boldsymbol{q}, t) = \begin{bmatrix} \boldsymbol{\Phi}^{external} \\ \boldsymbol{\Phi}^{internal} \end{bmatrix} = \begin{bmatrix} x_s - v_s t \\ \theta_s - \omega_s t \\ x_r - B_{ax,N} \\ \theta_r - \theta_g - B_{ang} \end{bmatrix} = \mathbf{0} \tag{A.1.12}$$

with

$$\frac{\partial \boldsymbol{\Phi}}{\partial \boldsymbol{q}} = \begin{bmatrix} 1 & 0 & 0 & 0 & 0 \\ 0 & 1 & 0 & 0 & 0 \\ 0 & 0 & 1 & 0 & 0 \\ 0 & 0 & 0 & 1 & -1 \end{bmatrix}, \qquad \frac{\partial \boldsymbol{\Phi}}{\partial t} = \begin{bmatrix} -v_s \\ -\omega_s \\ 0 \\ 0 \end{bmatrix}$$

The equations of motion are

$$\begin{bmatrix} m_s & 0 & 0 & 0 & 0 \\ 0 & I_s & 0 & 0 & 0 \\ 0 & 0 & m_r & 0 & 0 \\ 0 & 0 & 0 & I_r & 0 \\ 0 & 0 & 0 & 0 & I_g \end{bmatrix} \begin{bmatrix} \ddot{x}_s \\ \ddot{\theta}_s \\ \ddot{x}_r \\ \ddot{\theta}_r \\ \ddot{\theta}_g \end{bmatrix} - \begin{bmatrix} 1 & 0 & 0 & 0 \\ 0 & 1 & 0 & 0 \\ 0 & 0 & 1 & 0 \\ 0 & 0 & 0 & 1 \\ 0 & 0 & 0 & -1 \end{bmatrix} \begin{bmatrix} \lambda_1 \\ \lambda_2 \\ \lambda_3 \\ \lambda_4 \end{bmatrix} = \begin{bmatrix} F_s \\ 0 \\ 0 \\ 0 \\ 0 \end{bmatrix}^{app} - \begin{bmatrix} F_{sf} \\ M_{sf} \\ F_{rf} \\ M_{rf} \\ M_{gf} \end{bmatrix}^{fric} \tag{A.1.13}$$

where $F_{sf} = F_{sq} + C_{s\alpha}\, sign(\dot{x}_s)$, $M_{sf} = T_{sq} + C_s\dot{\theta}_s$, $F_{rf} = -F_{sq}$, $M_{rf} = -T_{sq} + C_r\, \dot{\theta}_r$, $M_{gf} = C_g\ \dot{\theta}_g$. Q^A is equal to the frictional forces $\left[F_{sf}, M_{sf}, F_{rf}, M_{rf}, M_{gf}\right]^{fric}$.

$$\begin{bmatrix} m_s & 0 & 0 & 0 & 0 & 1 & 0 & 0 & 0 \\ 0 & I_s & 0 & 0 & 0 & 0 & 1 & 0 & 0 \\ 0 & 0 & m_r & 0 & 0 & 0 & 0 & 1 & 0 \\ 0 & 0 & 0 & I_r & 0 & 0 & 0 & 0 & 1 \\ 0 & 0 & 0 & 0 & I_g & 0 & 0 & 0 & -1 \\ 1 & 0 & 0 & 0 & 0 & 0 & 0 & 0 & 0 \\ 0 & 1 & 0 & 0 & 0 & 0 & 0 & 0 & 0 \\ 0 & 0 & 1 & 0 & 0 & 0 & 0 & 0 & 0 \\ 0 & 0 & 0 & 1 & -1 & 0 & 0 & 0 & 0 \end{bmatrix} \begin{bmatrix} \ddot{x}_s \\ \ddot{\theta}_s \\ \ddot{x}_r \\ \ddot{\theta}_r \\ \ddot{\theta}_g \\ \lambda_1 \\ \lambda_2 \\ \lambda_3 \\ \lambda_4 \end{bmatrix} = \begin{bmatrix} F_s - F_{sf} \\ -M_{sf} \\ -F_{rf} \\ -M_{rf} \\ -M_{gf} \\ 0 \\ 0 \\ 0 \\ 0 \end{bmatrix} \tag{A.1.14}$$

and $\boldsymbol{\gamma} = [0\ 0\ 0\ 0]^T$.
The phase end condition is $h_\alpha = d_{mix}$.

A.1.5 Phase 1e-Equations

The cone force during mixed friction was derived in [8] as

$$F_c = \left[\frac{F_{dry} - F_{sq}}{t_{dry} - t_{vis}}\right](t - t_{vis}) \qquad T_c = \eta_1 F_c + \eta_2 + \eta_3 \omega_r \tag{A.1.15}$$

Where $\eta_i = \lambda_{cons}\, \chi_{\,i}$, $\lambda_{cons} = \frac{r_c}{\sin(\alpha)}\left(1 + \frac{1}{3}\left(\frac{b}{r_c}\right)^2 \sin^2(\alpha)\right)$ [8]

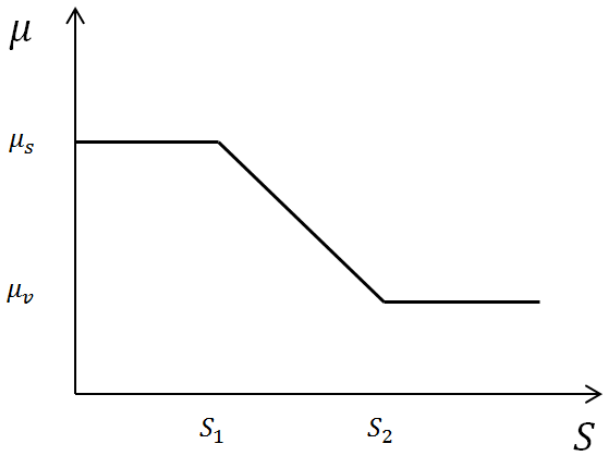

Figure 53: Stribeck diagram in case of linear mixed friction.

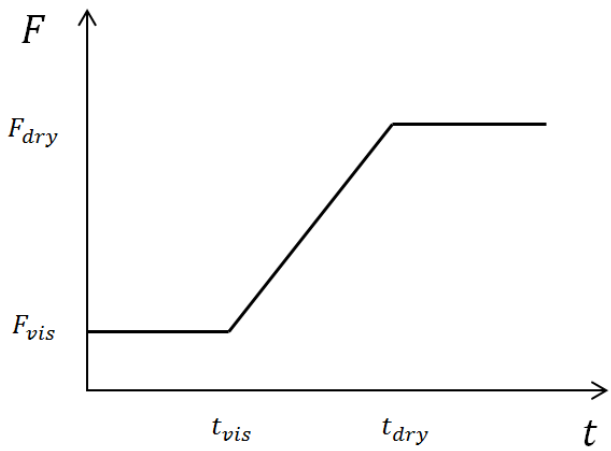

Figure 54: Linear increment of force from viscous friction to solid friction. [8]

The set of active constraint for the phase 1e is

$$\boldsymbol{\Phi}(\boldsymbol{q},t) = \begin{bmatrix} \boldsymbol{\Phi}^{external} \\ \boldsymbol{\Phi}^{internal} \end{bmatrix} = \begin{bmatrix} x_s - v_s t \\ \theta_s - \omega_s t \\ x_r - d_\alpha \\ \theta_r - \theta_g - B_{ang} \end{bmatrix} = \mathbf{0} \tag{A.1.16}$$

where x_r is independent of time.

$$\frac{\partial \boldsymbol{\Phi}}{\partial \boldsymbol{q}} = \begin{bmatrix} 1 & 0 & 0 & 0 & 0 \\ 0 & 1 & 0 & 0 & 0 \\ 0 & 0 & 1 & 0 & 0 \\ 0 & 0 & 0 & 1 & -1 \end{bmatrix}, \quad \frac{\partial \boldsymbol{\Phi}}{\partial t} = \begin{bmatrix} -v_s \\ -\omega_s \\ 0 \\ 0 \end{bmatrix}$$

The equations of motion are

$$\begin{bmatrix} m_s & 0 & 0 & 0 & 0 \\ 0 & I_s & 0 & 0 & 0 \\ 0 & 0 & m_r & 0 & 0 \\ 0 & 0 & 0 & I_r & 0 \\ 0 & 0 & 0 & 0 & I_g \end{bmatrix} \begin{bmatrix} \ddot{x}_s \\ \ddot{\theta}_s \\ \ddot{x}_r \\ \ddot{\theta}_r \\ \ddot{\theta}_g \end{bmatrix} - \begin{bmatrix} 1 & 0 & 0 & 0 \\ 0 & 1 & 0 & 0 \\ 0 & 0 & 1 & 0 \\ 0 & 0 & 0 & 1 \\ 0 & 0 & 0 & -1 \end{bmatrix} \begin{bmatrix} \lambda_1 \\ \lambda_2 \\ \lambda_3 \\ \lambda_4 \end{bmatrix} = \begin{bmatrix} F_s \\ 0 \\ 0 \\ 0 \\ 0 \end{bmatrix}^{app} - \begin{bmatrix} F_{sf} \\ M_{sf} \\ F_{rf} \\ M_{rf} \\ M_{gf} \end{bmatrix}^{fric} \tag{A.1.17}$$

Where $F_{sf} = F_c + C_{s\alpha}\, sign(\dot{x}_s)$, $M_{sf} = T_c + C_s\dot{\theta}_s$, $F_{rf} = -F_c$, $M_{rf} = -T_c + C_r\, \dot{\theta}_r$, $M_{gf} = C_g\ \dot{\theta}_g$. Q^A is equal to the frictional forces $\left[F_{sf}, M_{sf}, F_{rf}, M_{rf}, M_{gf}\right]^{fric}$.

$$\begin{bmatrix} m_s & 0 & 0 & 0 & 0 & 1 & 0 & 0 & 0 \\ 0 & I_s & 0 & 0 & 0 & 0 & 1 & 0 & 0 \\ 0 & 0 & m_r & 0 & 0 & 0 & 0 & 1 & 0 \\ 0 & 0 & 0 & I_r & 0 & 0 & 0 & 0 & 1 \\ 0 & 0 & 0 & 0 & I_g & 0 & 0 & 0 & -1 \\ 1 & 0 & 0 & 0 & 0 & 0 & 0 & 0 & 0 \\ 0 & 1 & 0 & 0 & 0 & 0 & 0 & 0 & 0 \\ 0 & 0 & 1 & 0 & 0 & 0 & 0 & 0 & 0 \\ 0 & 0 & 0 & 1 & -1 & 0 & 0 & 0 & 0 \end{bmatrix} \begin{bmatrix} \ddot{x}_s \\ \ddot{\theta}_s \\ \ddot{x}_r \\ \ddot{\theta}_r \\ \ddot{\theta}_g \\ \lambda_1 \\ \lambda_2 \\ \lambda_3 \\ \lambda_4 \end{bmatrix} = \begin{bmatrix} F_s - F_{sf} \\ -M_{sf} \\ -F_{rf} \\ -M_{rf} \\ M_{gf} \\ 0 \\ 0 \\ 0 \end{bmatrix} \tag{A.1.18}$$

and $\boldsymbol{\gamma} = [0\ 0\ 0\ 0]^T$.
The phase will end when the dry friction will start.

A.1.6 Phase 1f-Equations

The cone torque is

$$T_c = \lambda_{cons}\, \mu_\alpha\, F_s \tag{A.1.19}$$

where F_s is the applied shift force and F_{sq}^{mix} is shift force at end of the phase 1e. The set of active constraint for the phase 1f is

$$\boldsymbol{\Phi}(\boldsymbol{q}, t) = \begin{bmatrix} \boldsymbol{\Phi}^{external} \\ \boldsymbol{\Phi}^{internal} \end{bmatrix} = \begin{bmatrix} x_s - d_\alpha - B_{ax} \\ \theta_s - \omega_s t \\ x_r - x_s - d_\alpha \\ \theta_r - \theta_g - B_{ang} \end{bmatrix} = \mathbf{0} \tag{A.1.20}$$

Where x_r and x_s are independent of time.

$$\frac{\partial \boldsymbol{\Phi}}{\partial \boldsymbol{q}} = \begin{bmatrix} 1 & 0 & 0 & 0 & 0 \\ 0 & 1 & 0 & 0 & 0 \\ 1 & 0 & -1 & 0 & 0 \\ 0 & 0 & 0 & 1 & -1 \end{bmatrix}, \quad \frac{\partial \boldsymbol{\Phi}}{\partial t} = \begin{bmatrix} 0 \\ -\omega_s \\ 0 \\ 0 \end{bmatrix}$$

Equations of motion

$$\begin{bmatrix} m_s & 0 & 0 & 0 & 0 \\ 0 & I_s & 0 & 0 & 0 \\ 0 & 0 & m_r & 0 & 0 \\ 0 & 0 & 0 & I_r & 0 \\ 0 & 0 & 0 & 0 & I_g \end{bmatrix} \begin{bmatrix} \ddot{x}_s \\ \ddot{\theta}_s \\ \ddot{x}_r \\ \ddot{\theta}_r \\ \ddot{\theta}_g \end{bmatrix} - \begin{bmatrix} 1 & 0 & 1 & 0 \\ 0 & 1 & 0 & 0 \\ 0 & 0 & -1 & 0 \\ 0 & 0 & 0 & 1 \\ 0 & 0 & 0 & -1 \end{bmatrix} \begin{bmatrix} \lambda_1 \\ \lambda_2 \\ \lambda_3 \\ \lambda_4 \end{bmatrix} = \begin{bmatrix} F_s \\ 0 \\ 0 \\ 0 \\ 0 \end{bmatrix}^{app} - \begin{bmatrix} F_{sf} \\ M_{sf} \\ F_{rf} \\ M_{rf} \\ M_{gf} \end{bmatrix}^{fric} \tag{A.1.21}$$

Where $F_{sf} = 0$, $M_{sf} = T_c + C_s\dot{\theta}_s$, $F_{rf} = 0$, $M_{rf} = -T_c + C_r\, \dot{\theta}_r$, $M_{gf} = C_g\ \dot{\theta}_g$. Q^A is equal to the frictional forces $\left[F_{sf}, M_{sf}, F_{rf}, M_{rf}, M_{gf}\right]^{fric}$ and applied force $[F_s]^{app}$.

$$\begin{bmatrix} m_s & 0 & 0 & 0 & 0 & 1 & 0 & 1 & 0 \\ 0 & I_s & 0 & 0 & 0 & 0 & 1 & 0 & 0 \\ 0 & 0 & m_r & 0 & 0 & 0 & 0 & -1 & 0 \\ 0 & 0 & 0 & I_r & 0 & 0 & 0 & 0 & 1 \\ 0 & 0 & 0 & 0 & I_g & 0 & 0 & 0 & -1 \\ 1 & 0 & 0 & 0 & 0 & 0 & 0 & 0 & 0 \\ 0 & 1 & 0 & 0 & 0 & 0 & 0 & 0 & 0 \\ 1 & 0 & -1 & 0 & 0 & 0 & 0 & 0 & 0 \\ 0 & 0 & 0 & 1 & -1 & 0 & 0 & 0 & 0 \end{bmatrix} \begin{bmatrix} \ddot{x}_s \\ \ddot{\theta}_s \\ \ddot{x}_r \\ \ddot{\theta}_r \\ \ddot{\theta}_g \\ \lambda_1 \\ \lambda_2 \\ \lambda_3 \\ \lambda_4 \end{bmatrix} = \begin{bmatrix} F_s - F_{sf} \\ -M_{sf} \\ -F_{rf} \\ -M_{rf} \\ -M_{gf} \\ 0 \\ 0 \\ 0 \\ 0 \end{bmatrix} \tag{A.1.22}$$

and $\boldsymbol{\gamma} = [0\ 0\ 0\ 0]^T$.

The end condition is $F_{ax} \geq F_{spring} + F_{sq}^{mix}$.

A.1.7 Phase 2-Equation

The cone torque is

$$T_c = \lambda_{cons}\, \mu_\alpha\, F_s \tag{A.1.23}$$

where $\lambda_{cons} = \frac{r_c}{\sin(\alpha)}\left(1 + \frac{1}{3}\left(\frac{b}{r_c}\right)^2 \sin^2(\alpha)\right)$ [8] and F_s is applied shift force.

The set of active constraint for the phase 2 is

$$\boldsymbol{\Phi}(\boldsymbol{q}, t) = \begin{bmatrix} \boldsymbol{\Phi}^{external} \\ \boldsymbol{\Phi}^{internal} \end{bmatrix} = \begin{bmatrix} x_s - d_\alpha - B_{ax} \\ \theta_s - \omega_s t \\ x_r - x_s - d_\alpha \\ \theta_r - \theta_g - B_{ang} \end{bmatrix} = \mathbf{0} \tag{A.1.24}$$

with

$$\frac{\partial \boldsymbol{\Phi}}{\partial \boldsymbol{q}} = \begin{bmatrix} 1 & 0 & 0 & 0 & 0 \\ 0 & 1 & 0 & 0 & 0 \\ -1 & 0 & 1 & 0 & 0 \\ 0 & 0 & 0 & 1 & -1 \end{bmatrix}, \quad \frac{\partial \boldsymbol{\Phi}}{\partial t} = \begin{bmatrix} 0 \\ -\omega_s \\ 0 \\ 0 \end{bmatrix}$$

The equations of motion are

$$\begin{bmatrix} m_s & 0 & 0 & 0 & 0 \\ 0 & I_s & 0 & 0 & 0 \\ 0 & 0 & m_r & 0 & 0 \\ 0 & 0 & 0 & I_r & 0 \\ 0 & 0 & 0 & 0 & I_g \end{bmatrix} \begin{bmatrix} \ddot{x}_s \\ \ddot{\theta}_s \\ \ddot{x}_r \\ \ddot{\theta}_r \\ \ddot{\theta}_g \end{bmatrix} - \begin{bmatrix} 1 & 0 & -1 & 0 \\ 0 & 1 & 0 & 0 \\ 0 & 0 & 1 & 0 \\ 0 & 0 & 0 & 1 \\ 0 & 0 & 0 & -1 \end{bmatrix} \begin{bmatrix} \lambda_1 \\ \lambda_2 \\ \lambda_3 \\ \lambda_4 \end{bmatrix} = \begin{bmatrix} F_s \\ 0 \\ 0 \\ 0 \\ 0 \end{bmatrix}^{app} - \begin{bmatrix} 0 \\ M_{sf} \\ F_{rf} \\ M_{rf} \\ M_{gf} \end{bmatrix}^{fric} \tag{A.1.25}$$

where $F_{sf} = 0$, $M_{sf} = T_c + C_s\dot{\theta}_s$, $F_{rf} = 0$, $M_{rf} = -T_c + C_r\, \dot{\theta}_r$, $M_{gf} = C_g\ \dot{\theta}_g$. Q^A is equal to the frictional forces $\left[F_{sf}, M_{sf}, F_{rf}, M_{rf}, M_{gf}\right]^{fric}$, and applied force $[F_s]^{app}$.

$$\begin{bmatrix} m_s & 0 & 0 & 0 & 0 & 1 & 0 & -1 & 0 \\ 0 & I_s & 0 & 0 & 0 & 0 & 1 & 0 & 0 \\ 0 & 0 & m_r & 0 & 0 & 0 & 0 & 1 & 0 \\ 0 & 0 & 0 & I_r & 0 & 0 & 0 & 0 & 1 \\ 0 & 0 & 0 & 0 & I_g & 0 & 0 & 0 & -1 \\ 1 & 0 & 0 & 0 & 0 & 0 & 0 & 0 & 0 \\ 0 & 1 & 0 & 0 & 0 & 0 & 0 & 0 & 0 \\ 1 & 0 & -1 & 0 & 0 & 0 & 0 & 0 & 0 \\ 0 & 0 & 0 & 1 & -1 & 0 & 0 & 0 & 0 \end{bmatrix} \begin{bmatrix} \ddot{x}_s \\ \ddot{\theta}_s \\ \ddot{x}_r \\ \ddot{\theta}_r \\ \ddot{\theta}_g \\ \lambda_1 \\ \lambda_2 \\ \lambda_3 \\ \lambda_4 \end{bmatrix} = \begin{bmatrix} F_s \\ -M_{sf} \\ 0 \\ -M_{rf} \\ -M_{gf} \\ 0 \\ 0 \\ 0 \\ 0 \end{bmatrix} \tag{A.1.26}$$

and $\boldsymbol{\gamma} = [0\ 0\ 0\ 0]^T$.

A.1.8 Phase 3a-Synchronized-Equations

The cone torque is

$$T_c = \lambda \mu_\alpha F_s \tag{A.1.27}$$

The set of active constraint for the phase 3a is

$$\boldsymbol{\Phi}(q,t) = \begin{bmatrix} \boldsymbol{\Phi}^{external} \\ \boldsymbol{\Phi}^{internal} \end{bmatrix} = \begin{bmatrix} x_s - v_s t \\ \theta_s - \omega_s t \\ x_r - x_s - d_\alpha \\ \theta_g - \theta_r + B_{ang} - \dfrac{x_r - B_{ax}}{r_\beta} \tan\beta \end{bmatrix} = \mathbf{0} \tag{A.1.28}$$

with

$$\frac{\partial \boldsymbol{\Phi}}{\partial \boldsymbol{q}} = \begin{bmatrix} 1 & 0 & 0 & 0 & 0 \\ 0 & 1 & 0 & 0 & 0 \\ 1 & 0 & -1 & 0 & 0 \\ 0 & 0 & -\dfrac{1}{r_\beta}\tan\beta & -1 & 1 \end{bmatrix}, \qquad \frac{\partial \boldsymbol{\Phi}}{\partial t} = \begin{bmatrix} -v_s \\ -\omega_s \\ 0 \\ 0 \end{bmatrix} = \mathbf{0}$$

The equations of motion are

$$\begin{bmatrix} m_s & 0 & 0 & 0 & 0 \\ 0 & I_s & 0 & 0 & 0 \\ 0 & 0 & m_r & 0 & 0 \\ 0 & 0 & 0 & I_r & 0 \\ 0 & 0 & 0 & 0 & I_g \end{bmatrix} \begin{bmatrix} \ddot{x}_s \\ \ddot{\theta}_s \\ \ddot{x}_r \\ \ddot{\theta}_r \\ \ddot{\theta}_g \end{bmatrix} - \begin{bmatrix} 1 & 0 & 1 & 0 \\ 0 & 1 & 0 & 0 \\ 0 & 0 & -1 & -\dfrac{1}{r_\beta}\tan\beta \\ 0 & 0 & 0 & -1 \\ 0 & 0 & 0 & 1 \end{bmatrix} \begin{bmatrix} \lambda_1 \\ \lambda_2 \\ \lambda_3 \\ \lambda_4 \end{bmatrix} = \begin{bmatrix} F_s \\ 0 \\ 0 \\ 0 \\ 0 \end{bmatrix}^{app} - \begin{bmatrix} F_{sf} \\ M_{sf} \\ F_{rf} \\ M_{rf} \\ M_{gf} \end{bmatrix}^{fric} \tag{A.1.29}$$

where $F_s = (max(F_{ax} + F_s) - 5t)N/s$, $F_{sf} = C_{s\alpha}\, sign(\dot{x}_{sl})$, $M_{sf} = T_{sq} + C_s \dot{\theta}_s$, $F_{rf} = C_{r\beta}\, sign(\dot{x}_r)$, $M_{rf} = -T_c + C_r\, \dot{\theta}_r$, $M_{gf} = C_g\ \dot{\theta}_g$. Q^A is equal to the frictional forces $\left[F_{sf}, M_{sf}, F_{rf}, M_{rf}, M_{gf}\right]^{fric}$ and external force $[F_s]^{app}$.

$$
\begin{bmatrix}
m_s & 0 & 0 & 0 & 0 & 1 & 0 & 1 & 0 \\
0 & I_s & 0 & 0 & 0 & 0 & 1 & 0 & 0 \\
0 & 0 & m_r & 0 & 0 & 0 & 0 & -1 & -\frac{1}{r_\beta}\tan\beta \\
0 & 0 & 0 & I_r & 0 & 0 & 0 & 0 & -1 \\
0 & 0 & 0 & 0 & I_g & 0 & 0 & 0 & 1 \\
1 & 0 & 0 & 0 & 0 & 0 & 0 & 0 & 0 \\
0 & 1 & -1 & 0 & 0 & 0 & 0 & 0 & 0 \\
1 & 0 & 1 - B_{ax} & 0 & 0 & 0 & 0 & 0 & 0 \\
0 & 0 & -\frac{1 - B_{ax}}{r_\beta}\tan\beta & -1 & 1 & 0 & 0 & 0 & 0
\end{bmatrix}
\begin{bmatrix}
\ddot{x}_s \\ \ddot{\theta}_s \\ \ddot{x}_r \\ \ddot{\theta}_r \\ \ddot{\theta}_g \\ \lambda_1 \\ \lambda_2 \\ \lambda_3 \\ \lambda_4
\end{bmatrix}
= \begin{bmatrix}
F_s - F_{sf} \\ -M_{sf} \\ -F_{rf} \\ -M_{rf} \\ -M_{gf} \\ 0 \\ 0 \\ 0 \\ 0
\end{bmatrix}
\tag{A.1.30}
$$

and $\boldsymbol{\gamma} = [0\ 0\ 0\ 0]^T$.

A.1.9 Phase 3b-Synchronized-Equations

The set of active constraint for the phase 3b is

$$
\boldsymbol{\Phi}(\boldsymbol{q}, t) = \begin{bmatrix} \boldsymbol{\Phi}^{external} \\ \boldsymbol{\Phi}^{internal} \end{bmatrix} = \begin{bmatrix}
x_s - v_s t \\ \theta_s - \omega_s t \\ x_r - x_s - d_\alpha \\ \theta_r - \theta_s - \Delta\theta \\ \theta_g - \theta_r + B_{ang} - \frac{x_r - B_{ax}}{r_\beta}\tan\beta
\end{bmatrix} = \mathbf{0}
\tag{A.1.31}
$$

$\Delta\theta$ is taken as $\theta_s - \theta_r$ at end of the phase 3a.

$$
\frac{\partial \boldsymbol{\Phi}}{\partial \boldsymbol{q}} = \begin{bmatrix}
1 & 0 & 0 & 0 & 0 \\
0 & 1 & 0 & 0 & 0 \\
-1 & 0 & 1 & 0 & 0 \\
0 & -1 & 0 & 1 & 0 \\
0 & 0 & -\frac{1}{r_\beta}\tan\beta & -1 & 1
\end{bmatrix}, \frac{\partial \boldsymbol{\Phi}}{\partial t} = \begin{bmatrix} -v_s \\ -\omega_s \\ 0 \\ 0 \\ 0 \end{bmatrix} = \mathbf{0}
$$

The equations of motion are

$$\begin{bmatrix} m_s & 0 & 0 & 0 & 0 \\ 0 & I_s & 0 & 0 & 0 \\ 0 & 0 & m_r & 0 & 0 \\ 0 & 0 & 0 & I_r & 0 \\ 0 & 0 & 0 & 0 & I_g \end{bmatrix} \begin{bmatrix} \ddot{x}_s \\ \ddot{\theta}_s \\ \ddot{x}_r \\ \ddot{\theta}_r \\ \ddot{\theta}_g \end{bmatrix} - \begin{bmatrix} 1 & 0 & 1 & 0 & 0 \\ 0 & 1 & 0 & 1 & 0 \\ 0 & 0 & -1 & 0 & -\frac{1}{r_\beta}\tan\beta \\ 0 & 0 & 0 & -1 & -1 \\ 0 & 0 & 0 & 0 & 1 \end{bmatrix} \begin{bmatrix} \lambda_1 \\ \lambda_2 \\ \lambda_3 \\ \lambda_4 \\ \lambda_5 \end{bmatrix}$$
$$= \begin{bmatrix} F_s \\ 0 \\ 0 \\ 0 \\ 0 \end{bmatrix}^{app} - \begin{bmatrix} F_{sf} \\ M_{sf} \\ F_{rf} \\ M_{rf} \\ M_{gf} \end{bmatrix}^{fric} \tag{A.1.32}$$

where $F_s = \left(F_{s,3a} - 4000t\right)N/s$, $F_{sf} = C_{s\alpha}\, sign(\dot{x}_{sl})$, $M_{sf} = C_s\dot{\theta}_s$, $F_{rf} = C_{r\beta}\, sign(\dot{x}_r)$, $M_{rf} = C_r\, \dot{\theta}_r$, $M_{gf} = C_g\ \dot{\theta}_g$. Q^A is equal to the frictional forces $\left[F_{sf}, M_{sf}, F_{rf}, M_{rf}, M_{gf}\right]^{fric}$ and external force $[F_s]^{app}$. $F_{s,3a}$ is shift force at end of the phase 3a.

$$\begin{bmatrix} m_s & 0 & 0 & 0 & 0 & 1 & 0 & 1 & 0 & 0 \\ 0 & I_s & 0 & 0 & 0 & 0 & 1 & 0 & 1 & 0 \\ 0 & 0 & m_r & 0 & 0 & 0 & 0 & -1 & 0 & -\frac{1}{r_\beta}\tan\beta \\ 0 & 0 & 0 & I_r & 0 & 0 & 0 & 0 & -1 & -1 \\ 0 & 0 & 0 & 0 & I_g & 0 & 0 & 0 & 0 & 1 \\ 1 & 0 & 0 & 0 & 0 & 0 & 0 & 0 & 0 & 0 \\ 0 & 1 & -1 & 0 & 0 & 0 & 0 & 0 & 0 & 0 \\ 1 & 0 & 0 & 0 & 0 & 0 & 0 & 0 & 0 & 0 \\ 0 & 1 & 1 & -1 & 0 & 0 & 0 & 0 & 0 & 0 \\ 0 & 0 & -\frac{1}{r_\beta}\tan\beta & -1 & 1 & 0 & 0 & 0 & 0 & 0 \end{bmatrix} \begin{bmatrix} \ddot{x}_s \\ \ddot{\theta}_s \\ \ddot{x}_r \\ \ddot{\theta}_r \\ \ddot{\theta}_g \\ \lambda_1 \\ \lambda_2 \\ \lambda_3 \\ \lambda_4 \\ \lambda_5 \end{bmatrix} = \begin{bmatrix} F_s - F_{sf} \\ -M_{sf} \\ -F_{rf} \\ -M_{rf} \\ -M_{gf} \\ 0 \\ 0 \\ 0 \\ 0 \\ 0 \end{bmatrix} \tag{A.1.33}$$

and $\boldsymbol{\gamma} = [0\ 0\ 0\ 0\ 0]^T$.

A.1.10 Phase 3c-Synchronized Postsynchronization-Equations

Oil splash losses will not support turning of the gear. The set of active constraint for the phase 3c is

$$\boldsymbol{\Phi}(\boldsymbol{q}, t) = \begin{bmatrix} \boldsymbol{\Phi}^{external} \\ \boldsymbol{\Phi}^{internal} \end{bmatrix} = \begin{bmatrix} x_s - v_s t \\ \theta_s - \omega_s t \\ x_r - x_s - d_\alpha \\ \theta_r - \theta_g - \frac{B_{ang}}{2} \\ \theta_s - \theta_g + S_{ang} - \frac{x_s - (c + B_{ax})}{r_\delta}\tan\delta \end{bmatrix} = \mathbf{0} \tag{A.1.34}$$

with

$$\frac{\partial \boldsymbol{\Phi}}{\partial \boldsymbol{q}} = \begin{bmatrix} 1 & 0 & 0 & 0 & 0 \\ 0 & 1 & 0 & 0 & 0 \\ -1 & 0 & 1 & 0 & 0 \\ 0 & 0 & 0 & 1 & -1 \\ -\frac{1}{r_\delta}\tan\delta & 1 & 0 & 0 & -1 \end{bmatrix}, \frac{\partial \boldsymbol{\Phi}}{\partial t} = \begin{bmatrix} -v_s \\ -\omega_s \\ 0 \\ 0 \\ 0 \end{bmatrix} = \mathbf{0}$$

The equations of motion are

$$\begin{bmatrix} m_s & 0 & 0 & 0 & 0 \\ 0 & I_s & 0 & 0 & 0 \\ 0 & 0 & m_r & 0 & 0 \\ 0 & 0 & 0 & I_r & 0 \\ 0 & 0 & 0 & 0 & I_g \end{bmatrix} \begin{bmatrix} \ddot{x}_s \\ \ddot{\theta}_s \\ \ddot{x}_r \\ \ddot{\theta}_r \\ \ddot{\theta}_g \end{bmatrix} - \begin{bmatrix} 1 & 0 & 1 & 0 & -\frac{1}{r_\delta}\tan\delta \\ 0 & 1 & 0 & 0 & 1 \\ 0 & 0 & -1 & 0 & 0 \\ 0 & 0 & 0 & 1 & 0 \\ 0 & 0 & 0 & -1 & -1 \end{bmatrix} \begin{bmatrix} \lambda_1 \\ \lambda_2 \\ \lambda_3 \\ \lambda_4 \\ \lambda_5 \end{bmatrix} = \begin{bmatrix} F_s \\ 0 \\ 0 \\ 0 \\ 0 \end{bmatrix}^{app} - \begin{bmatrix} F_{sf} \\ M_{sf} \\ F_{rf} \\ M_{rf} \\ M_{gf} \end{bmatrix}^{fric} \tag{A.1.35}$$

where $F_s = \left(F_{s,3b} - 3000t\right)N/s$, $F_{sf} = C_{s\alpha}\, sign(\dot{x}_{sl})$, $M_{sf} = C_s\dot{\theta}_s$, $F_{rf} = C_{r\beta}\, sign(\dot{x}_r)$, $M_{rf} = C_r\, \dot{\theta}_r$, $M_{gf} = C_g\ \dot{\theta}_g$. Q^A is equal to the frictional forces $\left[F_{sf}, M_{sf}, F_{rf}, M_{rf}, M_{gf}\right]^{fric}$ and external force $[F_s]^{app}$. $F_{s,3b}$ is shift force at end of the phase 3b.

$$\begin{bmatrix} m_s & 0 & 0 & 0 & 0 & 1 & 0 & 1 & 0 & -\frac{1}{r_\delta}\tan\delta \\ 0 & I_s & 0 & 0 & 0 & 0 & 1 & 0 & 0 & 1 \\ 0 & 0 & m_r & 0 & 0 & 0 & 0 & -1 & 0 & 0 \\ 0 & 0 & 0 & I_r & 0 & 0 & 0 & 0 & 1 & 0 \\ 1 & 0 & 0 & 0 & I_g & 0 & 0 & 0 & -1 & -1 \\ 0 & 0 & 0 & 0 & 0 & 0 & 0 & 0 & 0 & 0 \\ 1 & 1 & 0 & 0 & 0 & 0 & 0 & 0 & 0 & 0 \\ 0 & 0 & -1 & 0 & 0 & 0 & 0 & 0 & 0 & 0 \\ -\frac{1}{r_\delta}\tan\delta & 0 & 0 & 1 & -1 & 0 & 0 & 0 & 0 & 0 \\ & 1 & 0 & 0 & -1 & 0 & 0 & 0 & 0 & 0 \end{bmatrix} \begin{bmatrix} \ddot{x}_s \\ \ddot{\theta}_s \\ \ddot{x}_r \\ \ddot{\theta}_r \\ \ddot{\theta}_g \\ \lambda_1 \\ \lambda_2 \\ \lambda_3 \\ \lambda_4 \\ \lambda_5 \end{bmatrix} = \begin{bmatrix} F_s - F_{sf} \\ -M_{sf} \\ -F_{rf} \\ -M_{rf} \\ -M_{gf} \\ 0 \\ 0 \\ 0 \\ 0 \\ 0 \end{bmatrix} \tag{A.1.36}$$

and $\boldsymbol{\gamma} = [0\ 0\ 0\ 0\ 0]^T$.

A.1.11 Phase 3c-Synchronized Desynchronization-Equations

The set of active constraint for the phase 3c is

$$\boldsymbol{\Phi}(\boldsymbol{q},t)=\begin{bmatrix}\boldsymbol{\Phi}^{external}\\ \boldsymbol{\Phi}^{internal}\end{bmatrix}=\begin{bmatrix} x_s-v_s t\\ \theta_s-\omega_s t\\ x_r-x_s-d_\alpha\\ \theta_r-\theta_s-\dfrac{B_{ang}}{2}\\ \theta_s-\theta_g+B_{ang}+\dfrac{x_s-(c+B_{ax})}{r_\delta}\tan\delta\end{bmatrix}=\mathbf{0} \qquad \text{(A.1.37)}$$

with

$$\frac{\partial\boldsymbol{\Phi}}{\partial\boldsymbol{q}}=\begin{bmatrix}1 & 0 & 0 & 0 & 0\\ 0 & 1 & 0 & 0 & 0\\ -1 & 0 & 1 & 0 & 0\\ 0 & -1 & 0 & 1 & 0\\ \frac{1}{r_\delta}\tan\delta & 0 & 0 & -1 & 1\end{bmatrix},\frac{\partial\boldsymbol{\Phi}}{\partial t}=\begin{bmatrix}-v_s\\ -\omega_s\\ 0\\ 0\\ 0\end{bmatrix}=\mathbf{0}$$

The equations of motion are

$$\begin{bmatrix}m_s & 0 & 0 & 0 & 0\\ 0 & I_s & 0 & 0 & 0\\ 0 & 0 & m_r & 0 & 0\\ 0 & 0 & 0 & I_r & 0\\ 0 & 0 & 0 & 0 & I_g\end{bmatrix}\begin{bmatrix}\ddot{x}_s\\ \ddot{\theta}_s\\ \ddot{x}_r\\ \ddot{\theta}_r\\ \ddot{\theta}_g\end{bmatrix}-\begin{bmatrix}1 & 0 & -1 & 0 & \frac{1}{r_\delta}\tan\delta\\ 0 & 1 & 0 & -1 & 0\\ 0 & 0 & 1 & 0 & 0\\ 0 & 0 & 0 & 1 & -1\\ 0 & 0 & 0 & 0 & 1\end{bmatrix}\begin{bmatrix}\lambda_1\\ \lambda_2\\ \lambda_3\\ \lambda_4\\ \lambda_5\end{bmatrix}=\begin{bmatrix}F_s\\ 0\\ 0\\ 0\\ 0\end{bmatrix}^{app}-\begin{bmatrix}F_{sf}\\ M_{sf}\\ F_{rf}\\ M_{rf}\\ M_{gf}\end{bmatrix}^{fric} \qquad \text{(A.1.38)}$$

$$\begin{bmatrix}m_s & 0 & 0 & 0 & 0 & 1 & 0 & -1 & 0 & \frac{1}{r_\delta}\tan\delta\\ 0 & I_s & 0 & 0 & 0 & 0 & 1 & 0 & -1 & 0\\ 0 & 0 & m_r & 0 & 0 & 0 & 0 & 1 & 0 & 0\\ 0 & 0 & 0 & I_r & 0 & 0 & 0 & 0 & 1 & -1\\ 1 & 0 & 0 & 0 & I_g & 0 & 0 & 0 & 0 & 1\\ 0 & 0 & 0 & 0 & 0 & 0 & 0 & 0 & 0 & 0\\ -1 & 1 & 0 & 0 & 0 & 0 & 0 & 0 & 0 & 0\\ 0 & 0 & 1 & 0 & 0 & 0 & 0 & 0 & 0 & 0\\ \frac{1}{r_\delta}\tan\delta & -1 & 0 & 1 & 0 & 0 & 0 & 0 & 0 & 0\\ & 0 & 0 & -1 & 1 & 0 & 0 & 0 & 0 & 0\end{bmatrix}\begin{bmatrix}\ddot{x}_s\\ \ddot{\theta}_s\\ \ddot{x}_r\\ \ddot{\theta}_r\\ \ddot{\theta}_g\\ \lambda_1\\ \lambda_2\\ \lambda_3\\ \lambda_4\\ \lambda_5\end{bmatrix}=\begin{bmatrix}F_s-F_{sf}\\ -M_{sf}\\ -F_{rf}\\ -M_{rf}\\ -M_{gf}\\ 0\\ 0\\ 0\\ 0\\ 0\end{bmatrix} \qquad \text{(A.1.39)}$$

and $\boldsymbol{\gamma}=[0\ 0\ 0\ 0]^T$.

A.1.12 Phase 4-Engagement-Equations

The set of active constraint for the phase 4 is

$$\boldsymbol{\Phi}(\boldsymbol{q},t)=\begin{bmatrix}\boldsymbol{\Phi}^{external}\\ \boldsymbol{\Phi}^{internal}\end{bmatrix}=\begin{bmatrix}x_s-v_s t\\ \theta_s-\omega_s t\\ x_r-x_s+d_\alpha\\ \theta_r-\theta_s+\Delta\theta_{r_s}\\ \theta_g-\theta_s+B_{ang}+\Delta\theta_{g_s}\end{bmatrix}=\mathbf{0} \tag{A.1.40}$$

$\Delta\theta_{r_s}=\theta_r-\theta_s$ and $\Delta\theta_{g_s}=\theta_g-\theta_s$ at end of phase 3c.

$$\frac{\partial\boldsymbol{\Phi}}{\partial\boldsymbol{q}}=\begin{bmatrix}1&0&0&0&0\\0&1&0&0&0\\-1&0&1&0&0\\0&-1&0&1&0\\0&-1&0&0&1\end{bmatrix},\frac{\partial\boldsymbol{\Phi}}{\partial t}=\begin{bmatrix}-v_s\\-\omega_s\\0\\0\\0\end{bmatrix}=\mathbf{0}$$

The equations of motion are

$$\begin{bmatrix}m_s&0&0&0&0\\0&I_s&0&0&0\\0&0&m_r&0&0\\0&0&0&I_r&0\\0&0&0&0&I_g\end{bmatrix}\begin{bmatrix}\ddot{x}_s\\\ddot{\theta}_s\\\ddot{x}_r\\\ddot{\theta}_r\\\ddot{\theta}_g\end{bmatrix}-\begin{bmatrix}1&0&-1&0&0\\0&1&0&-1&-1\\0&0&1&0&0\\0&0&0&1&0\\0&0&0&0&1\end{bmatrix}\begin{bmatrix}\lambda_1\\\lambda_2\\\lambda_3\\\lambda_4\\\lambda_5\end{bmatrix}=\begin{bmatrix}F_s\\0\\0\\0\\0\end{bmatrix}^{app}-\begin{bmatrix}F_{sf}\\M_{sf}\\F_{rf}\\M_{rf}\\M_{gf}\end{bmatrix}^{fric} \tag{A.1.41}$$

where $F_s=\left(F_{s,3c}-5t\right)N/s$, $F_{sf}=C_{s\alpha}\,sign(\dot{x}_{sl})$, $M_{sf}=C_s\dot{\theta}_s$, $F_{rf}=C_{r\beta}\,sign(\dot{x}_r)$, $M_{rf}=C_r\,\dot{\theta}_r$, $M_{gf}=C_g\;\dot{\theta}_g$. Q^A is equal to the frictional forces $\left[F_{sf},M_{sf},F_{rf},M_{rf},M_{gf}\right]^{fric}$ and external force $[F_s]^{app}$. $F_{s,3c}$ is shift force at end of the phase 3c.

$$\begin{bmatrix}m_s&0&0&0&0&1&0&1&0&0\\0&I_s&0&0&0&0&1&0&1&1\\0&0&m_r&0&0&0&0&-1&0&0\\0&0&0&I_r&0&0&0&0&-1&0\\0&0&0&0&I_g&0&0&0&0&-1\\1&0&0&0&0&0&0&0&0&0\\0&1&0&0&0&0&0&0&0&0\\1&0&-1&0&0&0&0&0&0&0\\0&1&0&-1&0&0&0&0&0&0\\0&1&0&0&-1&0&0&0&0&0\end{bmatrix}\begin{bmatrix}\ddot{x}_s\\\ddot{\theta}_s\\\ddot{x}_r\\\ddot{\theta}_r\\\ddot{\theta}_g\\\lambda_1\\\lambda_2\\\lambda_3\\\lambda_4\\\lambda_5\end{bmatrix}=\begin{bmatrix}F_s-F_{sf}\\-M_{sf}\\-F_{rf}\\-M_{rf}\\-M_{gf}\\0\\0\\0\\0\\0\end{bmatrix} \tag{A.1.42}$$

and $\boldsymbol{\gamma}=[0\;0\;0\;0]^T$.

A.2 Alternative case of phase 3: small clearance

A.2.1 Phase 3-synchronized

When dimensions of the synchronizer is such that the engaging teeth chamfers come in contact before the blocking teeth chamfers come out of contact.

A.2.2 Phase 3a-Synchronized

The phase 3a starts when the ring again starts to move axially and ends when the speed difference reduces to zero before the engaging teeth chamfers come in contact.

The rotational speeds of the sleeve and the ring are $\dot{\theta}_s$ and $\dot{\theta}_r$ respectively. The gearwheel will have the rotational speed $\dot{\theta}_{g_rel} = \frac{\dot{x}_r}{r_\beta}\tan\beta$ relative to the ring.

Time duration of the phase 3a depends upon rate of the shift force with angle of the cones and the blocker chamfers.

A.2.3 Phase 3a-Synchronized-Equations

The set of active constraint for the phase 3a is

$$\boldsymbol{\Phi}(\boldsymbol{q},t) = \begin{bmatrix} \boldsymbol{\Phi}^{external} \\ \boldsymbol{\Phi}^{internal} \end{bmatrix} = \begin{bmatrix} x_s - v_s t \\ \theta_s - \omega_s t \\ x_r - x_s - d_\alpha \\ \theta_g - \theta_r + B_{ang} - \dfrac{x_r - B_{ax}}{r_\beta}\tan\beta \end{bmatrix} = \mathbf{0} \qquad \text{(A.2.1)}$$

with

$$\frac{\partial \boldsymbol{\Phi}}{\partial \boldsymbol{q}} = \begin{bmatrix} 1 & 0 & 0 & 0 & 0 \\ 0 & 1 & 0 & 0 & 0 \\ -1 & 0 & 1 & 0 & 0 \\ 0 & 0 & -\dfrac{1}{r_\beta}\tan\beta & 1 & -1 \end{bmatrix}, \quad \frac{\partial \boldsymbol{\Phi}}{\partial t} = \begin{bmatrix} -v_s \\ -\omega_s \\ 0 \\ 0 \end{bmatrix} = \mathbf{0}$$

The equations of motion are

$$\begin{bmatrix} m_s & 0 & 0 & 0 & 0 \\ 0 & I_s & 0 & 0 & 0 \\ 0 & 0 & m_r & 0 & 0 \\ 0 & 0 & 0 & I_r & 0 \\ 0 & 0 & 0 & 0 & I_g \end{bmatrix} \begin{bmatrix} \ddot{x}_s \\ \ddot{\theta}_s \\ \ddot{x}_r \\ \ddot{\theta}_r \\ \ddot{\theta}_g \end{bmatrix} - \begin{bmatrix} 1 & 0 & -1 & 0 \\ 0 & 1 & 0 & 0 \\ 0 & 0 & 1 & -\dfrac{1}{r_\beta}\tan\beta \\ 0 & 0 & 0 & 1 \\ 0 & 0 & 0 & -1 \end{bmatrix} \begin{bmatrix} \lambda_1 \\ \lambda_2 \\ \lambda_3 \\ \lambda_4 \end{bmatrix} = \begin{bmatrix} F_s \\ 0 \\ 0 \\ 0 \\ 0 \end{bmatrix}^{app} - \begin{bmatrix} C_{s\alpha}\, sign(\dot{x}_{sl}) \\ C_s \dot{\theta}_s \\ C_{r\beta}\, sign(\dot{x}_r) \\ C_r\, \dot{\theta}_r \\ C_g\, \dot{\theta}_g \end{bmatrix} \qquad \text{(A.2.2)}$$

where $F_s = (max(F_{ax} + F_s) - 5t)N/s$, $F_{sf} = C_{s\alpha}\, sign(\dot{x}_{sl})$, $M_{sf} = C_s\dot{\theta}_s$, $F_{rf} = C_{r\beta}\, sign(\dot{x}_r)$, $M_{rf} = C_r\, \dot{\theta}_r$, $M_{gf} = C_g\ \dot{\theta}_g$. Q^A is equal to the frictional forces $\left[F_{sf}, M_{sf}, F_{rf}, M_{rf}, M_{gf}\right]^{fric}$ and external force $[F_s]^{app}$.

$$\begin{bmatrix} m_s & 0 & 0 & 0 & 0 & 1 & 0 & -1 & 0 \\ 0 & I_s & 0 & 0 & 0 & 0 & 1 & 0 & 0 \\ 0 & 0 & m_r & 0 & 0 & 0 & 0 & 1 & \frac{-1}{r_\beta}\tan\beta \\ 0 & 0 & 0 & I_r & 0 & 0 & 0 & 0 & 1 \\ 0 & 0 & 0 & 0 & I_g & 0 & 0 & 0 & -1 \\ 1 & 0 & 0 & 0 & 0 & 0 & 0 & 0 & 0 \\ 0 & 1 & 1 & 0 & 0 & 0 & 0 & 0 & 0 \\ -1 & 0 & 0 & 0 & 0 & 0 & 0 & 0 & 0 \\ 0 & 0 & \frac{-1}{r_\beta}\tan\beta & 1 & -1 & 0 & 0 & 0 & 0 \end{bmatrix} \begin{bmatrix} \ddot{x}_s \\ \ddot{\theta}_s \\ \ddot{x}_r \\ \ddot{\theta}_r \\ \ddot{\theta}_g \\ \lambda_1 \\ \lambda_2 \\ \lambda_3 \\ \lambda_4 \end{bmatrix} = \begin{bmatrix} F_s - F_{sf} \\ -M_{sf} \\ -F_{rf} \\ -M_{rf} \\ -M_{gf} \\ 0 \\ 0 \\ 0 \\ 0 \end{bmatrix} \qquad \text{(A.2.3)}$$

and $\boldsymbol{\gamma} = [0\ 0\ 0\ 0]^T$.

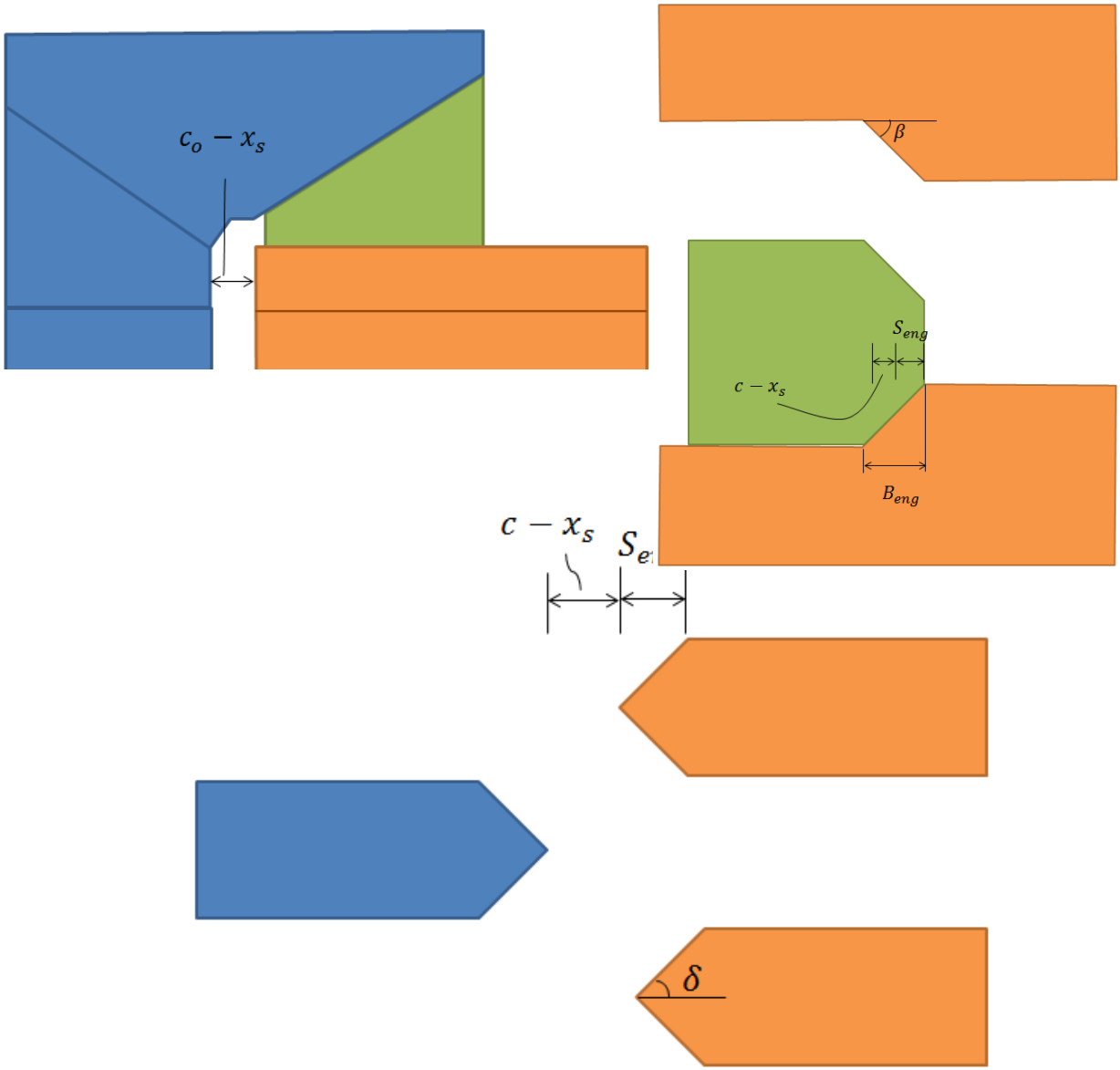

Figure 55: End position of the phase 3a-synchronized.

A.2.4 Phase 3b-Synchronized

From start of the phase 3b the ring and the sleeve will rotate and translate axially together. The gear will rotate with the speed $\dot{\theta}_{g_rel} = \frac{\dot{x}_r}{r_\beta} \tan\beta$. It is assumed that $B_{eng} = C + S_{eng}$. The phase 3b will end when the displacement equal to S_{eng} on the blocking chamfers decreases to zero. When engaging teeth chamfers are coming in contact, the nature of contact will be vary in each time of gear shifting. The nature of contact will depend upon the angular relative position of the engaging teeth.

Two kinds of possibilities of their contact are studied; first the engaging chamfers can contact at top and second the engaging chamfers can contact at bottom as shown in *Figure*

56. Beyond these two possibilities the contact can also be realistic but for simplicity of the model two positions in *Figure 56.* are considered as extreme positions.

A.2.5 Phase 3b-Synchronized-Equations

The set of active constraint for the phase 3b is

$$\boldsymbol{\Phi}(\boldsymbol{q},t)=\begin{bmatrix}\boldsymbol{\Phi}^{external}\\ \boldsymbol{\Phi}^{internal}\end{bmatrix}=\begin{bmatrix}x_s-v_s t\\ \theta_s-\omega_s t\\ x_r-x_s-d_\alpha\\ \theta_r-\theta_s-\theta_{r_s}\\ \theta_g-\theta_r+B_{ang}-\dfrac{x_r-B_{ax}}{r_\beta}\tan\beta\end{bmatrix}=\mathbf{0} \qquad \text{(A.2.4)}$$

If linear tangential velocity of the sleeve rotational speed (v_{ω_s}) is greater than its axial velocity (v_s), the term $\frac{x_r-B_{ax}}{r_\beta}\tan\beta$ will change by $\frac{x_s-B_{ax}}{r_\delta}\tan\delta$.

$$\frac{\partial\boldsymbol{\Phi}}{\partial\boldsymbol{q}}=\begin{bmatrix}1&0&0&0&0\\0&1&0&0&0\\-1&0&1&0&0\\0&-1&0&1&0\\0&0&-\dfrac{1}{r_\beta}\tan\beta&-1&1\end{bmatrix},\qquad \frac{\partial\boldsymbol{\Phi}}{\partial t}=\begin{bmatrix}-v_s\\-\omega_s\\0\\0\\0\end{bmatrix}=\mathbf{0}$$

The equations of motion are

$$\begin{bmatrix}m_s&0&0&0&0\\0&I_s&0&0&0\\0&0&m_r&0&0\\0&0&0&I_r&0\\0&0&0&0&I_g\end{bmatrix}\begin{bmatrix}\ddot{x}_s\\\ddot{\theta}_s\\\ddot{x}_r\\\ddot{\theta}_r\\\ddot{\theta}_g\end{bmatrix}-\begin{bmatrix}1&0&-1&0&0\\0&1&0&-1&0\\0&0&1&0&-\dfrac{1}{r_\beta}\tan\beta\\0&0&0&1&-1\\0&0&0&0&1\end{bmatrix}\begin{bmatrix}\lambda_1\\\lambda_2\\\lambda_3\\\lambda_4\\\lambda_5\end{bmatrix}=\begin{bmatrix}F_s\\0\\0\\0\\0\end{bmatrix}^{app}-\begin{bmatrix}F_{sf}\\M_{sf}\\F_{rf}\\M_{rf}\\M_{gf}\end{bmatrix}^{fric} \qquad \text{(A.2.5)}$$

where $F_s=(F_{s,3a}-4000t)N/s$, $F_{sf}=C_{s\alpha}\,sign(\dot{x}_{sl})$, $M_{sf}=C_s\dot{\theta}_s$, $F_{rf}=C_{r\beta}\,sign(\dot{x}_r)$, $M_{rf}=C_r\,\dot{\theta}_r$, $M_{gf}=C_g\,\dot{\theta}_g$. Q^A is equal to the frictional forces $[F_{sf},M_{sf},F_{rf},M_{rf},M_{gf}]^{fric}$ and external force $[F_s]^{app}$. $F_{s,3a}$ is applied shift force at end of phase 3a.

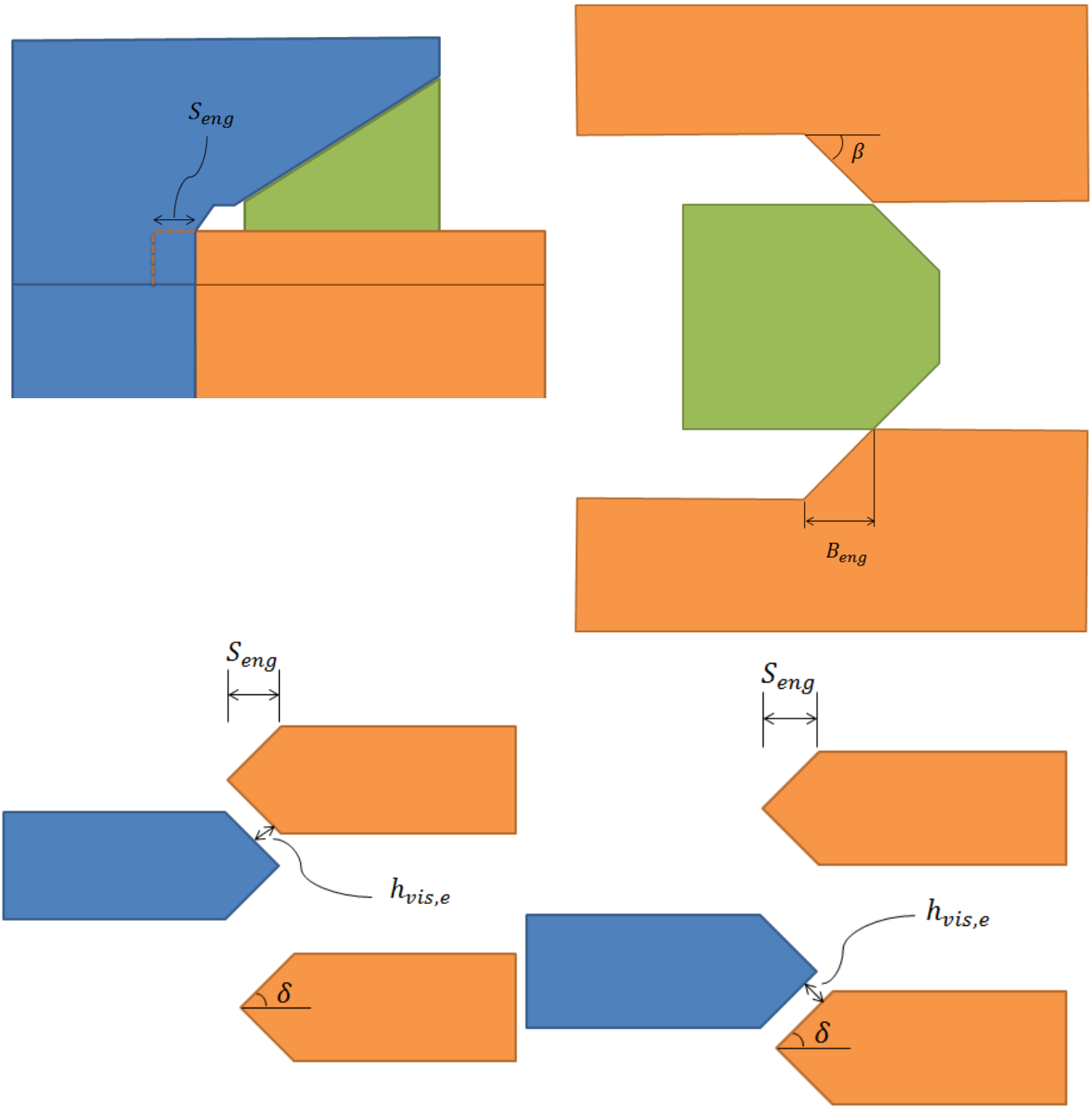

Figure 56: End position of the phase 3b-synchronized (a) post-synchronization (b) hang on-synchronization.

$$\begin{bmatrix} m_s & 0 & 0 & 0 & 0 & 1 & 0 & -1 & 0 & 0 \\ 0 & I_s & 0 & 0 & 0 & 0 & 1 & 0 & -1 & 0 \\ 0 & 0 & m_r & 0 & 0 & 0 & 0 & 1 & 0 & \frac{-1}{r_\beta}\tan\beta \\ 0 & 0 & 0 & I_r & 0 & 0 & 0 & 0 & 1 & -1 \\ 0 & 0 & 0 & 0 & I_g & 0 & 0 & 0 & 0 & 1 \\ 1 & 0 & 0 & 0 & 0 & 0 & 0 & 0 & 0 & 0 \\ 0 & 1 & 1 & 0 & 0 & 0 & 0 & 0 & 0 & 0 \\ -1 & 0 & 0 & 0 & 0 & 0 & 0 & 0 & 0 & 0 \\ 0 & -1 & \frac{-1}{r_\beta}\tan\beta & 1 & 0 & 0 & 0 & 0 & 0 & 0 \\ 0 & 0 & & -1 & 1 & 0 & 0 & 0 & 0 & 0 \end{bmatrix} \begin{bmatrix} \ddot{x}_s \\ \ddot{\theta}_s \\ \ddot{x}_r \\ \ddot{\theta}_r \\ \ddot{\theta}_g \\ \lambda_1 \\ \lambda_2 \\ \lambda_3 \\ \lambda_4 \\ \lambda_5 \end{bmatrix} = \begin{bmatrix} F_s - F_{sf} \\ -M_{sf} \\ -F_{rf} \\ -M_{rf} \\ -M_{gf} \\ 0 \\ 0 \\ 0 \\ 0 \\ 0 \end{bmatrix} \quad \text{(A.2.6)}$$

and $\boldsymbol{\gamma} = [0\ 0\ 0\ 0\ 0]^T$.

A.2.6 Phase 3c-Synchronized

Turning of the gear at top contact is called post-synchronization and holding of the gear at bottom contact is called hang-synchronization. The gear and the ring will rotate together. The sleeve and the ring will translate together. The rotational speed of the gear will be determined from the axial speed of the sleeve $\dot{\theta}_{g_rel} = \frac{\dot{x}_s}{r_\delta}\tan\delta$.

A.2.7 Post-synchronization

The shift force will increase to break the oil film and to turn the gear. This is the second increment which is called second bump in the shift force. The oil splash losses will support turning of the gear.

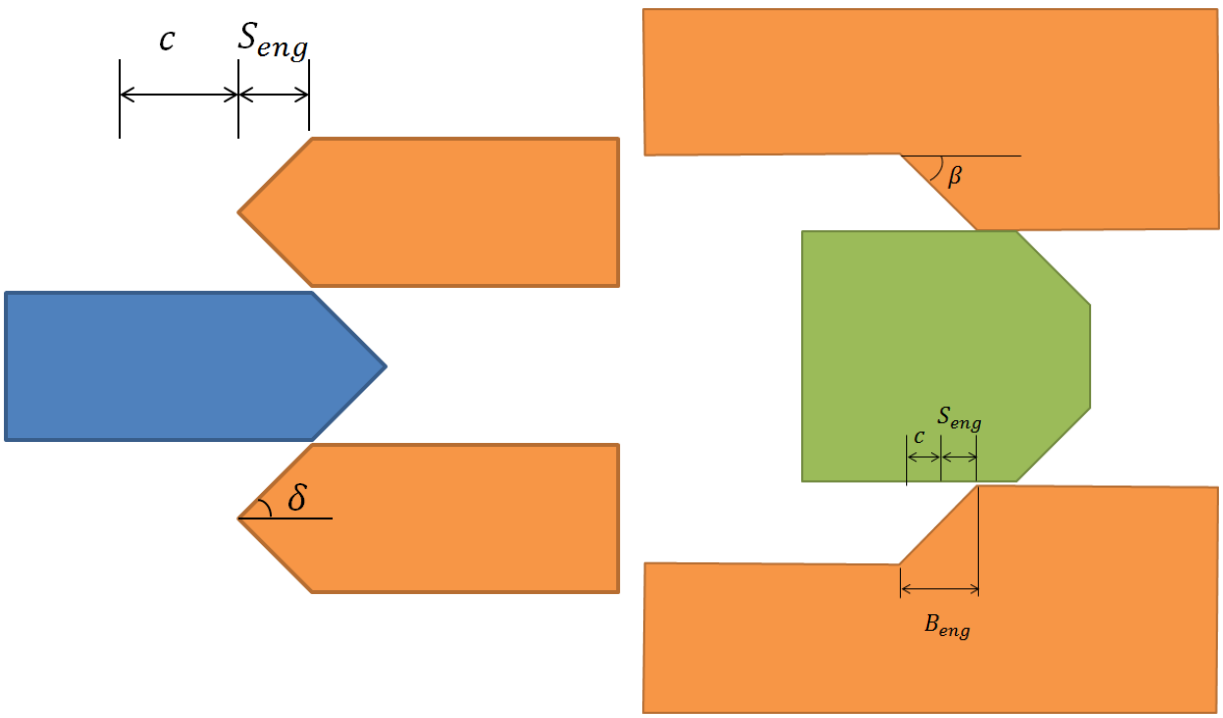

Figure 57: End position of the phase 3c-synchronized.

A.2.8 Phase 3c-Synchronized-Equations

The set of active constraint for the phase 3c is

$$\boldsymbol{\Phi}(\boldsymbol{q},t)=\begin{bmatrix}\boldsymbol{\Phi}^{external}\\ \boldsymbol{\Phi}^{internal}\end{bmatrix}=\begin{bmatrix} x_s-v_s t\\ \theta_s-\omega_s t\\ x_r-x_s-d_\alpha\\ \theta_r-\theta_g-\dfrac{B_{ang}}{2}\\ \theta_s-\theta_g+S_{ang}-\dfrac{x_s-(c+B_{ax})}{r_\delta}\tan\delta\end{bmatrix}=\mathbf{0} \qquad \text{(A.2.7)}$$

with

$$\frac{\partial\boldsymbol{\Phi}}{\partial\boldsymbol{q}}=\begin{bmatrix}1 & 0&0&0&0\\ 0 & 1&0&0&0\\ -1 & 0&1&0&0\\ 0 & 0&0&1&-1\\ -\dfrac{1}{r_\delta}\tan\delta & 1&0&0&-1\end{bmatrix},\frac{\partial\boldsymbol{\Phi}}{\partial t}=\begin{bmatrix}-v_s\\ -\omega_s\\ 0\\ 0\\ 0\end{bmatrix}=\mathbf{0}$$

The equations of motion are

$$\begin{bmatrix}m_s&0&0&0&0\\0&I_s&0&0&0\\0&0&m_r&0&0\\0&0&0&I_r&0\\0&0&0&0&I_g\end{bmatrix}\begin{bmatrix}\ddot{x}_s\\ \ddot{\theta}_s\\ \ddot{x}_r\\ \ddot{\theta}_r\\ \ddot{\theta}_g\end{bmatrix}-\begin{bmatrix}1&0&-1&0&\frac{-1}{r_\delta}\tan\delta\\0&1&0&0&1\\0&0&1&0&0\\0&0&0&1&0\\0&0&0&-1&-1\end{bmatrix}\begin{bmatrix}\lambda_1\\ \lambda_2\\ \lambda_3\\ \lambda_4\\ \lambda_5\end{bmatrix}=\begin{bmatrix}F_s\\0\\0\\0\\0\end{bmatrix}^{app}-\begin{bmatrix}F_{sf}\\M_{sf}\\F_{rf}\\M_{rf}\\M_{gf}\end{bmatrix}^{fric} \qquad \text{(A.2.8)}$$

where $F_s=\left(F_{s,3b}-3000t\right)N/s$, $F_{sf}=C_{s\alpha}\,sign(\dot{x}_{sl})$, $M_{sf}=C_s\dot{\theta}_s$, $F_{rf}=C_{r\beta}\,sign(\dot{x}_r)$, $M_{rf}=C_r\,\dot{\theta}_r$, $M_{gf}=C_g\;\dot{\theta}_g$. Q^A is equal to the frictional forces $\left[F_{sf},M_{sf},F_{rf},M_{rf},M_{gf}\right]^{fric}$ and external force $[F_s]^{app}$. $F_{s,3b}$ is applied shift force at end of phase 3b.

$$\begin{bmatrix}m_s&0&0&0&0&1&0&-1&0&\frac{-1}{r_\delta}\tan\delta\\0&I_s&0&0&0&0&1&0&0&1\\0&0&m_r&0&0&0&0&1&0&0\\0&0&0&I_r&0&0&0&0&1&0\\1&0&0&0&I_g&0&0&0&-1&-1\\0&0&0&0&0&0&0&0&0&0\\-1&1&0&0&0&0&0&0&0&0\\0&0&1&0&0&0&0&0&0&0\\0&0&0&1&-1&0&0&0&0&0\\\frac{-1}{r_\delta}\tan\delta&1&0&0&-1&0&0&0&0&0\end{bmatrix}\begin{bmatrix}\ddot{x}_s\\ \ddot{\theta}_s\\ \ddot{x}_r\\ \ddot{\theta}_r\\ \ddot{\theta}_g\\ \lambda_1\\ \lambda_2\\ \lambda_3\\ \lambda_4\\ \lambda_5\end{bmatrix}=\begin{bmatrix}F_s-F_{sf}\\-M_{sf}\\-F_{rf}\\-M_{rf}\\-M_{gf}\\0\\0\\0\\0\\0\end{bmatrix} \qquad \text{(A.2.9)}$$

and $\boldsymbol{\gamma}=[0\;0\;0\;0\;0]^T$.

A.2.9 Hang on-synchronization

When the engaging teeth will come in contact at bottom as shown in *Figure 56.*, this position either will hang the sleeve, the ring and the gear or will push back the sleeve. The sleeve and the ring will move together axially because of the cone contact but at same time the sleeve will turn the gear to desynchronize through engaging chamfers contact and the ring will turn the gear to post-synchronize through blocking chamfers contact.

Because the oil splash losses are supporting the hang-synchronization, the sleeve can be pushed back in this contact position.

A.2.10 Phase 3-Unsynchronized

The speed difference decreases to zero after the engaging teeth chamfers come in contact.

A.2.11 Phase 3a-Unsynchronized

The sleeve will cover the axial clearance c between the engaging teeth as shown in *Figure 58*. As it is a downshift case, at the same time chamfers of the engaging teeth will come closer at top. At end of the phase 3a the engaging chamfers come in contact through viscous oil film thickness $h_{vis,e}$.

At end of the phase 2 the pressure between the cones and the blocker angle will give the axial velocity. The shift force is decreasing and the axial speed is increasing. Speed difference at start of the phase will predict angular relative position of the engaging teeth and after increasing axial speed, rotational speed of the sleeve and varying rotational speed of the gear will give an impact of the engaging chamfers.

The impact can be between tips of the chamfers instead of between the chamfers at bottom but because of the speed difference the sleeve will rotate with higher speed and the chamfers afterwards will have impact again at top as shown in the *Figure 59*. Nature of the impact can vary during each shifting of gear. In this model only the impact in *Figure 59.* is considered.

If axial component of the resultant of all forces acting at the impact is greater/equal than tangential component of the resultant, the impact will forward the engagement. If the axial component is less than the tangential component, the impact will produce clashing and the next phase of the engagement will not start until the axial component exceeds the tangential component.

A.2.12 Phase 3a-Unsynchronized-Equations

The ring will also travel axially and its rotational speed increases at the same time because the torque transfers between the cones. The ring will turn the gear.

$$T_c = \lambda_{cons}\, \mu_\alpha (F_{ax} + F_s) \qquad \text{(A.2.10)}$$

where $\lambda_{cons} = \frac{r_c}{\sin(\alpha)}\left(1 + \frac{1}{3}\left(\frac{b}{r_c}\right)^2 \sin^2(\alpha)\right)$

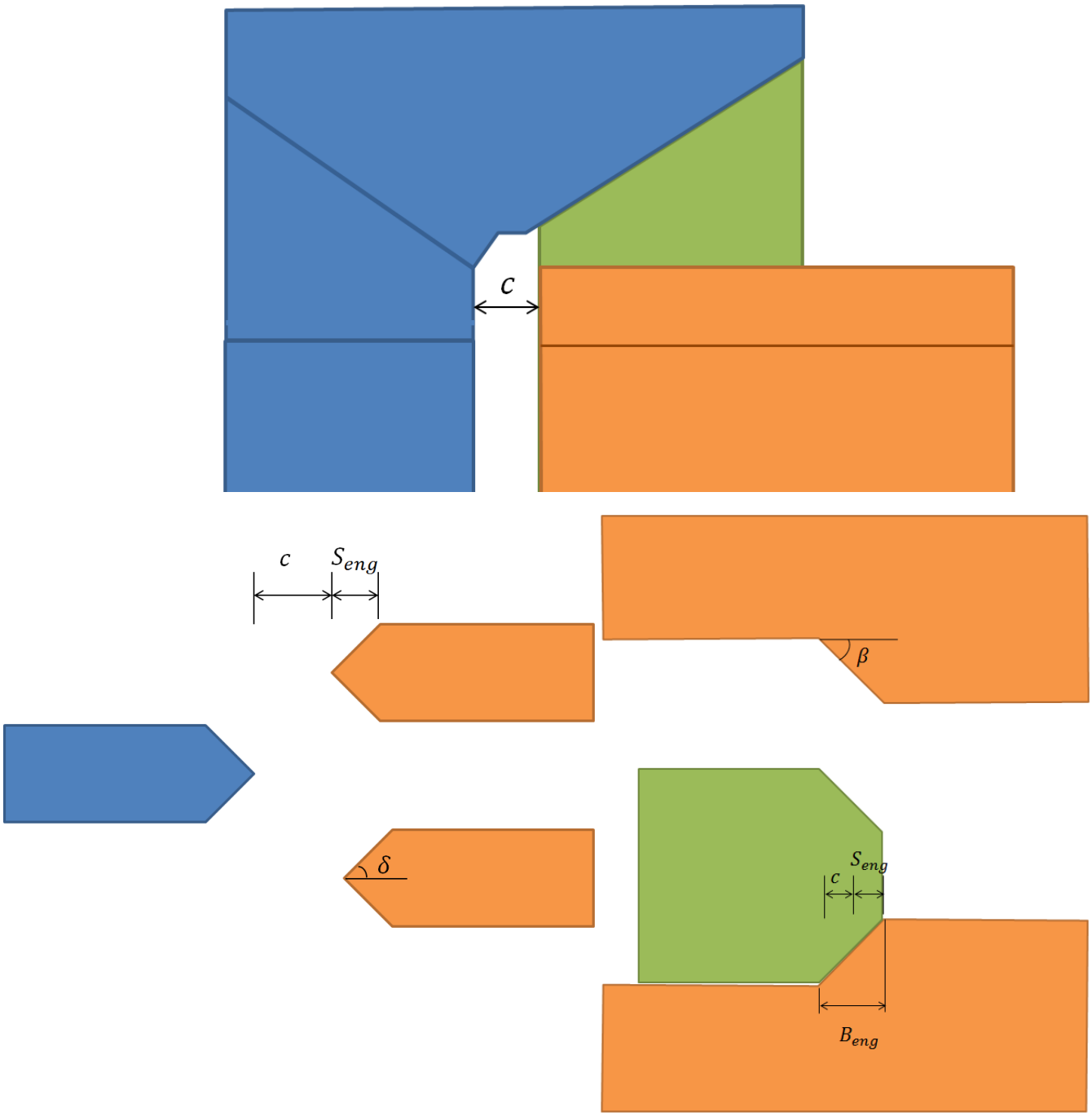

Figure 58: Starting position of the phase 3a-unsynchronized.

$\omega_r \leq \omega_s < \omega_g$ and $v_{\omega_s}(v_{\omega_s} = r\omega_s) > v_s$ OR $\omega_r \leq \omega_s < \omega_g$ and $v_{\omega_s}(v_{\omega_s} = r\omega_s) < v_s$

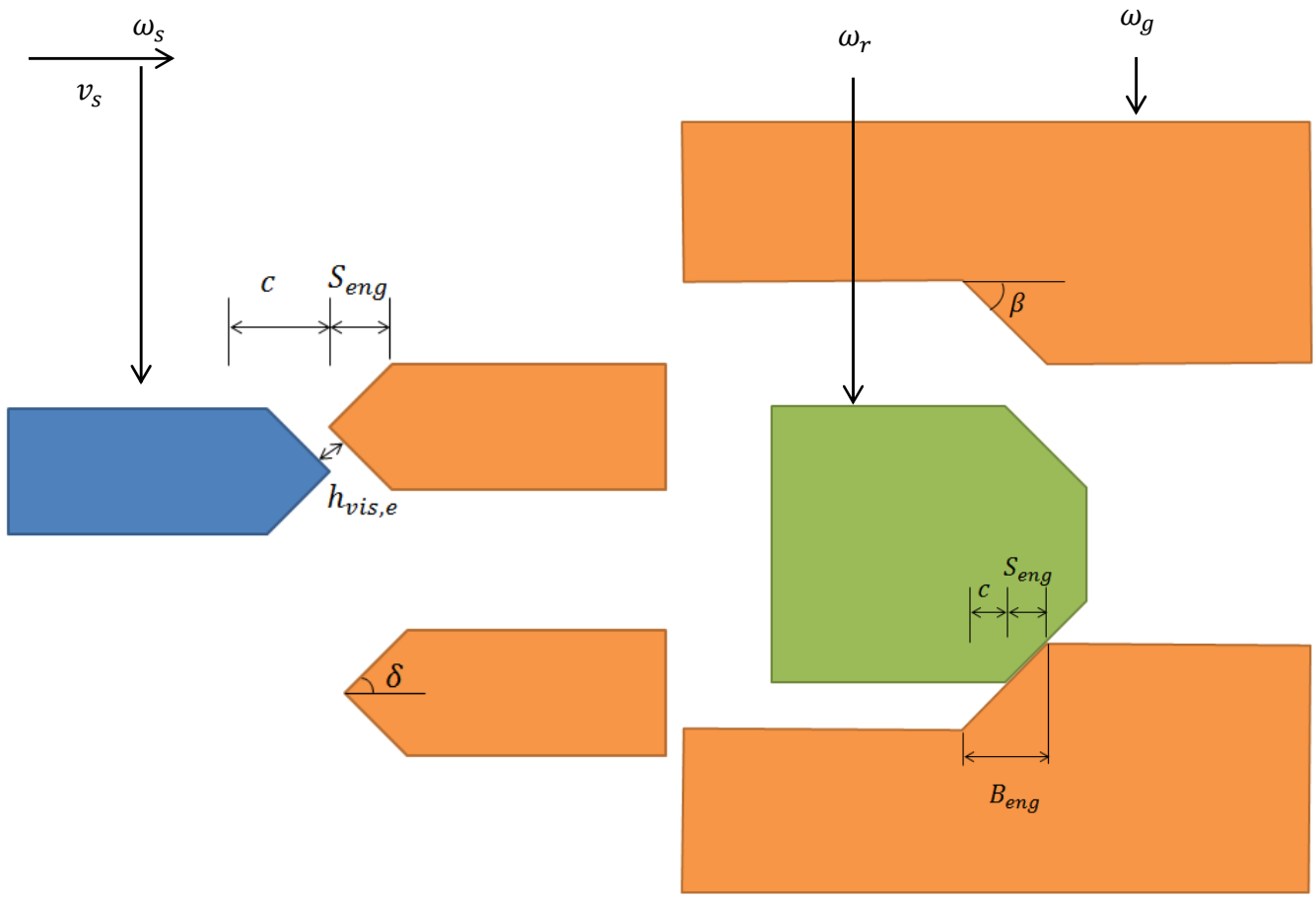

Figure 59: End position of the phase 3a-unsynchronized.

The set of active constraint for the phase 3a is

$$\boldsymbol{\Phi}(\boldsymbol{q},t) = \begin{bmatrix} \boldsymbol{\Phi}^{external} \\ \boldsymbol{\Phi}^{internal} \end{bmatrix} = \begin{bmatrix} x_s - v_s t \\ \theta_s - \omega_s t \\ x_r - x_s - d_\alpha \\ \theta_g - \theta_r + B_{ang} - \dfrac{x_r - B_{ax}}{r_\beta}\tan\beta \end{bmatrix} = \mathbf{0} \qquad \text{(A.2.11)}$$

with

$$\frac{\partial \boldsymbol{\Phi}}{\partial \boldsymbol{q}} = \begin{bmatrix} 1 & 0 & 0 & 0 & 0 \\ 0 & 1 & 0 & 0 & 0 \\ -1 & 0 & 1 & 0 & 0 \\ 0 & -1 & 0 & 1 & 0 \\ 0 & 0 & \dfrac{-1}{r_\beta}\tan\beta & -1 & 1 \end{bmatrix}, \frac{\partial \boldsymbol{\Phi}}{\partial t} = \begin{bmatrix} -v_s \\ -\omega_s \\ 0 \\ 0 \\ 0 \end{bmatrix} = \mathbf{0}$$

The equations of motion are

$$\begin{bmatrix} m_s & 0 & 0 & 0 & 0 \\ 0 & I_s & 0 & 0 & 0 \\ 0 & 0 & m_r & 0 & 0 \\ 0 & 0 & 0 & I_r & 0 \\ 0 & 0 & 0 & 0 & I_g \end{bmatrix} \begin{bmatrix} \ddot{x}_s \\ \ddot{\theta}_s \\ \ddot{x}_r \\ \ddot{\theta}_r \\ \ddot{\theta}_g \end{bmatrix} - \begin{bmatrix} 1 & 0 & 1 & 0 & 0 \\ 0 & 1 & 0 & 1 & 0 \\ 0 & 0 & -1 & 0 & \frac{-1}{r_\beta}\tan\beta \\ 0 & 0 & 0 & -1 & -1 \\ 0 & 0 & 0 & 0 & 1 \end{bmatrix} \begin{bmatrix} \lambda_1 \\ \lambda_2 \\ \lambda_3 \\ \lambda_4 \end{bmatrix} = \begin{bmatrix} F_s \\ 0 \\ 0 \\ 0 \\ 0 \end{bmatrix}^{app} - \begin{bmatrix} F_{sf} \\ M_{sf} \\ F_{rf} \\ M_{rf} \\ M_{gf} \end{bmatrix}^{fric} \tag{A.2.12}$$

where $F_s = (max(F_{ax} + F_s) - 5t)N/s$, $F_{sf} = F_{ax} + C_{s\alpha}\, sign(\dot{x}_{sl})$, $M_{sf} = T_{sq} + C_s\dot{\theta}_s$, $F_{rf} = -F_{ax} + C_{r\beta}\, sign(\dot{x}_r)$, $M_{rf} = -T_{sq} + C_r\, \dot{\theta}_r$, $M_{gf} = C_g\ \dot{\theta}_g$. Q^A is equal to the frictional forces $\left[F_{sf}, M_{sf}, F_{rf}, M_{rf}, M_{gf}\right]^{fric}$ and external force $[F_s]^{app}$.

$$\begin{bmatrix} m_s & 0 & 0 & 0 & 0 & 1 & 0 & 1 & 0 \\ 0 & I_s & 0 & 0 & 0 & 0 & 1 & 0 & 0 \\ 0 & 0 & m_r & 0 & 0 & 0 & 0 & -1 & \frac{-1}{r_\beta}\tan\beta \\ 0 & 0 & 0 & I_r & 0 & 0 & 0 & 0 & -1 \\ 0 & 0 & 0 & 0 & I_g & 0 & 0 & 0 & 1 \\ 1 & 0 & 0 & 0 & 0 & 0 & 0 & 0 & 0 \\ 0 & 1 & -1 & 0 & 0 & 0 & 0 & 0 & 0 \\ 1 & 0 & 0 & 0 & 0 & 0 & 0 & 0 & 0 \\ 0 & 0 & \frac{-1}{r_\beta}\tan\beta & -1 & 1 & 0 & 0 & 0 & 0 \end{bmatrix} \begin{bmatrix} \ddot{x}_s \\ \ddot{\theta}_s \\ \ddot{x}_r \\ \ddot{\theta}_r \\ \ddot{\theta}_g \\ \lambda_1 \\ \lambda_2 \\ \lambda_3 \\ \lambda_4 \end{bmatrix} = \begin{bmatrix} F_s - F_{sf} \\ -M_{sf} \\ -F_{rf} \\ -M_{rf} \\ -M_{gf} \\ 0 \\ 0 \\ 0 \\ 0 \end{bmatrix} \tag{A.2.13}$$

and $\boldsymbol{\gamma} = [0\ 0\ 0\ 0]^T$.

A.2.13 Phase 3b-Unsynchronized

The sleeve will continue its axial and rotational movement until tip of the sleeve chamfer will cover S_{eng} by maintaining the viscous oil thickness between the engaging teeth chamfers. Meanwhile the ring spline will come out from the blocking contact to initiate further engagement.

The sleeve has constant rotational speed and increasing axial speed during the phase 3b. The sleeve will turn the gear or the ring will turn the gear will depend on the comparison of the axial and the rotational speed of the sleeve. If the axial speed of the sleeve is higher with respect to its rotational speed, the ring will turn the gear otherwise the sleeve will turn the gear. In the model it is considered that the sleeve will turn the gear.

It is possible that somewhere during the phase speed difference between the cones reduces to zero otherwise at end of the phase the speed difference between the cones will be zero. After the engaging chamfers contact the cones speed difference is not important to take into account.

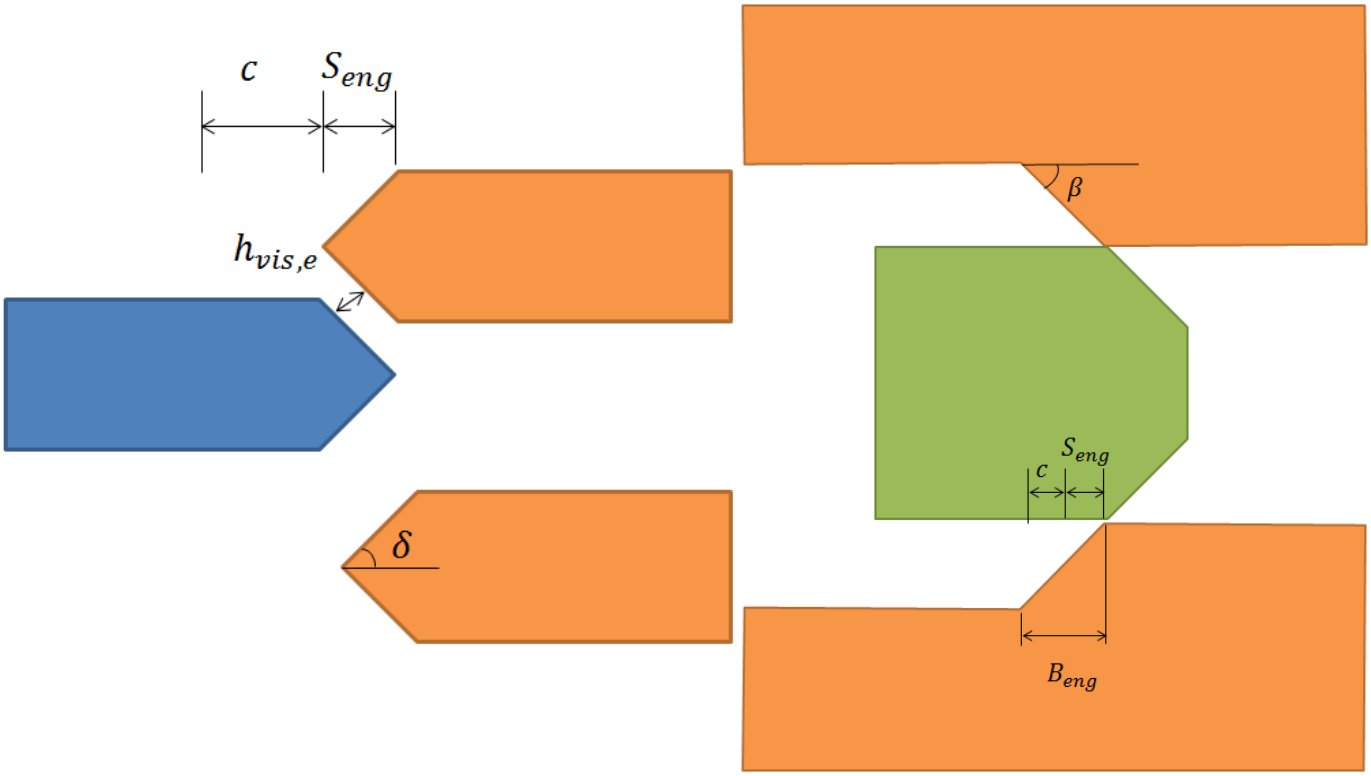

Figure 60: End position of the phase 3b-unsynchronized.

A.2.14 Phase 3b-Unsynchronized–Equations

The set of active constraint for the phase 3b is

$$\boldsymbol{\Phi}(\boldsymbol{q},t) = \begin{bmatrix} \boldsymbol{\Phi}^{external} \\ \boldsymbol{\Phi}^{internal} \end{bmatrix} = \begin{bmatrix} x_s - v_s t \\ \theta_s - \omega_s t \\ x_r - x_s - d_\alpha \\ \theta_r - \theta_s - \theta_{r_s} \\ \theta_g - \theta_r + B_{ang} - \dfrac{x_r - B_{ax}}{r_\beta}\tan\beta \end{bmatrix} = \mathbf{0} \qquad \text{(A.2.14)}$$

If linear tangential velocity of the sleeve rotational speed (v_{ω_s}) is greater than its axial velocity $(\dot{x}_s)$, the term $\frac{x_r - B_{ax}}{r_\beta}\tan\beta$ will change by $\frac{x_s - B_{ax}}{r_\delta}\tan\delta$.

$$\frac{\partial \boldsymbol{\Phi}}{\partial \boldsymbol{q}} = \begin{bmatrix} 1 & 0 & 0 & 0 & 0 \\ 0 & 1 & 0 & 0 & 0 \\ -1 & 0 & 1 & 0 & 0 \\ 0 & -1 & 0 & 1 & 0 \\ 0 & 0 & \frac{-1}{r_\beta}\tan\beta & -1 & 1 \end{bmatrix}, \frac{\partial \boldsymbol{\Phi}}{\partial t} = \begin{bmatrix} -v_s \\ -\omega_s \\ 0 \\ 0 \\ 0 \end{bmatrix} = \mathbf{0}$$

The equations of motion are

$$\begin{bmatrix} m_s & 0 & 0 & 0 & 0 \\ 0 & I_s & 0 & 0 & 0 \\ 0 & 0 & m_r & 0 & 0 \\ 0 & 0 & 0 & I_r & 0 \\ 0 & 0 & 0 & 0 & I_g \end{bmatrix} \begin{bmatrix} \ddot{x}_s \\ \ddot{\theta}_s \\ \ddot{x}_r \\ \ddot{\theta}_r \\ \ddot{\theta}_g \end{bmatrix} - \begin{bmatrix} 1 & 0 & -1 & 0 & 0 \\ 0 & 1 & 0 & -1 & 0 \\ 0 & 0 & 1 & 0 & \frac{-x_r}{r_\beta}\tan\beta \\ 0 & 0 & 0 & 1 & -1 \\ 0 & 0 & 0 & 0 & 1 \end{bmatrix} \begin{bmatrix} \lambda_1 \\ \lambda_2 \\ \lambda_3 \\ \lambda_4 \end{bmatrix} = \begin{bmatrix} F_s \\ 0 \\ 0 \\ 0 \\ 0 \end{bmatrix}^{app} - \begin{bmatrix} F_{sf} \\ M_{sf} \\ F_{rf} \\ M_{rf} \\ M_{gf} \end{bmatrix}^{fric} \tag{A.2.15}$$

where $F_s = \left(F_{s,3a} - 40000t\right)N/s$, $F_{sf} = C_{s\alpha}\, sign(\dot{x}_{sl})$, $M_{sf} = T_c + C_s\dot{\theta}_s$, $F_{rf} = C_{r\beta}\, sign(\dot{x}_r)$, $M_{rf} = -T_{sq} + C_r\, \dot{\theta}_r$, $M_{gf} = C_g\ \dot{\theta}_g$. Q^A is equal to the frictional forces $\left[F_{sf}, M_{sf}, F_{rf}, M_{rf}, M_{gf}\right]^{fric}$ and external force $[F_s]^{app}$. $F_{s,3a}$ is applied shift force at end of phase 3a.

$$\begin{bmatrix} m_s & 0 & 0 & 0 & 0 & 1 & 0 & -1 & 0 & 0 \\ 0 & I_s & 0 & 0 & 0 & 0 & 1 & 0 & -1 & 0 \\ 0 & 0 & m_r & 0 & 0 & 0 & 0 & 1 & 0 & \frac{-x_r}{r_\beta}\tan\beta \\ 0 & 0 & 0 & I_r & 0 & 0 & 0 & 0 & 1 & -1 \\ 0 & 0 & 0 & 0 & I_g & 0 & 0 & 0 & 0 & 1 \\ 1 & 0 & 0 & 0 & 0 & 0 & 0 & 0 & 0 & 0 \\ 0 & 1 & 0 & 0 & 0 & 0 & 0 & 0 & 0 & 0 \\ -1 & 0 & 1 & 0 & 0 & 0 & 0 & 0 & 0 & 0 \\ 0 & -1 & 0 & 1 & 0 & 0 & 0 & 0 & 0 & 0 \\ 0 & 0 & \frac{-x_r}{r_\beta}\tan\beta & -1 & 1 & 0 & 0 & 0 & 0 & 0 \end{bmatrix} \begin{bmatrix} \ddot{x}_s \\ \ddot{\theta}_s \\ \ddot{x}_r \\ \ddot{\theta}_r \\ \ddot{\theta}_g \\ \lambda_1 \\ \lambda_2 \\ \lambda_3 \\ \lambda_4 \end{bmatrix} = \begin{bmatrix} F_s - F_{sf} \\ -M_{sf} \\ -F_{rf} \\ -M_{rf} \\ -M_{gf} \\ 0 \\ 0 \\ 0 \\ 0 \end{bmatrix} \tag{A.2.16}$$

and $\boldsymbol{\gamma} = [0\ 0\ 0\ 0]^T$.

A.2.15 Phase 3c-Unsynchronized

The shift force increases to break the viscous oil film thickness and to turn the slave to move the master axially. This second increment in the shift force is called second bump. If the speed difference between the cones becomes zero at least before start of the phase 3b, the cones will stuck over each other during the phase 3b because of the releasing heat and the decreasing diameter. The shift force will increase in double bump during the phase 3c to release the cones by turning the gear and the ring together.

If there is tangential clearance between splines of the engaging teeth at bottom, the splines will go in the engagement position without breaking the oil film. When full engagement is done and clutch is released, the film will be squeezed out by the drag torque between the splines.

It is desirable that the sleeve has axial velocity with the shift force to free the stuck cones but this value should not be higher than the required otherwise it will lead to a high second bump.

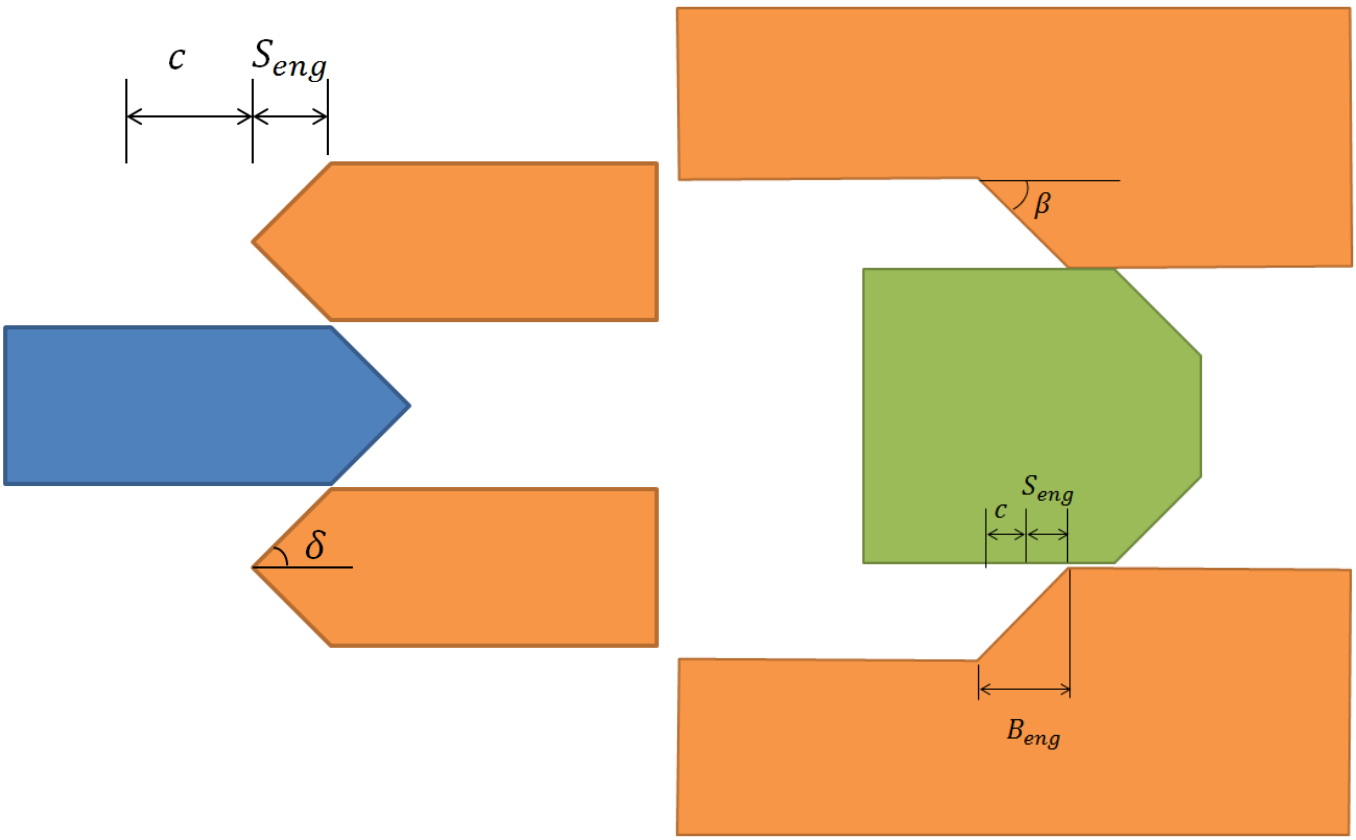

Figure 61: End position of the phase 3c-unsynchronized.

A.2.16 Phase 3c-Unsynchronized–Equations

The set of active constraint for the phase 3c is

$$\boldsymbol{\Phi}(\boldsymbol{q},t)=\begin{bmatrix}\boldsymbol{\Phi}^{external}\\ \boldsymbol{\Phi}^{internal}\end{bmatrix}=\begin{bmatrix}x_s-v_s t\\ \theta_s-\omega_s t\\ x_r-x_s-d_\alpha\\ \theta_r-\theta_s-\theta_{r_s}\\ \theta_g-\theta_r+B_{ang}-\dfrac{x_s-(C-B_{ax})}{r_\delta}\tan\delta\end{bmatrix}=\mathbf{0} \qquad \text{(A.2.17)}$$

with

$$\frac{\partial\boldsymbol{\Phi}}{\partial\boldsymbol{q}}=\begin{bmatrix}1 & 0 & 0 & 0 & 0\\ 0 & 1 & 0 & 0 & 0\\ -1 & 0 & 1 & 0 & 0\\ 0 & -1 & 0 & 1 & 0\\ \dfrac{-1}{r_\delta}\tan\delta & 0 & 0 & -1 & 1\end{bmatrix},\frac{\partial\boldsymbol{\Phi}}{\partial t}=\begin{bmatrix}-v_s\\ -\omega_s\\ 0\\ 0\\ 0\end{bmatrix}=\mathbf{0}$$

The equations of motion are

$$\begin{bmatrix}m_s & 0 & 0 & 0 & 0\\ 0 & I_s & 0 & 0 & 0\\ 0 & 0 & m_r & 0 & 0\\ 0 & 0 & 0 & I_r & 0\\ 0 & 0 & 0 & 0 & I_g\end{bmatrix}\begin{bmatrix}\ddot{x}_s\\ \ddot{\theta}_s\\ \ddot{x}_r\\ \ddot{\theta}_r\\ \ddot{\theta}_g\end{bmatrix}-\begin{bmatrix}1 & 0 & -1 & 0 & \dfrac{-1}{r_\delta}\tan\delta\\ 0 & 1 & 0 & -1 & 0\\ 0 & 0 & 1 & 0 & 0\\ 0 & 0 & 0 & 1 & -1\\ 0 & 0 & 0 & 0 & 1\end{bmatrix}\begin{bmatrix}\lambda_1\\ \lambda_2\\ \lambda_3\\ \lambda_4\end{bmatrix}$$
$$=\begin{bmatrix}F_s\\ 0\\ 0\\ 0\\ 0\end{bmatrix}^{app}-\begin{bmatrix}F_{sf}\\ M_{sf}\\ F_{rf}\\ M_{rf}\\ M_{gf}\end{bmatrix}^{fric} \qquad \text{(A.2.18)}$$

Where $F_s=\left(F_{s,3b}-3000t\right)N/s$, $F_{sf}=C_{s\alpha}\,sign(\dot{x}_{sl})$, $M_{sf}=C_s\dot{\theta}_s$, $F_{rf}=C_{r\beta}\,sign(\dot{x}_r)$, $M_{rf}=C_r\,\dot{\theta}_r$, $M_{gf}=C_g\;\dot{\theta}_g$. Q^A is equal to the frictional forces $\left[F_{sf},M_{sf},F_{rf},M_{rf},M_{gf}\right]^{fric}$ and external force $[F_s]^{app}$. $F_{s,3b}$ is applied shift force at end of phase 3b.

$$\begin{bmatrix} m_s & 0 & 0 & 0 & 0 & 1 & 0 & -1 & 0 & \frac{-1}{r_\delta}\tan\delta \\ 0 & I_s & 0 & 0 & 0 & 0 & 1 & 0 & -1 & 0 \\ 0 & 0 & m_r & 0 & 0 & 0 & 0 & 1 & 0 & 0 \\ 0 & 0 & 0 & I_r & 0 & 0 & 0 & 0 & 1 & -1 \\ 1 & 0 & 0 & 0 & I_g & 0 & 0 & 0 & 0 & 1 \\ 0 & 0 & 0 & 0 & 0 & 0 & 0 & 0 & 0 & 0 \\ -1 & 1 & 0 & 0 & 0 & 0 & 0 & 0 & 0 & 0 \\ 0 & 0 & 1 & 0 & 0 & 0 & 0 & 0 & 0 & 0 \\ \frac{-1}{r_\delta}\tan\delta & -1 & 0 & 1 & 0 & 0 & 0 & 0 & 0 & 0 \\ & 0 & 0 & -1 & 1 & 0 & 0 & 0 & 0 & 0 \end{bmatrix} \begin{bmatrix} \ddot{x}_s \\ \ddot{\theta}_s \\ \ddot{x}_r \\ \ddot{\theta}_r \\ \ddot{\theta}_g \\ \lambda_1 \\ \lambda_2 \\ \lambda_3 \\ \lambda_4 \end{bmatrix} = \begin{bmatrix} F_s - F_{sf} \\ -M_{sf} \\ -F_{rf} \\ -M_{rf} \\ -M_{gf} \\ 0 \\ 0 \\ 0 \\ 0 \end{bmatrix} \qquad \text{(A.2.19)}$$

and $\boldsymbol{\gamma} = [0\ 0\ 0\ 0]^T$.

If the shift force needed to squeeze out the oil film thickness is higher than the shift force needed to release the cones and to turn the slave, the gear will turn first and after oil film will squeeze out. Position of the chamfers contact is shown in *Figure 62*.

If the shift force needed to squeeze out the oil film thickness is less than the shift force needed to release the cones and to turn the slave, oil film will squeeze out first and after the gear will turn. Position of the chamfers contact is shown in *Figure 63*.

But in both cases it is assumed that the shift force is higher than the oil splash losses.

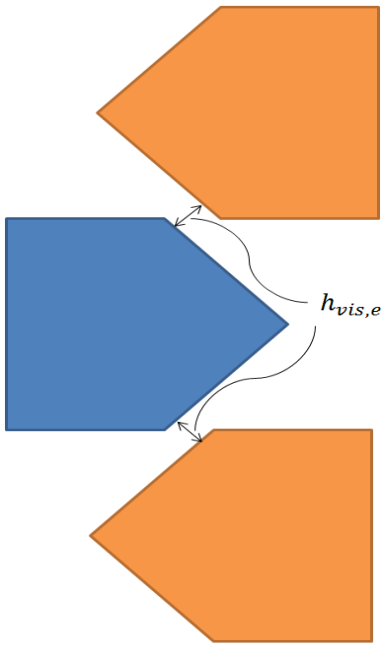

Figure 62: Possible position of the phase 3c-unsynchronized with high viscosity and density oil.

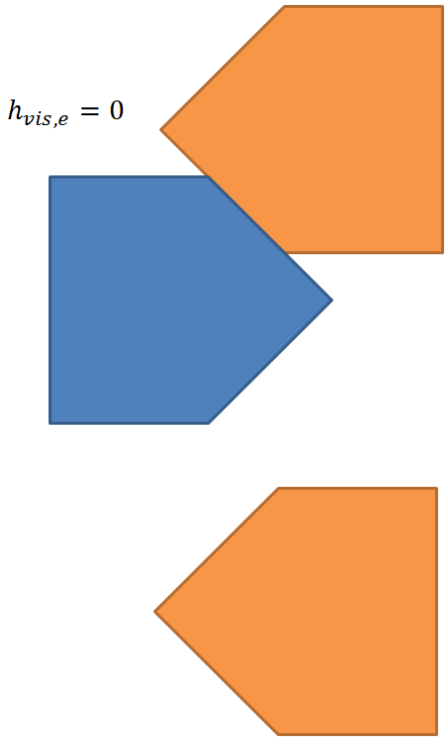

Figure 63: Possible position of the phase 3c-unsynchronized with low viscosity and density oil.

A.3 Modified synchronizer for test rig comparison

Here, the constraints pertinent to the modified model are given.

A.3.1 Phase 1a neutral to spring contact

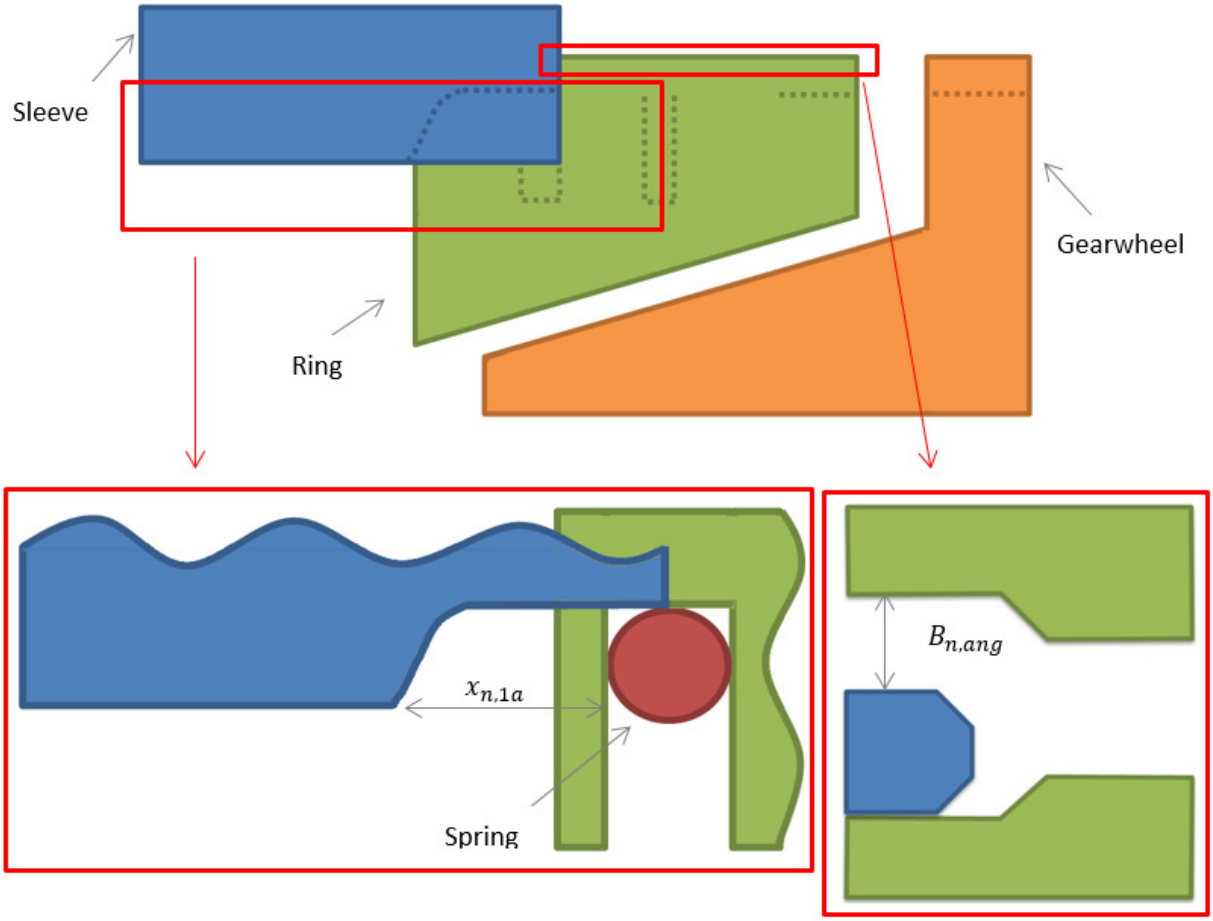

Figure 64: The modified generic synchronizer, start of the phase 1a.

The sleeve moves axially from neutral position and covers a displacement $x_{n,1a}$. At end of the phase the sleeve comes in contact with spring. The ring will stay at its axial position. The ring and the sleeve will rotate together.

The sleeve travel $d_{n\alpha}$ axial displacement and c_{ns} is the sliding friction.

$$\boldsymbol{\Phi}(\boldsymbol{q},t) = \begin{bmatrix} \theta_s - \omega_s t \\ \theta_s - \theta_r \\ x_r \end{bmatrix} = \mathbf{0}$$

A.3.2 Phase 1b Angular indexing

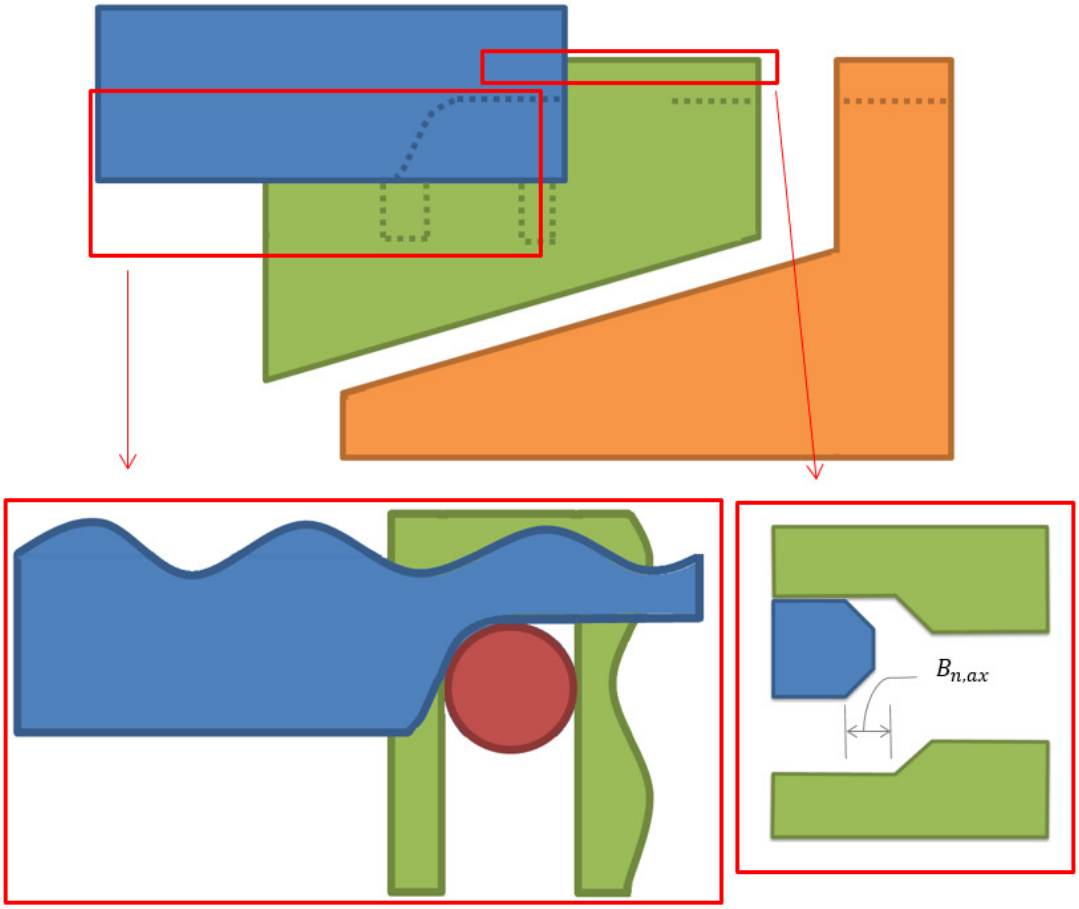

Figure 65: The modified generic synchronizer, the phase 1b.

The applied shift force is small such that after the sleeve and the spring contact the sleeve will not move further, giving the ring time to get angular indexing during the phase 1b and gets an angular displacement $B_{n,ang}$.

The sleeve and the ring will not move axially.

$$\boldsymbol{\Phi}(\boldsymbol{q},t) = \begin{bmatrix} x_s - x_{n,1a} \\ \theta_s - \omega_s t \\ x_s - x_r - x_{n,1a} \end{bmatrix} = \mathbf{0}$$

A.3.3 Phase 1c towards axial indexing

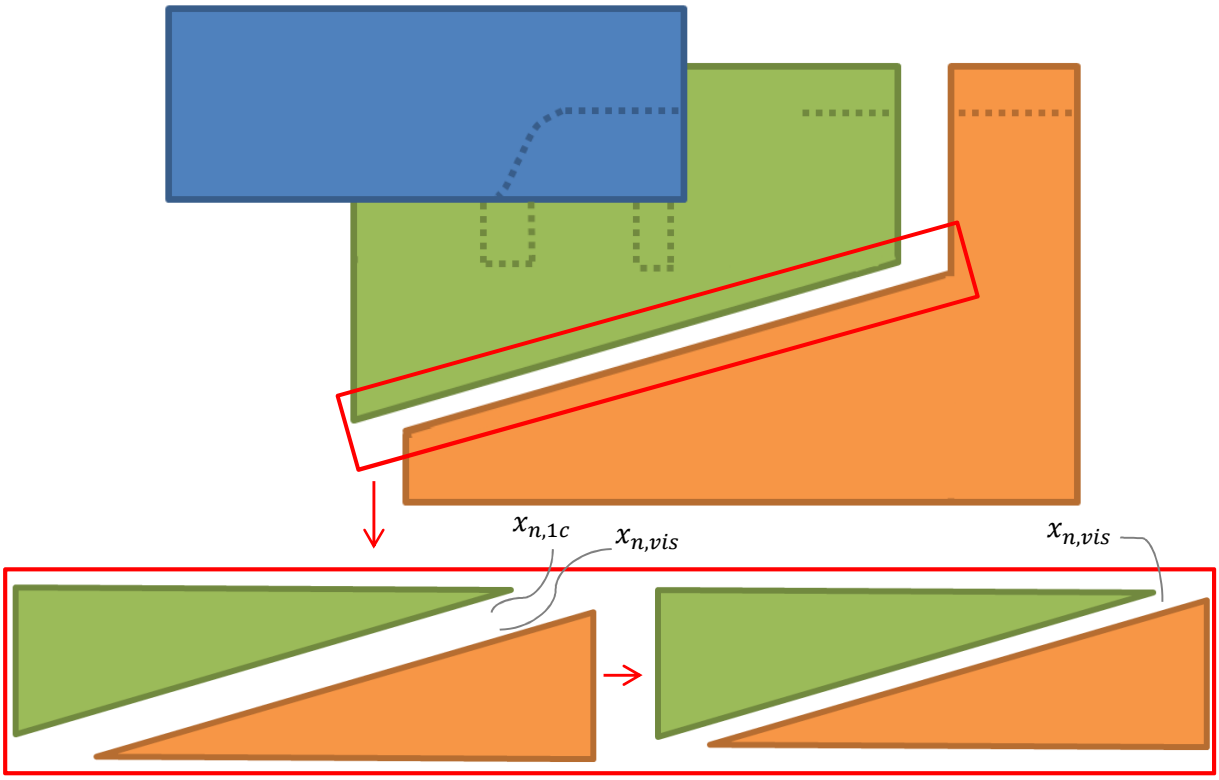

Figure 66: The modified generic synchronizer, the phase 1c.

In this phase 1c the axial distance between the cones will decrease until the viscous friction starts while the sleeve and the ring will move axially and rotationally together. Because of the insufficient oil friction between the cones the gear will get a small increment in rotational speed.

The applied sleeve force overcomes the sliding friction c_{nss} of the sleeve and the ring to translate axially during the phase to cover the displacement $x_{n,1c}$.

$$\boldsymbol{\Phi}(\boldsymbol{q},t) = \begin{bmatrix} \theta_s - \omega_s t \\ \theta_s - \theta_r - B_{n,ang} \\ x_s - x_r - x_{n,1a} \end{bmatrix} = \mathbf{0}$$

A.3.4 Phase 1d axial indexing/Spring force

The force needed to squeeze out the oil between the cones is much higher than the spring stiffness. So during the phase the sleeve will push the spring down by increasing the applied shift force with higher increasing rate than so far. The ring will maintain its axial position. At end of the phase the sleeve chamfer will comes in contact with the ring chamfer to complete the axial indexing and covers the axial displacement $B_{n,ax}$.

$$\boldsymbol{\Phi}(\boldsymbol{q},t) = \begin{bmatrix} \theta_s - \omega_s t \\ \theta_s - \theta_r - B_{n,ang} \\ x_r - x_{n,1c} \end{bmatrix} = \mathbf{0}$$

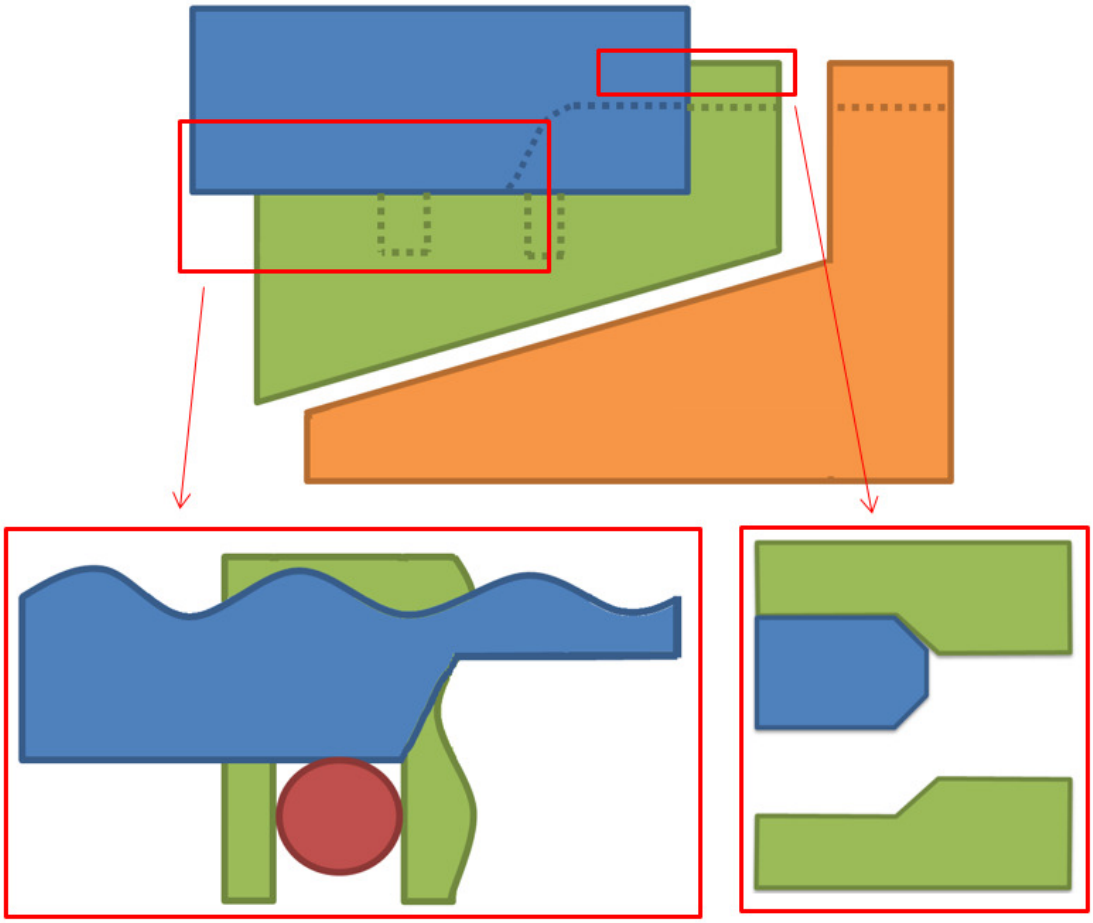

Figure 67: The modified generic synchronizer, end of the phase 1d.

A.3.5 Phase 1e viscous friction

In the final sub-phase of the presynchronization phase 1 the oil will squeeze out between the cones and the cones contact will shift from viscous friction to dry friction. The sleeve moves axially by a displacement $x_{n,vis}$.

$$\boldsymbol{\Phi}(\boldsymbol{q},t) = \begin{bmatrix} \theta_s - \omega_s t \\ \theta_s - \theta_r - B_{n,ang} \\ x_s - x_r - x_{n,1a} - x_{n,1c} \end{bmatrix} = \mathbf{0}$$

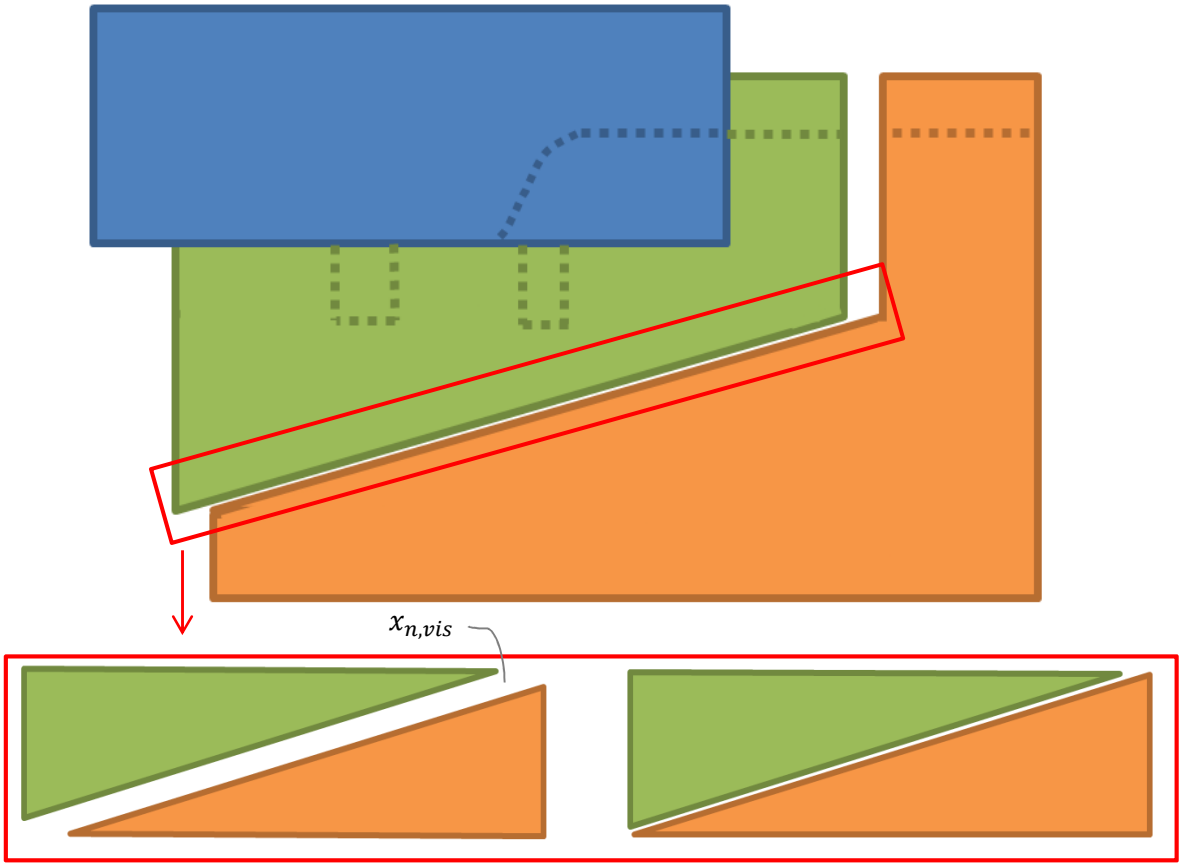

Figure 68: The modified generic synchronizer, the phase 1e.

A.3.6 Phase 2 Dry friction/main synchronization

Three bodies of the modified generic synchronizer hold their axial position while speed difference decreases by the cones sliding over each other due to dry friction.

$$\boldsymbol{\Phi}(\boldsymbol{q},t) = \begin{bmatrix} \theta_s - \omega_s t \\ \theta_s - \theta_r - B_{n,ang} \\ x_s - x_r - x_{n,1a} - x_{n,1c} \end{bmatrix} = \mathbf{0}$$